Characterization of symbiotically important processes in *Sinorhizobium meliloti*

Hardik Zatakia

Dissertation submitted to the faculty of the Virginia Polytechnic Institute and State University in partial fulfillment of the requirements for the degree of

Doctor of Philosophy

in

Biological Sciences

Birgit Scharf, Chair
John Jelesko
David Popham
Ann Stevens

August 7th, 2015
Blacksburg, VA

Keywords: Chemotaxis, exopolysaccharides, motility, nodulation, type IVb pili

Characterization of symbiotically important processes in *Sinorhizobium meliloti*

Hardik Zatakia

ABSTRACT

Bacteria perform biological nitrogen fixation (BNF) which leads to conversion of N_2 to ammonia. One of the best studied models of BNF is the symbiotic association of *Sinorhizobium meliloti – Medicago sativa* (alfalfa). Since alfalfa is a major source of animal feed and the fourth largest crop grown in the USA, enhanced understanding of this symbiosis can have implications for increasing crop yields, reducing environmental contamination and food costs. Studies discussed here focus on two symbiotically important bacterial traits, type IVb pili and chemotaxis.

Chapter 2 characterizes *S. meliloti* type IVb pili encoded by *flp-1* and establishes their role in nodulation. Bundle-forming pili were visualized in wild-type cells, while cells lacking *pilA1*, the pilin-encoding gene, showed an absence of pili. Competitive nodulation assays with alfalfa concluded that cells lacking pili had a significant nodulation defect. Regulation of *pilA1* expression via a quorum sensing regulator, ExpR, was confirmed.

Chapter 3 describes the role of the *flp-2* cluster in establishing symbiosis. PilA2 is a pilin subunit encoded from *flp-2*. The *pilA2* deletion strain was defective in nodulation by 31% as compared to the wild type. A non-significant change in nodulation was seen in Δ*pilA1pilA2* strain. Thus, both *flp-1* and *flp-2* have a significant role in establishing symbiosis.

Chapter 4 focuses on the deviations of *S. meliloti* chemotaxis from the enterobacterial paradigm. Transcriptional fusions showed that *S. meliloti* chemoreceptors (MCPs) are class III genes and regulated by FlbT. Quantitative immunoblots determined the cellular amounts of chemoreceptors. Chemoreceptors were grouped in three classes; high, low, and extremely-low

abundance, similar to the high and low abundance chemoreceptors of *Escherichia coli*. Importantly, the MCP:CheA ratio in an *S. meliloti* cell was observed to be 37:1, similar to that in *Bacillus subtilis* of 24:1, but quite different from that in *E. coli* of 3.4:1. In conclusion, our data indicates that soil bacteria may have optimized their chemotaxis system based on their milieu, which is different from enteric bacteria.

These studies have enhanced our understanding of two symbiotically important processes in *S. meliloti*, and pave the way for future manipulations of the system to increase symbiosis and reduce our dependence on synthetic fertilizers.

ACKNOWLEDGEMENTS

I would like express my deepest gratitude for Dr. Birgit Scharf for giving me the opportunity to study under her guidance. None of the studies presented here would have been possible without her excellent mentorship, inspiring passion for science, and overall optimism. Referring to Dr. Scharf as my 'Thesis Advisor' would be underplaying her role in my personal growth. She has kept me motivated through the toughest moments of my life. I will be forever indebted to her.

I would like to thank my wife, Kuntan Dhanoya, for everything and much much more. I would also like to thank my parents and family for their continuous support and belief in me.

I have been fortunate to have had an excellent committee under whose supervision all of my work has come to fruition. Thank you Dr. Jelesko, Dr. Popham, and Dr. Stevens for our productive meetings, for all the constructive comments, and always having your doors open for me.

Ben Webb, with a personality that is my polar opposite, it was a pleasure getting to know you and to have worked with you. Thank you for taking me 'outside' the box and sharing experiences with me that I would have perhaps never had. I will always cherish the times we've played Frisbee, biked together, and those spent on the balcony contemplating. Katherine Broadway, it is truly amazing to have watched you start as an undergraduate researcher and be a very successful graduate student. Thank you for being a fellow caffeine fiend, a wonderful colleague, and an even better friend. I would like to thank Cassandra Nelson and Anjali Sharma

for the help and support during my early years in the Scharf lab. What can I say about the members of the Scharf Lab (Tim, Rafael, Amanda, and Jose)? It is craziness personified. And for that I am extremely thankful. You'll made working hard a lot of fun.

I would like thank Dr. Revathy Ramachandran for her help with the DNA-Protein studies, Dr. Keith Ray for his help with protein analyses, Sean Mury for his help with the fluorescence microscope, and other members of the Microbiology group at Life Sciences 1.

I would also like to express my gratitude towards Prof. (Mrs.) Prabha Padmanabha and Dr. Srividya Shivakumar for their mentorship during my undergraduate and Masters' studies.

Last, but certainly not the least, I would like to thank Earl Sheehan for our very insightful conversations about life.

Contents

LIST OF FIGURES

Chapter 1

Chapter 2

Chapter 3

Chapter 4

LIST OF TABLES

Chapter 2

Chapter 3

Chapter 4

Chapter 1 - Introduction

Nitrogen is essential to survival of any living cell as it is required to synthesize amino acids that make up proteins and nucleic acids which form the genetic material of a cell. Nitrogen is the most abundant element in the atmosphere. However, most living cells cannot utilize it directly as its present in the N_2 form which has a very stable triple covalent bond. Nitrogen fixation is the conversion of inorganic nitrogen in the environment to an organic and a readily utilizable form. Nitrogen fixation is an integral part of the nitrogen cycle as it counter-balances the loss of nitrogen in the environment via denitrification. Nitrogen can be fixed chemically by the Haber-Bosch process to produce nitrogenous fertilizers. Bacteria, both symbiotic and free-living, perform biological nitrogen fixation (BNF) which leads to the nitrogenase-catalyzed conversion of atmospheric nitrogen to ammonia.

Increased use of synthetic nitrogenous fertilizers in agriculture has resulted in various deleterious effects on the environment like eutrophication of water bodies and increased acidity and salinity of soil. Thus, BNF combats these detrimental processes and is a more environmentally sustainable alternative (1). The ability to fix nitrogen is widespread in prokaryotes. While it is restricted to methanogens in archaea, it is found in almost all bacterial groups including green-sulphur bacteria, actinomycetes, cyanobacteria, and all sub-divisions of proteobacteria. Some free-living bacteria like the aerobic *Azotobacter* spp. and the facultative anaerobic *Klebsiella* spp. exhibit the capacity to fix nitrogen. Symbiotic BNF can occur between bacteria associated with plants and their plant hosts (2). The symbioses between legumes and bacteria present in their root nodules is perhaps one of the best studied host-microbe relationship (3). It is estimated that BNF itself contributes about 200 to 300 million tons of fixed nitrogen every year (4). About 10 % of this amount is a direct consequence of the rhizobia-legume symbiosis (5).

Symbiosis

One widely studied plant-bacterial interactions occurs between the rhizobial species and their leguminous plant hosts like soybean and alfalfa. Rhizobia are usually portrayed to be root-nodule-forming, nitrogen-fixing plant symbionts from the genera *Azorhizobium, Bradyrhizobium, Mesorhizobium, Rhizobium*, and *Sinorhizobium*. The formation of a symbiotic relationship between leguminous plants and rhizobia is a complex process. Exchanges of surface molecules from both partners and various mechanisms are implicated in this process.

Attachment of rhizobia on plants is generally thought to be mediated by plant lectins, which act as receptors for bacterial surface polysaccharides (6-8). A Ca^{2+}-binding bacterial protein called rhicadhesin is also involved in rhizobial infection of plants. Rhicadhesin is believed to have two binding domains, one for binding to the receptor on the bacterial surface and another for anchoring to the root-hair surface (9). However, the lectin/rhicadhesin-mediated binding is weak and reversible. A stronger secondary binding takes place in form of the attachment of bacterial fibrils to plant surfaces (10).

Legumes secrete some aromatic compounds called flavonoids which induce the transcription of *nod* genes in bacteria. This, in turn, leads to production of lipochitooligosaccharide compounds in bacteria called Nod factors (11). As shown in Fig. 1.1, Nod factors in turn induce various responses in plants like calcium spiking and induction of infection threads, both of which are essential for effective nodulation. Once on the plant root surface, the bacteria alter the growth of root hairs and cause them to curl. Root hair curling traps the bacteria, which induces cell division in the inner cortex, leading to the formation of nodule meristem (12).

Trapped bacteria induce the formation of an infection thread, which are thin tubes filled with bacterial cells that invade the plant cortical cells (3, 13). Plant cells then enclose the invading bacteria in host membrane bound organelles. The entire structure consisting of a bacterium and the surrounding endocytic plant membrane is called a symbiosome (14). Symbiosomes provide the right nutrients and microaerobic conditions required for nitrogen fixation. Once within a symbiosome, the bacterium undergoes morphogenesis to acquire a bacteroid form. Bacteroids are generally elongated rods which are usually branched. Synthesis of nitrogen fixing enzymes only occurs in differentiated bacteroids. (3).

Sinorhizobium meliloti (formerly *Rhizobium meliloti*) is a Gram negative bacterium belonging to the α-class of proteobacteria. *S. meliloti* forms a symbiotic relationship with three genera of leguminous plants namely *Medicago*, *Melilotus*, and *Trigonella*. Since *Medicago sativa* (alfalfa) is extensively grown in the United States and an important fodder crop, the *S. meliloti* – *M. sativa* symbiosis model is widely studied in many laboratories across the globe.

Like many members of the α-proteobacteria, *S. meliloti* has a multi-partite genome organization. The *S. meliloti* genome consists of three replicons: a chromosome (3.65 Mb) and two megaplasmids, pSymA (1.35 Mb) and pSymB (1.68 Mb) (15). There are many genes on both the megaplasmids that are required for the symbiotic life cycle of *S. meliloti*. The pSymA megaplasmid contains the *nif*/*fix* and the *nod* genes essential for nitrogen fixation and nodulation, respectively (16). Similarly, pSymB contains the *exo* genes which code for symbiotically important exopolysaccharides (succinoglycan) (17, 18). It also codes for Arg-tRNA, the cell's only t-RNA that recognizes CCG (Arg) (19). This makes pSymB essential for protein synthesis and growth.

The chromosome of *S. meliloti* is characteristic of an aerobic, heterotrophic bacterium. The megaplasmid, pSymB, confers upon the bacterium varied metabolic capabilities, while acquisition of pSymA gave the ability of nodulation and surviving under low oxygen conditions, which is important during the bacteroid stage. It is suggested that the two megaplasmids were acquired separately by an ancestor. Analyses of the G+C content shows that pSymB was acquired before pSymA (15). Interestingly, the cell can be cured of pSymA while approximately 200-kb of several pSymB regions is essential for cell viability. Apart from these three replicons, many strains of *S. meliloti* possess one or more accessory plasmids.

The following factors play a vital role in establishment of symbioses in *S. meliloti*.

1. Quorum sensing
2. Exopolysaccharide production
3. Type IV pili
4. Motility & chemotaxis

Quorum sensing (QS)

Quorum sensing is a mechanism that allows the cells within a population to act as a group rather than individuals and bring about appropriate changes in their physiology. Quorum sensing (QS) can be defined as coordinated changes in physiology based on local cell density (20). The cells are able to gage the local population density via the production and sensing of signaling molecules. The best characterized signaling molecules are acyl-homoserine lactones (AHLs) produced by many proteobacteria. Each cell extrudes and uptakes these AHLs and can sense the amount of AHLs present in the environment. When the amounts of AHLs reach a critical threshold, the cells induce changes in their physiology. This usually takes place by activation or repression of a transcriptional regulator, which then alters gene expression (21). During nodulation, as the bacteria cluster at the plant roots, they sense the rise in their cell population and induce the expression of genes involved in the nodulation. Thus, quorum sensing is a key factor in effective nodulation (13).

S. meliloti can have up to three QS systems (Fig. 1.2) (13). The s*inRI* system, which is encoded on the chromosome, is common to all *S. meliloti* strains. The s*inRI* system comprises two transcriptional regulators, ExpR and SinR, and a SinR-controlled autoinducer synthase, SinI (22). The autoinducer, N-acyl homoserine lactone, along with ExpR, control a plethora of genes

including ones responsible for exopolysaccharide biosynthesis, biofilm production, motility and chemotaxis (23-25). Differential sensitivity to varying levels of AHLs provides for a strict temporal control exerted by the *sinRI* system on the expression of downstream genes (26).

S. meliloti strain 1021 (Sm1021) is a sequenced strain and is widely considered to be the 'wild-type strain' amongst laboratories studying *S. meliloti* across the world. However, it has a mutated copy of ExpR due to which it grows as dry colonies (since ExpR is involved in exopolysaccharide synthesis) (27, 28). Contrarily, *S. meliloti* strain 8530 has a functional copy of ExpR and therefore shows a mucoid phenotype. This is important as both these strains are used in these studies.

The second system which utilizes short chain AHLs is called the *mel* system. Currently, the targets of *mel* system are unknown. The *tra* system, which is the third QS system, is found only in some *S. meliloti* strains as it is encoded on the plasmid pRme41a. Sm1021 strain does not contain the pRme41a plasmid and thus is deficient of the *tra* system (29). The function of the *tra* system is not yet identified.

Exopolysaccharide (EPS) production

The exopolysacccharides extruded from *S. meliloti* are known to play a role in symbiosis (12). *S. meliloti* synthesizes two exopolysaccharides namely EPS I (succinoglycan) and EPS II (galactoglucan) (27). Both EPS I and EPS II are synthesized in a low-molecular-weight (LMW) and a high-molecular-weight (HMW) form.

A 27-kb *exo* gene cluster on the pSymB plasmid encodes the proteins used for synthesis of EPS I. The *exo*$^{-}$ mutants are known to be defective in nodulation and could not fix nitrogen (30). However, it was shown that exogenous addition of EPSI rescued this phenotype in the *exo*$^{-}$ mutants (31). The biosynthetic genes for EPS II (*exp*) are located in a 23-kb cluster on the pSymB megaplasmid (32).

LMW EPS I is the primary EPS that is recognized by plants to induce nodulation (31, 33, 34). ExpR is the quorum sensing regulator which regulates EPS I via *exoI* and EPS II via *wgeB* (35). In Sm1021, since EPS I production is impaired due to the mutated copy of *expR*; the capsular polysaccharide (K antigen) fulfills the role of LMW EPS I and helps in nodulation. It has also been shown that LMW EPS II can induce nodulation, although it is significantly less efficient in nodule induction as compared to LMW EPS I (27).

Type IV pili

Attachment of bacterial cells to various surfaces is important for their survival. It could be the attachment to a substratum to form a biofilm or a eukaryotic host in case of pathogens. *S. meliloti* is thought to express Type IV pili (Tfp) at its surface. Type IV pili are long, extracellular, hair-like structures composed of a structural subunit called a pilin. Various proteins, cytoplasmic and membrane-bound, comprise the Tfp synthesis machinery. The sequences of leader peptides on pilin proteins are cleaved by prepilin peptidases. The ability to reversibly assemble into long fibers is a unique characteristic of Tfp. This is achieved due to the concerted action of two cytoplasmic ATPases, one involved in polymerization and the other in depolymerization. In addition, proteins forming a Type II secretion system-like membrane pore are part of the assembly machinery (36).

Tfp are further classified into Type IVa (Tfpa) and Type IVb (Tfpb) based on the length of pilin leader peptide and the residue at the N-terminus of the mature pilin. Leader peptides of Tfpb pilins can be longer as compared to the Type IVa pilins by as much as 15 amino acids (aa). Moreover, Type IVb pilins consist of either long (longer than Type IVa) mature peptides of 180 - 200 aa or short mature peptides only about 40-50 aa in length (37). The latter are similar to the members of the Flp (fimbrial low molecular weight) family, which were first described in *Actinobacillus* sp. The *S. meliloti* genome contains two pilin-encoding genes, *pilA1* and *pilA2*. The length of these pilin genes in *S. meliloti* suggests they encode members of the Flp family of Type IVb pili (38).

An important distinguishing character between Tfpa and Tfpb is gene organization. While Tfpa-synthesis machinery genes are usually scattered across the genome, Tfpb genes on the bacterial genomes are mostly organized in contiguous clusters. Such an organization points to the acquisition of Tfpb genes via horizontal gene transfer (39). *S. meliloti* has two *pil* gene clusters,

one each on the chromosome and the pSymA plasmid. There are two insertion sequences flanking *pil1* on the chromosome, which suggests that the *pil1* cluster was acquired horizontally. It is postulated that *pil2* came into existence after a gene duplication event of the *pil1* cluster (40, 41). The *pil2* cluster is immediately downstream of the *che2* operon and a diguanylate cyclase phosphodiesterase system. It has been shown in *Pseudomonas* sp. that Type IV pili can be regulated through a chemotaxis-like system (Pil-Chp system) (42). In addition, c-di-GMP is known to regulate the expression of Tfp in *Vibrio cholerae* (43). It can be postulated that such a regulation of the *pil2* gene cluster via the *che2* operon and the diguanylate cyclase phosphodiesterase system may occur in *S. meliloti* as well.

Tfp first came into light in *Acinetobacter* sp., *Moraxella* sp., and *Pseudomonas* sp. due to their association with flagellar-independent motility known as twitching motility (44). However, pilus-mediated motility is only seen in bacterial exhibiting Tfpa pili. The marked absence of the retracting ATPase in cells expressing Tfpb pili precludes their role in any pili-mediated motility. However, the only exception to that is the longus pilus in the enterotoxigenic *Escherichia coli*, which is a Tfpb pili and plays a role in motility (45). Instead, Tfpb have been associated with attachment and adherence to various biotic and abiotic surfaces like metals and eukaryotic hosts in bacteria across different phylogenetic families. In the same vein, the first report of a role for Tfp's in biofilm formation came in *Pseudomonas aeruginosa* (46). Tfp are also known to confer competence to bacterial cells and thus aid in DNA uptake as in the case of *Haemophilus* spp. and *Neisseria spp*. (47).

Tfpb have well-documented roles as virulence factors in various pathogens. Non-piliated mutants of enteropathogenic *E. coli* (EPEC) showed a reduction in virulence (48). The only reports, thus far, of Tfpb in plant-microbe interactions are those in plant pathogens. In *Ralstonia*

solanacearum and *Pseudomonas syringae*, Tfpb act as virulence factors in infecting the potato and tobacco plant, respectively (49, 50).

Despite the widespread presence of Tfp genes in rhizosphere bacteria, their significance in plant-bacteria symbiosis is not understood. The presence of two *pil* systems in *S. meliloti* calls for an in-depth probe to analyze whether or not they play a role in establishment of a symbiotic relationship by *S. meliloti*.

Motility & chemotaxis

Many bacteria use flagella for locomotion. Swimming motility, which is powered by the rotation of flagella through liquid, is the most widely understood form of motility. Several other kinds of motility like twitching, swarming, and gliding exist to enable bacterial locomotion on varied surfaces. Swarming motility like swimming is known to be flagella-dependent, while Type IV pili are required for twitching motility and some gliding motility (51). Bacterial swimming motility is effected by a series of 'runs' and 'tumbles'. Runs can be described as long relatively straight moves, while a tumble is a rather short random turn. By modulating the frequency of runs and tumbles, the bacteria are able to move in a desired direction, and this is termed as 'biased random walk' (52).

The ability of bacteria to move towards attractants and away from repellents is called chemotaxis. Chemotaxis allows bacteria to sense and adapt to their environment. Both motility and chemotaxis have been shown to play a role in a variety of bacterial processes like pathogenesis, biofilm formation, and host-microbe interactions (46, 53, 54). *E. coli* has been used as a model system for studying motility and chemotaxis (55-57).

In *E. coli*, the flagellum rotates both counter-clock-wise (CCW, run) and clock wise (CW, tumble). The flagellar filament is made up of thousands of flagellin subunits and has a certain helicity to it to be able to exert thrust. A flagellar motor at the base of the flagellar filament drives the rotation of the filament. The basal body comprises more than 20 proteins forming several structures among which are various rings spanning the cell wall and proteins involved in using the proton motive force that powers the motor (58). When the motor is turning CCW, the flagellar filament exhibits left-handed helicity. The flagellar filament changes helicity to right-handedness when the motor switches to the CW direction. The synchronous CCW rotation of all the flagellar

filaments on an *E. coli* cell results in the formation of the flagellar bundle. A CCW rotating flagellar bundle enables the cell to run in the desired direction. Asynchronous rotation of flagellar motors, due to the switching of one or more motors to CW direction, causes the flagellar bundle to splay apart and the cell to tumble (59-61). In contrast, *S. meliloti* flagellar filaments are locked in right-handed helicity and the flagellar motor only rotates in the CW mode (62, 63). For the cell to tumble, one or more of the flagellar motors has to slow down, which causes the flagellar bundle to fall apart, thereby enabling the cell to tumble (64). Motility, although not essential, is important for *S. meliloti* infection of leguminous plants. Non-motile cells are less competitive in nodule formation (65).

In *S. meliloti*, chemotaxis has been implicated in playing a role in establishing symbiosis with its host plant *M. sativa* (alfalfa) (66). Bacterial chemotaxis functions by sensing environmental signals and relaying that information via the concerted action of various chemotaxis proteins to ultimately cause a physiological change. While enterobacterial chemotaxis is well studied, several other species including *S. meliloti* have shown marked deviations from this paradigm (67-70). *S. meliloti* strain RU11/001 is known to me more motile and chemotactic than the generally considered wild type strain Sm1021 (62). Thus, our studies understanding the cellular stoichiometries of chemotaxis proteins were performed with strain RU11/001.

The environmental signals are sensed by bacterial transmembrane proteins called methyl-accepting chemotaxis proteins (MCPs). Different species have different numbers of chemoreceptors. While *Mesorhizobium loti* has only one, *V. cholerae* has 45 (70). *E. coli* has five MCPs: Tar, Tsr, Trg, Tap, and Aer. Tar recognizes aspartate and maltose and Trg recognize sugars like ribose and galactose. Tsr senses serine and Tap responds to dipeptides. Aer acts as an oxygen sensor (57). In contrast, *S. meliloti* has six transmembrane chemoreceptors (McpT, McpU, McpV,

McpW, McpX, and McpZ). It also has two soluble cytosolic receptors (McpY and IcpA) (71). The identification of ligands for *S. meliloti* MCPs is an area of active research. Webb *et. al*. have shown that the chemoreceptor McpU in *S. meliloti* plays a role in plant-host exudate sensing, particularly in sensing host-derived proline. (72). MCPs typically consist of a periplasmic ligand-binding domain, two transmembrane domains, and a cytoplasmic signaling domain and form stable homodimers. When a ligand binds to the periplasmic domain, it causes a piston-like movement through the transmembrane domains to the cytoplasmic domain, which then acts as a signal to the internal chemotaxis proteins. While there is a lot of sequence variation in the periplasmic domains of MCPs, presumably to bind different ligands, there is tremendous sequence conservation in the cytoplasmic signaling domains, even between different species (57).

A two component system using a histidine-aspartate phosphorelay (HAP) mediates the chemotactic signal transduction from the chemoreceptor cluster to the flagellar motor complex. The first component, CheA, is the histidine protein kinase that binds to the cytoplasmic domain of the MCPs via a coupling protein, CheW (73). The second component, CheY, is the response regulator that interacts with the flagellar motor complex when phosphorylated. In *E. coli*, CheZ is a phosphatase which increases the dephosphorylation rate of CheY-P and thereby allows for signal termination (74-76). A direct phosphatase mechanism is absent in *S. meliloti* (Fig. 1.3). In its place, it employs an indirect phosphate sink mechanism for signal termination. In this system, instead of a CheZ homolog, phosphate groups from the response regulator CheY2 are shuttled back via CheA to another response regulator protein CheY1. In fact, CheY1 directly competes with CheY2 for the initial phosphate from CheA-P (77). A small novel 97-amino acid protein, CheS, in *S. meliloti* increases the interaction of CheA and CheY1 and has been shown to aid in increased dephosphorylation of CheY1-P. Although CheS homologs are present in other α-proteobacteria

like *Agrobacterium tumefaciens* and *Caulobacter crescentus*, they are absent in enterobacteria (78).

In *E. coli*, when an attractant is bound to the periplasmic domain of an MCP, a conformational change in the MCP inhibits the autophosphorylating activity of CheA. Thus, there is no signal being passed on to the flagellar motor, which would then continue in the CCW direction resulting in a run. In absence of a bound attractant or presence of a repellent, CheA autophosphorylation is stimulated. Phosphorylated CheA (CheA-P) acts as a substrate for CheY which undergoes phosphorylation at a conserved aspartate residue. CheY-P interacts with FliM of the flagellar motor complex and signals the motor to switch to the CW direction (74, 79). An adaptation system is also employed by *E. coli* for increased sensitivity and real-time modulation of motility based on the local environment. CheR is a methyltransferase which constitutively adds methyl groups on conserved sites on the cytoplasmic signaling domain of MCPs. CheB is an enzyme that competes with CheY for the phosphate from CheA-P. CheB-P can remove the methyl groups from MCPs via its methylesterase activity (57, 70). In *E.*coli, only the high abundant MCPs (Tar and Tsr) have a conserved pentapeptide NWETF found at the C-terminus of the cytoplasmic domain, which serves as the site for CheR and CheB docking, enabling them to conduct their methyltransferase and methylesterase activities, respectively (80). The concerted addition and removal of methyl groups by CheR and CheB, respectively, brings about the conformational changes in MCPs required for resetting and adaptation of the chemotaxis system (81, 82).

Another important deviation in *S. meliloti* chemotaxis from the enterobacterial paradigm is the presence of another novel chemotaxis protein, CheT. It is an uncharacterized chemotaxis protein and in its absence the cells exhibit faster swimming speeds and reduced chemotaxis (B. Scharf, personal communication). CheD is a protein whose function in *S. meliloti* is not known but

an analog in *B. subtilis* has been shown to play a role in adaptation via deamidation of the chemoreceptors (83).

In *E. coli*, the chemotaxis, flagellar, and motility genes are located in four different gene clusters (84). Conversely, in *S. meliloti* 45 genes responsible for chemotaxis (*che*), flagellar synthesis (*fla*), and motility (*mot*) are clustered on the chromosome in one 56-kb contiguous region. This region is called the 'flagellar regulon' (85, 86). Flagellar synthesis and motility is metabolically expensive. Thus, a strict temporal hierarchy exists in the transcription of the genes of the flagellar regulon (87, 88).

The whole regulon is divided into four classes based on the hierarchy in which they are transcribed. Class IA contains two global regulators of the LuxR family, VisN and VisR (87). The VisNR complex acts as the activator of transcription of another regulator called Rem, which belongs to class IB of the regulon. Rem activates class II genes which comprises the class IIA (basal body structure and flagellar export) and class IIB (*mot*) genes. Chemotaxis and flagellin genes belonging to the class III genes are the last to be transcribed. They require the transcription of class IIA genes for their transcription (88).

Further analyses of *S. meliloti* motility and chemotaxis will shed light on the unique features of *S. meliloti* systems, as compared to the systems in *E. coli*, which may have enabled optimal function for two different lifestyles (free-living and symbiotic).

Cross-regulation

While each of the abovementioned processes are individually important in *S. meliloti*, only their concerted, sequential, and regulated action can help in establishment of a successful symbiotic relationship. Since the cell has to devote many resources for each of these processes to function properly, there exists a cross-regulation between EPS production, motility, quorum sensing, and biofilm formation. Fig. 1.4 summarizes the cross-regulation of these processes in S. meliloti via the concerted activity of various transcriptional regulators.

ExpR, a LuxR homolog, is part of the quorum sensing system and is a global transcriptional regulator (89). It is known to control motility via the repression of *visN/R*, which is a regulator of the motility and chemotaxis genes in *S. meliloti* (25, 87, 90). ExpR also acts as a direct link between succinoglycan (EPS I) and galactoglucan (EPS II) by regulating their biosynthesis (35, 91).

MucR, a zinc finger protein, positively regulates succinoglycan (EPS I) synthesis while repressing galactoglucan (EPS II) production. MucR also affects chemotaxis and motility by inhibiting Rem, a class IB regulator in the transcriptional hierarchy of the flagellar and chemotaxis genes in *S. meliloti* (88, 92). The symbiosis regulator CbrA positively controls transcription of *visN* and *visR* (93). *emmABC* is an operon where *emmB* and *emmC* encode a two-component system whose products have been found to regulate motility and exopolysaccharide production. Interestingly, mutations in this operon also affects host invasion and therefore nodule formation (94).

If Type IVb pili prove to be important in symbiosis, it would be interesting to elucidate if its synthesis is also a part of the crossregulation network regulated by the various regulators mentioned above.

Objectives of this work

Symbiotic nitrogen fixation (SNF) plays an extremely important role in the nitrogen cycle. Moreover, it reduces our dependence on synthetic nitrogenous fertilizers which are both detrimental to the environment and expensive. SNF saves almost $10 billion annually in the United States alone (95). Alfalfa (*Medicago sativa*) is the fourth largest crop grown in the United States and is a major source of animal feed. Our deeper understanding of *Sinorhizobium meliloti-Medicago sativa* symbiosis could not only potentially help us increase crop yields but also do so in an environmentally sustainable manner. Bacterial Type IV pili and chemotaxis are important aspects that help establish this relationship and are the focus of this study.

Chapter 2 characterizes the Type IV pili encoded by the *pil1* gene cluster on the *S. meliloti* genome. Their structure and organization is visualized by transmission electron microscopy. A very unique pattern of lateral localization of a pilus synthesis machinery protein is observed using fluorescence microscopy. Evidence for the importance of Tfpb in effective nodulation by *S. meliloti* is also provided. Furthermore, this chapter establishes that Tfpb synthesis in *S. meliloti* is regulated by a quorum sensing regulator, ExpR, which also controls motility, chemotaxis, and exopolysaccharide production. Chapter 3 shows the importance of the pilin encoded from the *pil2* gene cluster in effective nodulation. It also demonstrates the absence of an additive defect when pilins encoded from both clusters are deleted.

For chemotaxis to work proficiently, precise fine-tuning of all its components is absolutely essential (76). To better understand the deviations of *S. meliloti* chemotaxis from the enterobacterial paradigm and their corresponding effects of the life-cycle of bacteria, the cellular stoichiometry of chemoreceptor proteins is discussed in chapter 4. The values obtained from this

study would form the backbone on which computational models can be based for greater analyses of the differences between chemotactic behavior and responses in different model systems (96).

Taken together, these results enhance the understanding of the exact molecular processes that enable the plant and bacteria to enter into a successful symbiotic relationship. This knowledge will also pave the way for experimentation in further optimization of these processes to help increase crop yields and benefit the environment.

REFERENCES

1. **Dixon R, Kahn D.** 2004. Genetic regulation of biological nitrogen fixation. Nat Rev Microbiol **2:**621-631.
2. **Franche C, Lindström K, Elmerich C.** 2009. Nitrogen-fixing bacteria associated with leguminous and non-leguminous plants. Plant and soil **321:**35-59.
3. **Jones KM, Kobayashi H, Davies BW, Taga ME, Walker GC.** 2007. How rhizobial symbionts invade plants: the *Sinorhizobium-Medicago* model. Nat Rev Microbiol **5:**619-633.
4. **Galloway JN, Schlesinger WH, Levy H, Michaels A, Schnoor JL.** 1995. Nitrogen fixation: Anthropogenic enhancement-environmental response. Global Biogeochemical Cycles **9:**235-252.
5. **Smil V.** 2001. Enriching the earth: Fritz Haber, Carl Bosch, and the transformation of world food. The MIT Press, Cambridge, United Kingdom.
6. **Rüdiger H, Gabius H-J.** 2001. Plant lectins: Occurrence, biochemistry, functions and applications. Glycoconjugate Journal **18:**589-613.
7. **Hirsch AM.** 1999. Role of lectins (and rhizobial exopolysaccharides) in legume nodulation. Current Opinion in Plant Biology **2:**320-326.
8. **Ridge RW, Kim R, Yoshida F.** 1998. The diversity of lectin-detectable sugar residues on root hair tips of selected legumes correlates with the diversity of their host ranges for rhizobia. Protoplasma **202:**84-90.
9. **Smit G, Tubbing DMJ, Kijne JW, Lugtenberg BJJ.** 1991. Role of Ca^{2+} in the activity of rhicadhesin from *Rhizobium leguminosarum* biovar *viciae* which mediates the first step in attachment of *Rhizobiaceae* cells to plant root hair tips. Archives of Microbiology **155:**278-283.
10. **Robertson JL, Holliday T, Matthysse AG.** 1988. Mapping of *Agrobacterium tumefaciens* chromosomal genes affecting cellulose synthesis and bacterial attachment to host cells. J Bacteriol **170:**1408-1411.
11. **Perret X, Staehelin C, Broughton WJ.** 2000. Molecular basis of symbiotic promiscuity. Microbiol Mol Biol Rev **64:**180-201.
12. **Rodriguez-Navarro DN, Dardanelli MS, Ruiz-Sainz JE.** 2007. Attachment of bacteria to the roots of higher plants. FEMS Microbiol Lett **272:**127-136.
13. **Gonzalez JE, Marketon MM.** 2003. Quorum sensing in nitrogen-fixing rhizobia. Microbiol Mol Biol Rev **67:**574-592.
14. **Anonymous.** 2004. Plant Cell Wall Remodelling in the Rhizobium-Legume Symbiosis. Critical Reviews in Plant Sciences **23:**293-316.
15. **Galibert F, Finan TM, Long SR, Pühler A, Abola P, Ampe F, Barloy-Hubler F, Barnett MJ, Becker A, Boistard P, Bothe G, Boutry M, Bowser L, Buhrmester J, Cadieu E, Capela D, Chain P, Cowie A, Davis RW, Dreano S, Federspiel NA, Fisher RF, Gloux S, Godrie T, Goffeau A, Golding B, Gouzy J, Gurjal M, Hernandez-Lucas I, Hong A, Huizar L, Hyman RW, Jones T, Kahn D, Kahn ML, Kalman S, Keating DH, Kiss E, Komp C, Lelaure V, Masuy D, Palm C, Peck MC, Pohl TM, Portetelle D, Purnelle B, Ramsperger U, Surzycki R, Thebault P, Vandenbol M, et al.** 2001. The composite genome of the legume symbiont *Sinorhizobium meliloti*. Science **293:**668-672.
16. **Banfalvi Z, Sakanyan V, Koncz C, Kiss A, Dusha I, Kondorosi A.** 1981. Location of nodulation and nitrogen fixation genes on a high molecular weight plasmid of *R. meliloti*. Mol Gen Genet **184:**318-325.
17. **Glucksmann MA, Reuber TL, Walker GC.** 1993. Genes needed for the modification, polymerization, export, and processing of succinoglycan by *Rhizobium meliloti*: a model for succinoglycan biosynthesis. J Bacteriol **175:**7045-7055.
18. **Reuber TL, Walker GC.** 1993. Biosynthesis of succinoglycan, a symbiotically important exopolysaccharide of *Rhizobium meliloti*. Cell **74:**269-280.
19. **Finan TM, Kunkel B, De Vos GF, Signer ER.** 1986. Second symbiotic megaplasmid in *Rhizobium meliloti* carrying exopolysaccharide and thiamine synthesis genes. J Bacteriol **167:**66-72.
20. **Whitehead NA, Barnard AM, Slater H, Simpson NJ, Salmond GP.** 2001. Quorum-sensing in Gram-negative bacteria. FEMS Microbiol Rev **25:**365-404.
21. **Gurich N, González JE.** 2009. Role of quorum sensing in *Sinorhizobium meliloti*-Alfalfa symbiosis. J Bacteriol **191:**4372-4382.
22. **Marketon MM, González JE.** 2002. Identification of two quorum-sensing systems in *Sinorhizobium meliloti*. J Bacteriol **184:**3466-3475.
23. **Marketon MM, Glenn SA, Eberhard A, González JE.** 2003. Quorum sensing controls exopolysaccharide production in *Sinorhizobium meliloti*. J Bacteriol **185:**325-331.

24. **Rinaudi LV, González JE.** 2009. The low-molecular-weight fraction of exopolysaccharide II from *Sinorhizobium meliloti* is a crucial determinant of biofilm formation. J Bacteriol **191:**7216-7224.
25. **Hoang HH, Gurich N, González JE.** 2008. Regulation of motility by the ExpR/Sin quorum-sensing system in *Sinorhizobium meliloti*. J Bacteriol **190:**861-871.
26. **Charoenpanich P, Meyer S, Becker A, McIntosh M.** 2013. Temporal Expression Program of Quorum Sensing-Based Transcription Regulation in *Sinorhizobium meliloti*. J Bacteriol **195:**3224-3236.
27. **Glazebrook J, Walker GC.** 1989. A Novel Exopolysaccharide Can Function in Place of the Calcofluor-Binding Exopolysaccharide in Nodulation of Alfalfa by *Rhizobium-Meliloti*. Cell **56:**661-672.
28. **Pellock BJ, Teplitski M, Boinay RP, Bauer WD, Walker GC.** 2002. A LuxR homolog controls production of symbiotically active extracellular polysaccharide II by *Sinorhizobium meliloti*. J Bacteriol **184:**5067-5076.
29. **Marketon MM, Gronquist MR, Eberhard A, Gonzalez JE.** 2002. Characterization of the *Sinorhizobium meliloti sinR/sinI* locus and the production of novel N-acyl homoserine lactones. J Bacteriol **184:**5686-5695.
30. **Leigh JA, Lee CC.** 1988. Characterization of Polysaccharides of *Rhizobium-Meliloti* Exo Mutants That Form Ineffective Nodules. J Bacteriol **170:**3327-3332.
31. **Battisti L, Lara JC, Leigh JA.** 1992. Specific oligosaccharide form of the *Rhizobium meliloti* exopolysaccharide promotes nodule invasion in alfalfa. Proc Natl Acad Sci U S A **89:**5625-5629.
32. **Skorupska A, Janczarek M, Marczak M, Mazur A, Krol J.** 2006. Rhizobial exopolysaccharides: genetic control and symbiotic functions. Microb Cell Fact **5:**7.
33. **Gonzalez JE, Reuhs BL, Walker GC.** 1996. Low molecular weight EPS II of *Rhizobium meliloti* allows nodule invasion in *Medicago sativa*. Proc Natl Acad Sci U S A **93:**8636-8641.
34. **Wang LX, Wang Y, Pellock B, Walker GC.** 1999. Structural characterization of the symbiotically important low-molecular-weight succinoglycan of *Sinorhizobium meliloti*. J Bacteriol **181:**6788-6796.
35. **Janczarek M.** 2011. Environmental signals and regulatory pathways that influence exopolysaccharide production in rhizobia. International journal of molecular sciences **12:**7898-7933.
36. **Giltner CL, Nguyen Y, Burrows LL.** 2012. Type IV pilin proteins: versatile molecular modules. Microbiol Mol Biol Rev **76:**740-772.
37. **Pelicic V.** 2008. Type IV pili: *e pluribus unum*? Mol Microbiol **68:**827-837.
38. **Kachlany SC, Planet PJ, Desalle R, Fine DH, Figurski DH, Kaplan JB.** 2001. *flp-1*, the first representative of a new pilin gene subfamily, is required for non-specific adherence of *Actinobacillus actinomycetemcomitans*. Mol Microbiol **40:**542-554.
39. **Roux N, Spagnolo J, de Bentzmann S.** 2012. Neglected but amazingly diverse type IVb pili. Res Microbiol **163:**659-673.
40. **Planet PJ, Kachlany SC, Fine DH, DeSalle R, Figurski DH.** 2003. The Widespread Colonization Island of *Actinobacillus actinomycetemcomitans*. Nat Genet **34:**193-198.
41. **Tomich M, Planet PJ, Figurski DH.** 2007. The *tad* locus: postcards from the widespread colonization island. Nat Rev Microbiol **5:**363-375.
42. **Kato J, Kim HE, Takiguchi N, Kuroda A, Ohtake H.** 2008. *Pseudomonas aeruginosa* as a model microorganism for investigation of chemotactic behaviors in ecosystem. J Biosci Bioeng **106:**1-7.
43. **Tischler AD, Camilli A.** 2004. Cyclic diguanylate (c-di-GMP) regulates *Vibrio cholerae* biofilm formation. Mol Microbiol **53:**857-869.
44. **Henrichsen J.** 1975. The occurrence of twitching motility among gram-negative bacteria. Acta Pathol Microbiol Scand B **83:**171-178.
45. **Mazariego-Espinosa K, Cruz A, Ledesma MA, Ochoa SA, Xicohtencatl-Cortes J.** 2010. Longus, a type IV pilus of enterotoxigenic *Escherichia coli*, is involved in adherence to intestinal epithelial cells. J Bacteriol **192:**2791-2800.
46. **O'Toole GA, Kolter R.** 1998. Flagellar and twitching motility are necessary for *Pseudomonas aeruginosa* biofilm development. Mol Microbiol **30:**295-304.
47. **Carruthers MD, Tracy EN, Dickson AC, Ganser KB, Munson RS, Jr., Bakaletz LO.** 2012. Biological roles of nontypeable *Haemophilus influenzae* type IV pilus proteins encoded by the *pil* and *com* operons. J Bacteriol **194:**1927-1933.
48. **Zahavi EE, Lieberman JA, Donnenberg MS, Nitzan M, Baruch K, Rosenshine I, Turner JR, Melamed-Book N, Feinstein N, Zlotkin-Rivkin E, Aroeti B.** 2011. Bundle-forming pilus retraction enhances enteropathogenic *Escherichia coli* infectivity. Mol Biol Cell **22:**2436-2447.
49. **Nguyen LC, Taguchi F, Tran QM, Naito K, Yamamoto M, Ohnishi-Kameyama M, Ono H, Yoshida M, Chiku K, Ishii T, Inagaki Y, Toyoda K, Shiraishi T, Ichinose Y.** 2012. Type IV pilin is glycosylated

in *Pseudomonas syringae* pv. *tabaci* 6605 and is required for surface motility and virulence. Mol Plant Pathol **13:**764-774.
50. **Wairuri CK, van der Waals JE, van Schalkwyk A, Theron J.** 2012. *Ralstonia solanacearum* needs Flp pili for virulence on potato. Mol Plant Microbe Interact **25:**546-556.
51. **Harshey RM.** 2003. Bacterial Motility on a Surface: Many Ways to a Common Goal. Annual Review of Microbiology **57:**249-273.
52. **Berg HC.** 1993. Random walks in biology. Princeton University Press.
53. **Hawes MC, Smith LY.** 1989. Requirement for chemotaxis in pathogenicity of *Agrobacterium tumefaciens* on roots of soil-grown pea plants. J Bacteriol **171:**5668-5671.
54. **Pratt LA, Kolter R.** 1998. Genetic analysis of *Escherichia coli* biofilm formation: roles of flagella, motility, chemotaxis and type I pili. Mol Microbiol **30:**285-293.
55. **Manson MD.** 1992. Bacterial motility and chemotaxis. Adv Microb Physiol **33:**277-346.
56. **Macnab RM, Aizawa S-I.** 1984. Bacterial motility and the bacterial flagellar motor. Annual review of biophysics and bioengineering **13:**51-83.
57. **Wadhams GH, Armitage JP.** 2004. Making sense of it all: Bacterial chemotaxis. Nat Rev Mol Cell Bio **5:**1024-1037.
58. **Berg HC.** 2003. The rotary motor of bacterial flagella. Annual Review of Biochemistry **72:**19-54.
59. **Turner L, Ryu WS, Berg HC.** 2000. Real-time imaging of fluorescent flagellar filaments. J Bacteriol **182:**2793-2801.
60. **Darnton NC, Turner L, Rojevsky S, Berg HC.** 2007. On torque and tumbling in swimming *Escherichia coli*. J Bacteriol **189:**1756-1764.
61. **Macnab RM.** 2003. How bacteria assemble flagella. Annu Rev Microbiol **57:**77-100.
62. **Scharf B, Schmitt R.** 2002. Sensory transduction to the flagellar motor of *Sinorhizobium meliloti*. Journal of molecular microbiology and biotechnology **4:**183-186.
63. **Attmannspacher U, Scharf B, Schmitt R.** 2005. Control of speed modulation (chemokinesis) in the unidirectional rotary motor of *Sinorhizobium meliloti*. Mol Microbiol **56:**708-718.
64. **Platzer J, Sterr W, Hausmann M, Schmitt R.** 1997. Three genes of a motility operon and their role in flagellar rotary speed variation in *Rhizobium meliloti*. J Bacteriol **179:**6391-6399.
65. **Ames P, Bergman K.** 1981. Competitive advantage provided by bacterial motility in the formation of nodules by *Rhizobium meliloti*. J Bacteriol **148:**728-908 p.
66. **Caetano-Anollés G, Wall LG, De Micheli AT, Macchi EM, Bauer WD, Favelukes G.** 1988. Role of Motility and Chemotaxis in Efficiency of Nodulation by *Rhizobium meliloti*. Plant Physiol **86:**1228-1235.
67. **Schmitt R.** 2002. *Sinorhizobial* chemotaxis: a departure from the enterobacterial paradigm. Microbiology **148:**627-631.
68. **Boin MA, Austin MJ, Hase CC.** 2004. Chemotaxis in *Vibrio cholerae*. FEMS Microbiol Lett **239:**1-8.
69. **Sampedro I, Parales RE, Krell T, Hill JE.** 2015. *Pseudomonas* chemotaxis. FEMS Microbiol Rev **39:**17-46.
70. **Szurmant H, Ordal GW.** 2004. Diversity in chemotaxis mechanisms among the bacteria and archaea. Microbiol Mol Biol Rev **68:**301-319.
71. **Meier VM, Müschler P, Scharf BE.** 2007. Functional analysis of nine putative chemoreceptor proteins in *Sinorhizobium meliloti*. J Bacteriol **189:**1816-1826.
72. **Webb BA, Hildreth S, Helm RF, Scharf BE.** 2014. *Sinorhizobium meliloti* chemoreceptor McpU mediates chemotaxis toward host plant exudates through direct proline sensing. Appl Environ Microbiol **80:**3404-3415.
73. **Gegner JA, Graham DR, Roth AF, Dahlquist FW.** 1992. Assembly of an MCP receptor, CheW, and kinase CheA complex in the bacterial chemotaxis signal transduction pathway. Cell **70:**975-982.
74. **McEvoy MM, Bren A, Eisenbach M, Dahlquist FW.** 1999. Identification of the binding interfaces on CheY for two of its targets, the phosphatase CheZ and the flagellar switch protein fliM. J Mol Biol **289:**1423-1433.
75. **Baker MD, Wolanin PM, Stock JB.** 2006. Signal transduction in bacterial chemotaxis. Bioessays **28:**9-22.
76. **Parkinson JS, Hazelbauer GL, Falke JJ.** 2015. Signaling and sensory adaptation in *Escherichia coli* chemoreceptors: 2015 update. Trends Microbiol **23:**257-266.
77. **Sourjik V, Schmitt R.** 1998. Phosphotransfer between CheA, CheY1, and CheY2 in the chemotaxis signal transduction chain of *Rhizobium meliloti*. Biochemistry **37:**2327-2335.
78. **Dogra G, Purschke FG, Wagner V, Haslbeck M, Kriehuber T, Hughes JG, Van Tassell ML, Gilbert C, Niemeyer M, Ray WK, Helm RF, Scharf BE.** 2012. *Sinorhizobium meliloti* CheA complexed with CheS

exhibits enhanced binding to CheY1, resulting in accelerated CheY1 dephosphorylation. J Bacteriol **194:**1075-1087.

79. **Bren A, Eisenbach M.** 1998. The N terminus of the flagellar switch protein, FliM, is the binding domain for the chemotactic response regulator, CheY. J Mol Biol **278:**507-514.
80. **Feng X, Baumgartner JW, Hazelbauer GL.** 1997. High- and low-abundance chemoreceptors in *Escherichia coli*: differential activities associated with closely related cytoplasmic domains. J Bacteriol **179:**6714-6720.
81. **Djordjevic S, Stock AM.** 1998. Chemotaxis receptor recognition by protein methyltransferase CheR. Nat Struct Biol **5:**446-450.
82. **Anand GS, Goudreau PN, Stock AM.** 1998. Activation of methylesterase CheB: evidence of a dual role for the regulatory domain. Biochemistry **37:**14038-14047.
83. **Glekas GD, Plutz MJ, Walukiewicz HE, Allen GM, Rao CV, Ordal GW.** 2012. Elucidation of the multiple roles of CheD in *Bacillus subtilis* chemotaxis. Mol Microbiol **86:**743-756.
84. **Macnab RM.** 1992. Genetics and Biogenesis of Bacterial Flagella. Annual Review of Genetics **26:**131-158.
85. **Sourjik V, Sterr W, Platzer J, Bos I, Haslbeck M, Schmitt R.** 1998. Mapping of 41 chemotaxis, flagellar and motility genes to a single region of the *Sinorhizobium meliloti* chromosome. Gene **223:**283-290.
86. **Capela D, Barloy-Hubler F, Gouzy J, Bothe G, Ampe F, Batut J, Boistard P, Becker A, Boutry M, Cadieu E, Dreano S, Gloux S, Godrie T, Goffeau A, Kahn D, Kiss E, Lelaure V, Masuy D, Pohl T, Portetelle D, Pühler A, Purnelle B, Ramsperger U, Renard C, Thebault P, Vandenbol M, Weidner S, Galibert F.** 2001. Analysis of the chromosome sequence of the legume symbiont *Sinorhizobium meliloti* strain 1021. Proc Natl Acad Sci U S A **98:**9877-9882.
87. **Sourjik V, Müschler P, Scharf B, Schmitt R.** 2000. VisN and VisR are global regulators of chemotaxis, flagellar, and motility genes in *Sinorhizobium* (*Rhizobium*) *meliloti*. J Bacteriol **182:**782-788.
88. **Rotter C, Muhlbacher S, Salamon D, Schmitt R, Scharf B.** 2006. Rem, a new transcriptional activator of motility and chemotaxis in *Sinorhizobium meliloti*. J Bacteriol **188:**6932-6942.
89. **Hoang HH, Becker A, González JE.** 2004. The LuxR homolog ExpR, in combination with the Sin quorum sensing system, plays a central role in *Sinorhizobium meliloti* gene expression. J Bacteriol **186:**5460-5472.
90. **McIntosh M, Krol E, Becker A.** 2008. Competitive and cooperative effects in quorum-sensing-regulated galactoglucan biosynthesis in *Sinorhizobium meliloti*. J Bacteriol **190:**5308-5317.
91. **Yao SY, Luo L, Har KJ, Becker A, Ruberg S, Yu GQ, Zhu JB, Cheng HP.** 2004. *Sinorhizobium meliloti* ExoR and ExoS proteins regulate both succinoglycan and flagellum production. J Bacteriol **186:**6042-6049.
92. **Bahlawane C, McIntosh M, Krol E, Becker A.** 2008. *Sinorhizobium meliloti* regulator MucR couples exopolysaccharide synthesis and motility. Mol Plant Microbe Interact **21:**1498-1509.
93. **Gibson KE, Barnett MJ, Toman CJ, Long SR, Walker GC.** 2007. The symbiosis regulator CbrA modulates a complex regulatory network affecting the flagellar apparatus and cell envelope proteins. J Bacteriol **189:**3591-3602.
94. **Morris J, Gonzalez JE.** 2009. The novel genes *emmABC* are associated with exopolysaccharide production, motility, stress adaptation, and symbiosis in *Sinorhizobium meliloti*. J Bacteriol **191:**5890-5900.
95. **van Rhijn P, Vanderleyden J.** 1995. The *Rhizobium*-plant symbiosis. Microbiological Reviews **59:**124-142.
96. **Levin MD, Morton-Firth CJ, Abouhamad WN, Bourret RB, Bray D.** 1998. Origins of individual swimming behavior in bacteria. Biophys J **74:**175-181.
97. **Zatakia HM, Nelson CE, Syed UJ, Scharf BE.** 2014. ExpR coordinates the expression of symbiotically important, bundle-forming Flp pili with quorum sensing in *Sinorhizobium meliloti*. Appl Environ Microbiol **80:**2429-2439.

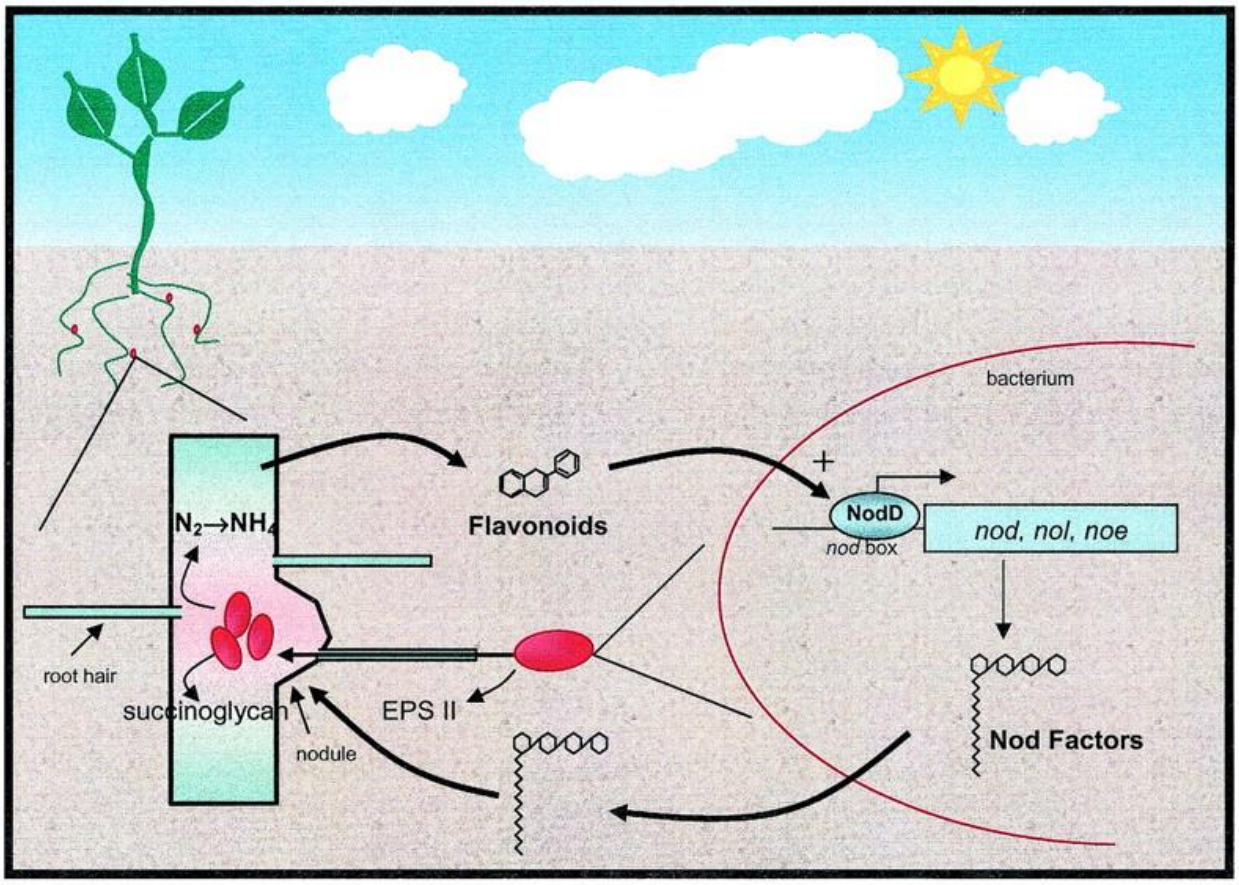

Fig. 1.1: *Rhizobium*-legume symbiosis model. Signals from both the bacteria and the plant host are exchanged in the rhizosphere. On nodule invasion, the bacteria undergo metamorphosis into bacteroids which are capable of fixing atmospheric nitrogen leading to successful symbiosis (13). (Used with permission from RightsLink in 2015)

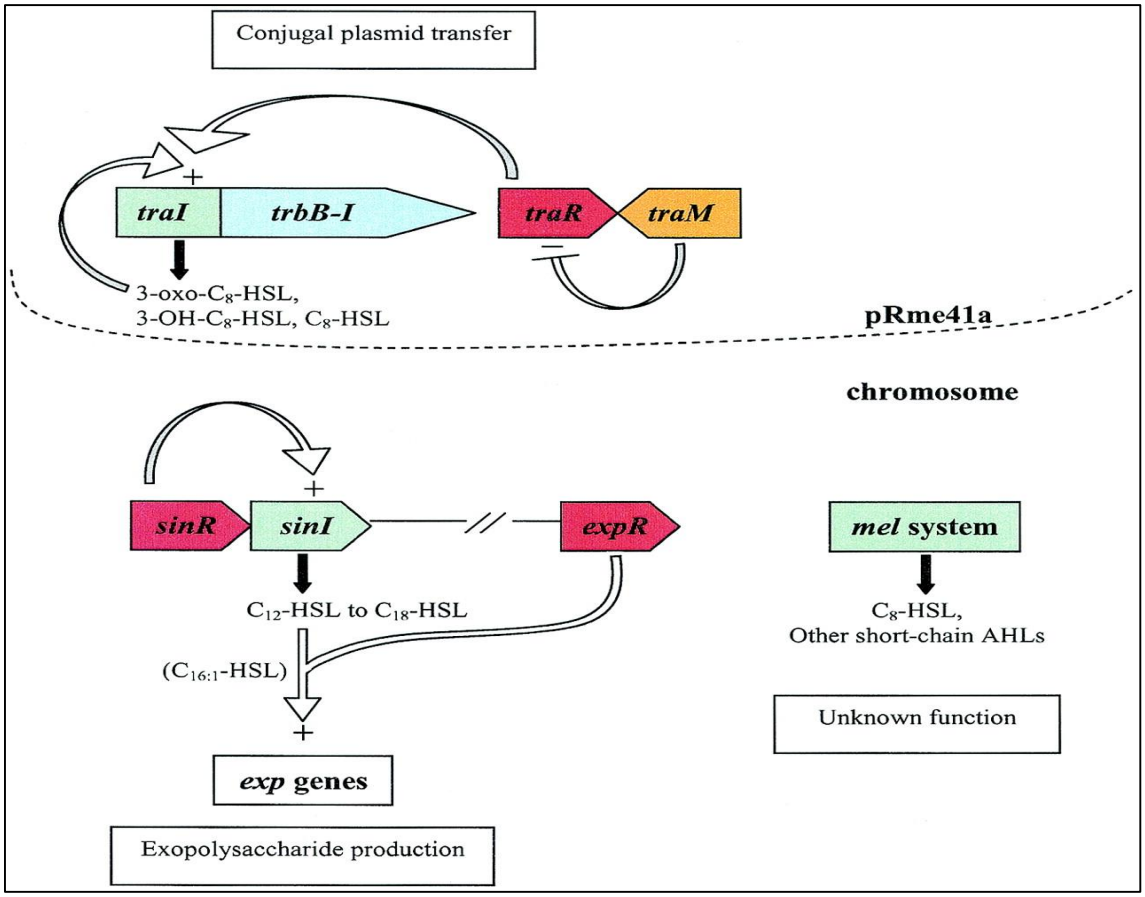

Fig 1.2: *S. meliloti* quorum-sensing systems. The *sinRI* system and the *mel* system are on the chromosome, while the *tra* system is encoded from the pRme41 plasmid. The role of *sinRI* system in regulating processes like exopolysaccharide production and motility and chemotaxis is well documented. The function of the *tra* and the *mel* systems are yet unknown (13). (Used with permission from RightsLink in 2015)

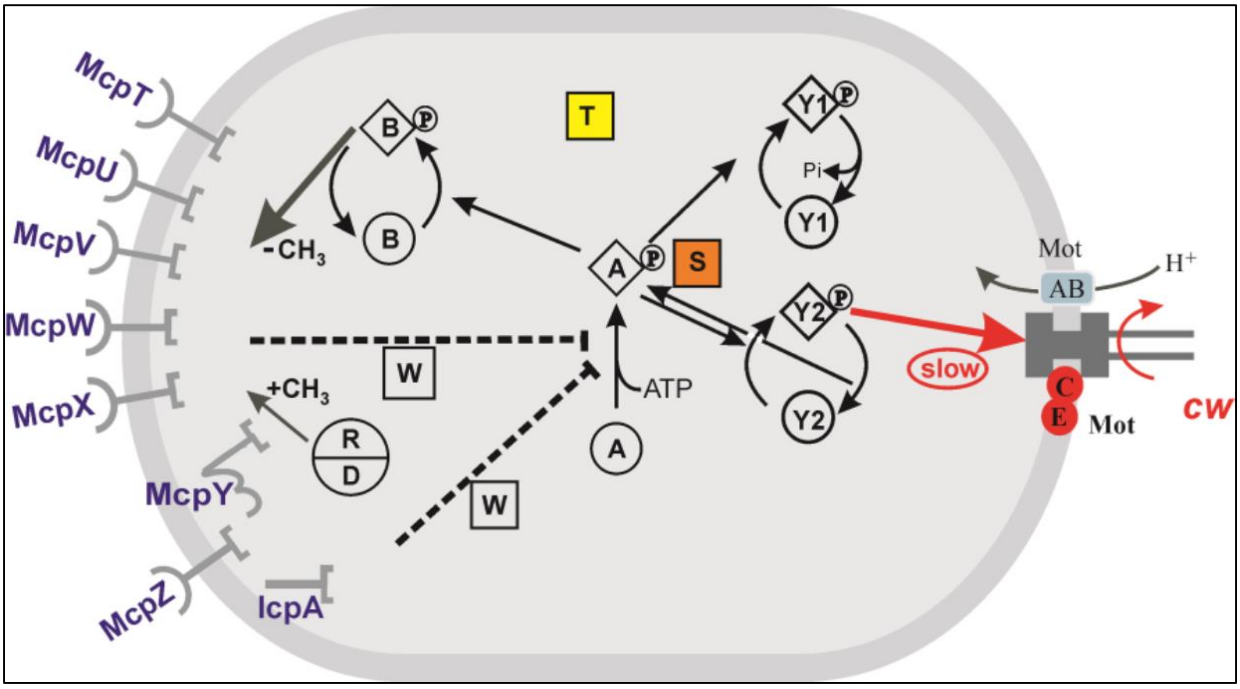

Fig 1.3: Chemotaxis pathway in *S. meliloti*. Molecular mechanism of the signal transduction pathway involved in chemotaxis in *S. meliloti*. The three primary components of the chemotaxis pathway are the chemoreceptors, the two-component system involving CheA and CheY2, and the flagellar motor complex (for details see the text). (B. Scharf, Modified from (62))

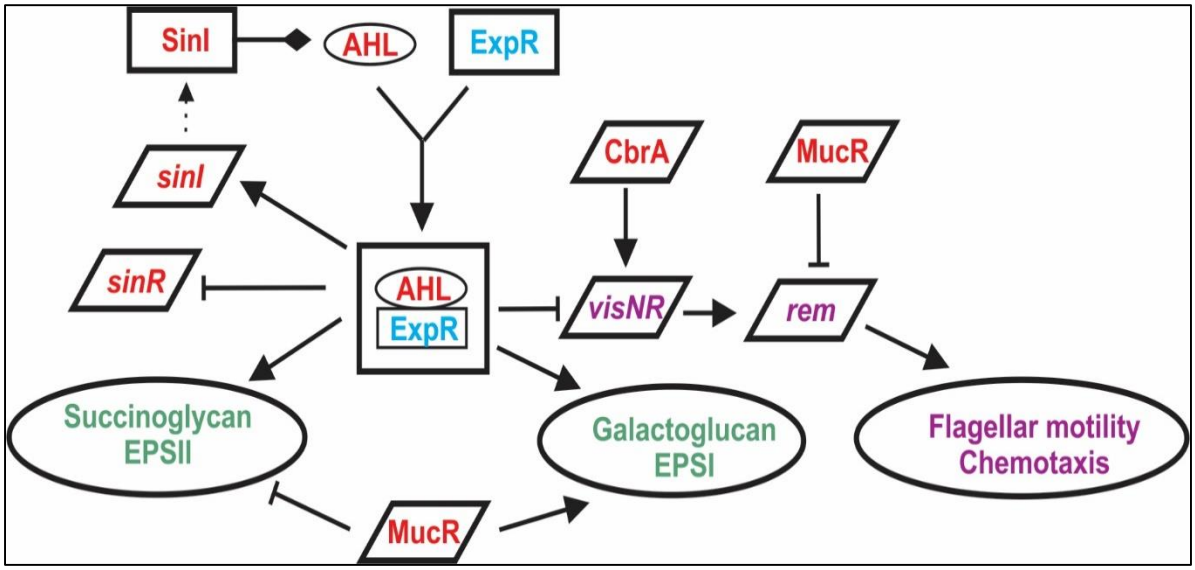

Fig 1.4: ExpR-mediated crossregulation in *S. meliloti*. AHL-activated ExpR regulates various physiological processes in *S. meliloti* like *sinRI* quorum sensing system, exopolysaccharide production, and motility and chemotaxis. Another regulator MucR regulates both EPS I and EPS II synthesis and also directly regulates motility and chemotaxis via repression of Rem. CbrA is an additional regulator of motility and chemotaxis. (Modified from (97)).

Chapter 2 - ExpR coordinates the expression of symbiotically important, bundle-forming Flp pili with quorum sensing in *Sinorhizobium meliloti*

HARDIK M. ZATAKIA, CASSANDRA E. NELSON, UMAIR J. SYED, AND BIRGIT E. SCHARF*

Department of Biological Sciences, Virginia Tech, Life Sciences I, Blacksburg, VA 24061

Running title: ExpR regulates Flp pili expression is *S. meliloti*

Key words: exopolysaccharides, nodulation, quorum sensing, rhizosphere, type IVb pili

* For correspondence:
E-mail bscharf@vt.edu
Tel: (+1) 540 231 0757
Fax: (+1) 540 231 4043
Biological Sciences, Life Sciences I
Virginia Tech
Blacksburg, VA 24061, USA

Present address: Cassandra E. Nelson, Department of Biological Sciences, University of Maryland, Baltimore, MD 21250.

Appl. Environ. Microbiol. AEM.04088-13; Accepted manuscript posted online 7 February 2014, doi:10.1128/AEM.04088-13

Attribution: HMZ has generated the data shown here in Fig. 2.1 - Fig. 2.6. UJS helped in generation of data shown in Fig. 2.2, while CEN helped in data shown in Fig 2.3. HMZ and BES drafted the final manuscript.

ABSTRACT

Type IVb pili in enteropathogenic bacteria function as a host-colonization factor by mediating tight adherence to host cells, but their role in bacteria-plant symbiosis is currently unknown. The genome of the symbiotic soil bacterium *Sinorhizobium meliloti* contains two clusters encoding proteins for Type IVb pili of the Flp (fimbrial low-molecular-weight protein) subfamily. To establish the role of Flp pili in the symbiotic interaction of *S. meliloti* and its host *Medicago sativa*, we deleted *pilA1* that encodes the putative pilin subunit in the chromosomal *flp-1* cluster and conducted competitive nodulation assays. The *pilA1* deletion strain formed 27% fewer nodules than wild type. Transmission electron microscopy revealed the presence of bundle-forming pili protruding from the polar and lateral region of *S. meliloti* wild-type cells. The putative pilus assembly ATPase, CpaE1, fused to mCherry showed a predominantly unilateral localization. Transcriptional reporter gene assays demonstrated that expression of *pilA1* peaks in early stationary phase and is repressed by the quorum sensing regulator ExpR, which also controls production of exopolysaccharides and motility. Binding of acyl homoserine lactone-activated ExpR to the *pilA1* promoter was confirmed with electrophoretic mobility shift assays. A 17-bp consensus sequence for ExpR binding was identified within the 28-bp protected region by DNase I detected by footprinting analyses. Our results show that Flp pili are important for efficient symbiosis of *S. meliloti* with its plant host. The temporal inverse regulation of exopolysaccharides and pili by ExpR enables *S. meliloti* to achieve a coordinated expression of cellular processes during early stages of host interaction.

INTRODUCTION

Nitrogen is one of the essential elements for biotic growth. Despite high concentrations of nitrogen in the atmosphere, most living cells cannot utilize it directly. Thus, it is important that nitrogen is converted into its readily assimilated forms. Several bacterial species can fix atmospheric nitrogen either in a free living state or through symbioses with plants. Legumes such as soybeans, peas, and alfalfa establish symbiotic relationships with soil bacteria from the Rhizobiaceae family resulting in the fixation of atmospheric nitrogen into ammonia (1, 2). The association between *Sinorhizobium meliloti* and its host plant *Medicago sativa* (alfalfa) is a widely used model to study nitrogen-fixing plant-microbe interaction (3). The coordination of events, namely bacterial chemotaxis towards the rhizosphere, exchange of bacterial and plant signaling molecules, bacterial exopolysaccharide (EPS) production, and lowering of plant defenses, is essential for establishing a successful symbiotic relationship (4-7). Plant roots release flavonoids into the soil, which results in rhizobial production of a class of lipochitooligosaccharides called Nod factors. These factors cause root hair curling, which entraps bacterial cells towards the plant roots (3, 8). The bacteria then induce the development of a plant-derived infection thread, leading to their deposition into plant cells and ultimately nodule formation. In the developing nodules, bacteria undergo metamorphosis into bacteroids that fix atmospheric nitrogen (3, 4, 8). Thus, the ability of rhizobia to attach to host plant roots is a crucial step in mediating specificity and initializing symbiosis (9, 10). In addition to Nod factors, further classes of bacterial components involved in host attachment include a Ca^{2+}-binding protein called rhicadhesin and bacterial surface polysaccharides (10).

Other cell surface components that have been previously implicated in the attachment to biotic and abiotic surfaces in various bacterial species are Type IV pili (Tfp). Tfp are one of the most widely found bacterial extracellular appendages (11, 12). Structurally, they are hair-like filaments, several

micrometers in length, and composed of thousands of protein subunits called pilin (12). Tfp are well-known for facilitating twitching motility in the model opportunistic pathogen *Pseudomonas aeruginosa* (13). In host-microbe interactions, Tfp mediate biofilm formation in *P. aeruginosa* (14, 15) and host colonization in the human pathogen *Moraxella catarrhalis* (16). Moreover, the importance of Tfp in plant-pathogen interactions is demonstrated in *Xylella fastidiosa* where they help in the spread of the pathogen through grape vines (17). They also act as a virulence factor for *P. syringae* in tobacco and *Ralstonia solanacearum* in potato plants (18, 19). Despite the presence of Tfp genes in rhizobia, their role in bacteria-plant symbiosis is currently unknown.

Tfp are further classified into two subcategories, namely Type IVa (Tfpa) and Type IVb (Tfpb), based on the length of the leader sequence of prepilin, length of the mature pilin, and identity of the N-terminal residue of the mature pilin (20). While genes encoding the Tfpa synthesis apparatus are typically scattered throughout the bacterial genome, Tfpb genes are mostly organized in contiguous clusters, which are usually operons (21). The *S. meliloti* genome is lacking Tfpa genes, but contains two gene clusters coding for Tfpb: *flp-1* which is located on the chromosome and *flp-2* on the pSymA megaplasmid. Tfpb were first described in enteropathogenic *Escherichia coli* as bundle forming pili (Bfp; (22)) and in *Vibrio cholera* as toxin-coregulated pili (Tcp;(20)). Tfpb are considered to have no role in bacterial motility with the exception of the longus pilus in enterotoxigenic *E. coli* (23). The two *S. meliloti* Tfpb gene clusters are similar to the *tad* (tight adherence) loci found in *Aggregatibacter* sp. and *Caulobacter crescentus*. (24). The *flp-1* locus is flanked by insertion sequences immediately upstream and downstream suggesting that the entire locus was acquired in a single horizontal gene transfer event, whereas *flp-2* presumably resulted from a gene duplication event after the transfer of the *flp-1* locus (24, 25). Each *S. meliloti flp* region contains a putative pilin encoding gene, namely *pilA1* and *pilA2*. Bioinformatics analyses

of their gene products have revealed that *pilA1* and *pilA2* belong to the Flp (fimbrial low-molecular-weight protein) subfamily of Tfpb, which was first described in *A. actinomycetemcomitans* (26, 27). Members of the Flp family have a wide range of functions (21). *A. actinomycetemcomitans* Flp pili mediate non-specific adhesion leading to host colonization and pathogenesis (27). In contrast, *Yersinia enterocolitica* Flp pili do not affect attachment to any biotic or abiotic surface, but instead have a role in microcolony formation (28).

In this study, we established that Flp pili encoded from *flp-1* form unilateral and polar bundles. *S. meliloti* Flp pili are required for competitive symbiosis of *S. meliloti* with the host *Medicago sativa*. Furthermore, we show that *pilA1* expression is under direct control of ExpR, the master transcriptional regulator of EPS synthesis. The activity of ExpR is regulated by the binding of acyl homoserine lactones (AHLs), which are produced by the autoinducer synthase SinI (29-31). Activated ExpR regulates various quorum-sensing gene targets, including EPS production and flagellar motility in *S. meliloti* (29, 32-37). In summary, our studies demonstrate that expression of symbiotically active Tfpb is integrated into the regulatory network of quorum sensing in *S. meliloti*.

MATERIALS AND METHODS

Bacterial strains and plasmids

Derivatives of *E. coli* K-12 and *S. meliloti* Sm1021 and Sm8530 and the plasmids used are listed in Table 2.1.

Media and growth conditions

Alfalfa (*Medicago sativa*, cultivar Iroquois and cultivar 'Guardsman II', developed from cultivar Iroquois (38)) for nodulation assays were grown in hydroponic (HP) medium without nitrogen source (50 mM KH_2PO_4, 25 mM K_2HPO_4, 100 mM K_2SO_4, 100 mM $MgSO_4$, 0.88 mM $CaSO_4$, 0.13 mM EDTA-Fe[III], 0.5 mM $NaMoO_4$, 46 mM H_3BO_3, 0.8 mM $CuSO_4$, 1.9 mM $ZnSO_4$, 1.8 mM $MnSO_4$ [pH 7.5, adjusted with KOH]) (39, 40). *S. meliloti* strains for nodulation assays were grown in TYC (0.5% tryptone, 0.3% yeast extract, 0.13% $CaCl_2$ x $6H_2O$ [pH 7.0]) at 30°C (41). *S. meliloti* strains for β-galactosidase, sliding, and twitching motility assays were grown in *Sinorhizobium* motility medium (SMM; RB [6.1 mM K_2HPO_4, 3.9 mM KH_2PO_4, 1 mM $MgSO_4$, 1 mM $(NH_4)_2SO_4$, 0.1 mM $CaCl_2$, 0.1 mM NaCl, 0.01 mM Na_2MoO_4, 0.001 mM $FeSO_4$, 2 µg/l biotin], 0.2 % mannitol, 2 % TY) (42, 43) at 30°C. *E. coli* for expression of ExpR was grown in lysogeny broth (LB) (44) at 37°C. The following antibiotics were used in their final concentrations: for *E. coli*, ampicillin at 100 µg/ml, kanamycin at 50 µg/ml; for *S. meliloti* grown in TYC, neomycin at 40 µg/ml, streptomycin at 600 µg/ml, and tetracycline at 10 µg/ml, for *S. meliloti* grown in SMM, streptomycin was omitted and tetracycline was used at 2.5 µg/ml.

Genetic manipulations and DNA methods

Promoter regions and genes were amplified according to standard PCR protocols using genomic

or plasmid DNA as template. The promoter-less plasmid pPHU234 (45) was utilized to make the *pilA1* promoter region-*lacZ* translational fusion, pBBR1MCS-2 (46) for *pilA1* complementation, pBBR1MCS-2 containing $lacI^q$ (pBS189) for CpaE1 localization, and pQE30 for ExpR expression and purification. Broad-host range plasmids were used to transform *E. coli* S17-1 and then transferred conjugally to *S. meliloti* by streptomycin-tetracycline or streptomycin-neomycin double selection (47). In-frame deletion constructs of *pilA1* (using oligonucleotides M409: ATAGTCATGAAGACCATTCCGAACGCCCCGTAACGG, M410: CCGTTACGGGGCGTTCGGAATGGTCTTCATGACTAT, M411: GTGTTCGAATTCGCCAGAAGTGCAGTG, and M412: GTGTTCAAGCTTGCCGCGAATAGGGCG) and *sinI* (using oligonucleotides M405: ATGATCAGGATAGTGAACCGCAGCGTAGGCATCTGA, M406: TCAGATGCCTACGCTGCGGTTCACTATCCTGATCAT, M407: GTGTTCGAATTCTCGGCATATCCGAGC, and M408: GTGTTCAAGCTTCCGTCGCGAGCACAT) were generated *in vitro* by overlap extension PCR as described by Higuchi (48). Constructs containing the mutations were cloned into the mobilizable suicide vector pK18*mobsacB*, used to transform *E. coli* S17-1, and conjugally transferred to *S. meliloti* by filter mating according to the method of Simon *et al.* (49). Allelic replacement was achieved by sequential selections on neomycin and 10% sucrose as described previously (50). Confirmation of allelic replacement and elimination of the vector was obtained by gene-specific primer PCR, DNA-sequencing, and Southern blotting.

Competitive nodulation assays

Alfalfa seeds were surface sterilized with 2.5% $HgCl_2$ and placed on sterile filter paper discs in

Petri dishes with 4 ml sterile water for 2 days at 30°C for germination. Individual germinated seeds were placed on filter paper strips (12 x 2 cm^2) in 50 ml glass tubes (with two thirds of bottom wrapped in aluminum foil) containing 10 ml of HP medium and kept in dark at room temperature for 3 days. Plants were grown in a plant growth chamber (Conviron Adaptis A1000, Canada) with 16 hours day (light) cycle at 24°C with 50% humidity and 8 hours night (dark) cycle at 16-18°C with 50% humidity. After about 2 weeks of growth, when plant roots reached into the medium, they were co-inoculated with equal amounts of competing *S. meliloti* strains (Wt/pGUS3 versus test strain). For each experiment, *S. meliloti* cultures were grown to an optical density (OD_{600}) between 0.5 and 0.8 with the individual OD_{600} being ± 0.02 of each other. To correlate OD_{600} with cell numbers, colony-forming units for each culture were determined by plating serial dilutions on TYC selection plates. Next, 0.2 ml of each strain was mixed with 19.6 ml of sterile H_2O, and 1 ml of this mixture was added to each plant tube. After 2 weeks of inoculation, plants roots were harvested, washed three times with sterile water, and incubated with 50 mM 5-bromo-4-chloro-3 indolyl-β-d-glucuronide (X-Gluc), 1% sodium dodecyl sulfate (SDS), 100 mM NaP_i [pH 7] at 37°C overnight (51). The number of blue and white nodules per plant were counted and the nodulation efficiency for each test strain was calculated as follows: [(*n*/*N*)*100]*2 where *n*, number of white nodules of test strain in a plant and *N*, total (blue and white) number of nodules on the same plant (39). The factor 2 was included for better representation of data. Data were analyzed for statistically significant differences using a one-way analysis of variance (ANOVA). A post hoc Tukey's test was applied for pairwise comparisons.

Motility assays

For motility assays, stationary phase cultures of *S. meliloti* were diluted to an OD_{600} of 0.02 in

SMM medium. To observe sliding motility, 2 µl of diluted cultures were spotted on SMM plates containing 0.6% agar, and plates were analyzed after 48-hour incubation in a humidity chamber at 30°C (52). For twitching motility assays, diluted cultures were inoculated on SMM plates containing 1.0% or 1.5% agar between the bottom layer of the agar and the plastic surface using a sterile toothpick. Plates were analyzed for twitching motility after 48 hours of incubation in a humidity chamber at 30°C (11, 13).

β-galactosidase assays

Stationary phase cultures of *S. meliloti* containing *lacZ* fusion plasmids were diluted to an OD_{600} of 0.02 in SMM medium and incubated at 30 ºC for 48 hours. Samples were taken every 2 hours, diluted 1:4 in Z buffer (53), permeabilized with 30 µL of 0.1% SDS and chloroform, and assayed for β-galactosidase activity by the method of Miller (1972) as previously described (43, 54).

Purification of His_6-ExpR

ExpR was purified essentially using the method described by Bartels *et al.* (55) with some modifications. Briefly, His_6-ExpR was overproduced from plasmid pBS1077 in *E. coli* M15/pREP4 (Table 2.1). Cells were grown in 1 L of LB containing 100 µg/ml ampicillin and 25 µg/ml kanamycin to an OD_{600} of 0.6-0.8, gene expression was induced with 0.02 mM isopropyl-β-D-thiogalactopyranoside (IPTG), and cultivation continued overnight at 25°C. Cells were harvested by centrifugation at 11,900 × *g* and suspended in 20 ml lysis buffer containing 20 mM imidazole, 0.5 M NaCl, 50 mM Tris [pH 8.0], 0.5% Triton-X 100, supplemented with 0.02 mM phenylmethanesulfonyl fluoride (PMSF), and 0.1 µg/ml DNase I (Roche, Indianapolis, IN). Cells were lysed by three passages through a French pressure cell at 16,000 psi (SLM Aminco, Silver

Spring, MD) and the soluble fraction was loaded onto a 5 ml HiTrap Chelating HP column (GE Healthcare Life Sciences, Pittsburgh, PA). The column was washed with 30 ml lysis buffer followed by 50 ml of 20 mM imidazole, 0.5 M NaCl, 50 mM Tris [pH 8.0]. His_6-ExpR was eluted with a 75-ml linear gradient of 0.02 M imidazole, 0.5 M NaCl, 50 mM Tris [pH 8.0] to 1 M imidazole, 0.5 M NaCl, 50 mM Tris [pH 8.0]. His_6-ExpR containing fractions were combined, protein concentration determined using the Bradford assay (Bio-Rad Laboratories, Hercules, CA), and stored at 4°C.

Electrophoretic mobility shift assay

Electrophoretic mobility shift assays were conducted as described by Bartels et al. (2007) (55) with the following modifications. 0.7 pmol of DNA PCR fragments (273-bp P*visN*, 254-bp P*pilA1*, and 327-bp P*fliF*, the latter included 122-bp flanking sequences derived from the pUCBM20 vector) were mixed with 15 pmol His_6-ExpR in an EMSA buffer (20 mM Tris-HCl [pH 8.0], 50 mM KCl) at a final volume of 20 µl. *N*-(3-Oxotetradecanoyl)-L-homoserine lactone (3-oxo-C_{14}-HSL; Sigma-Aldrich, St. Louis, MO), dissolved in 0.01 % acidified ethyl acetate, was added to a final concentration of 10 µM, and reactions were incubated at 24°C for 20 min. Reactions were stopped by addition of loading dye (50% glycerol, 10 mM EDTA, 0.2% bromophenol blue, 0.2% xylene cyanol, 40 mM Tris, 20 mM glacial acetic acid), and separated by electrophoresis in a 1.5% agarose gel at 8.5 V/cm for 1 h at 4°C. The gel was stained with SYBR® Green I nucleic acid gel stain (Invitrogen, Grand Island, NY) for 40 min and imaged using a Typhoon Trio Variable Mode Imager (GE Healthcare Life Sciences, Pittsburgh, PA).

DNase I footprinting analysis

DNase I footprinting analysis was carried out based on the method published by Zianni *et al.* (56).

Labeled *pilA1* promoter fragments were generated using standard PCR with a 5'-(6-FAM) labeled forward primer. Next, 373 μM of labeled probe and 373 nM of His_6-ExpR and 10 μM of 3-oxo-C_{14}-HSL were mixed in DNase I footprinting buffer (50 mM KCl, 5 mM $MgCl_2$, 2 mM $CaCl_2$, 20mM Tris-HCl [pH 8.0]) and incubated at 24°C for 20 min. Reactions were incubated for 60 sec in the presence of 0.025 μg/μl of DNase I and stopped by the addition of 5 μl of 1% SDS, 200 mM NaCl, 20 mM EDTA. DNA was purified using Wizard® SV Gel and PCR Clean-Up system (Promega, Madison, WI) and fragment analysis was performed with Genescan™-500 LIZ® on an Applied Biosystems 3130 (Applied Biosystems, Grand Island, NY) at the Virginia Bioinformatics Institute (Blacksburg, VA). To determine the sequence of the ExpR-binding region, sequencing reactions using non-labeled oligonucleotides and Thermo Sequenase Dye Primer Manual Cycle Sequencing Kit (Affymetrix, Santa Clara, CA) were used according to the manufacturer's instructions.

Transmission electron microscopy

Stationary phase cultures of *S. meliloti* Sm1021 WT and Sm1021 Δ*pilA1* were diluted to an OD_{600} of 0.02 in SMM medium, and incubated under shaking conditions at 75 rpm at 30°C for 40 hours to an OD_{600} of 0.5-0.6. Cells were diluted 1:4 in sterile water and 4 μl of this sample were placed on carbon-coated formvar copper or gold grids and allowed to air dry for 5 min. The grids were then stained with 1% uranyl acetate or 0.5% phosphotungstic acid (pH 7.2) for 30 sec and excess stain was removed. Grids were visualized using a JEOL JEM 1400 with an 80kV beam. Images were captured using the Orius Gatan charge-coupled device (CCD) camera.

Fluorescence microscopy

Stationary phase cultures of *S. meliloti* containing derivatives of pBBR1MCS-2 (Table 2.1) were diluted to an OD_{600} of 0.02 in TYC with the addition of appropriate antibiotics and 50 - 200 µM IPTG, and grown at 30°C for 14 to 16 hours to an OD_{600} of 0.5. Cells were immobilized on a slide coated with 1% (w/v) poly-L-lysine solution (Sigma Aldrich, St. Louis, MO). A coverslip was placed on top of the culture droplet and the edges were sealed with acrylic polymer to prevent drying. Images were taken with an Olympus 1X71/1X51 inverted research fluorescent microscope, using a 100x NA 1.4UPIanSApo objective lens equipped with a CCD camera (Photometrics CoolSNAP HQ2CCD) and analyzed using SoftWorx software (Applied Precision). Fluorescence signals (excitation 580 nm) were detected using mCherry filter (630 nm).

RESULTS

Flp pili in *S. meliloti* form polar and lateral bundles

One of the two *flp* gene clusters present in the *S. meliloti* genome is located on the chromosome (*flp-1*) and flanked on each site by an insertion sequence, ISRm22. Utilizing Pfam (protein families database of alignments, (57)), the ten open reading frames (ORFs) in this locus are predicted to encode one pilin subunit protein (PilA1) and nine Flp pilus assembly proteins similar to the bacterial type II secretion system (Smc04115, CpaA1, CpaB1, CpaC1, CpaD1, CpaE1, CpaF1, Smc02821, and Smc02822). In addition, two ORFs (Smc04117, Smc04118) upstream of ISRm22 and one ORF (Smc02824) downstream of the other ISRm22 encode putative pilus assembly proteins.

To assess localization and function of Flp pili in *S. meliloti* strain Sm1021, we used allelic replacement to generate an unmarked in-frame deletion in the *pilA1* gene, which is predicted to encode the precursor of the major structural component of Flp pili. The resulting strain Sm1021Δ*pilA1* (Table 2.1) and its parental strain were examined for the presence of Flp pili by transmission electron microscopy (TEM). Due to the fragile nature of the pili structures, standard washing procedures prior to staining were omitted, leading to micrographs with a higher content of debris. Negative staining of *S. meliloti* wild-type cells revealed the presence of two types of cell surface appendages, flagella and pili (Fig. 2.1A-C). Most cells (> 75%) exhibited a single bundle of several pilus filaments. These bundled pili were usually polar or sub-polar in location. Occasionally, cells with two or three lateral bundles were observed, which characteristically originated on one side of the cell (Fig. 2.1C). In contrast, pili-like filaments were mostly absent in Sm1021Δ*pilA1* cells (Fig. 2.1D). It should be mentioned, however, that a small percentage of cells (< 2%) displayed isolated, mostly detached pili-like structures (data not shown). We also analyzed

negatively stained cells of Sm1021Δ*pilA1* complemented with the broad-host range plasmid pBS396, expressing the *pilA1* gene *in trans*. Complementation restored the wild-type phenotype, although pili bundles appeared to be fragile and less abundant (data not shown). In conclusion, *S. meliloti* forms polar and unilateral bundles of Flp pili using PilA1 as major pilin subunit.

The putative Flp pilus assembly ATPase, CpaE1, exhibits lateral localization

The assembly and function of Tfp depends on a macromolecular secretion machinery extending from the cytosol to the outer membrane. To assess the localization of the Flp pili assembly apparatus in *S. meliloti*, we fluorescently labeled two predicted cytosolic proteins, CpaE1 and CpaF1, using C-terminal mCherry fusions. CpaE1 contains an AAA domain (ATPase associated with diverse cellular activities; (58, 59)), while CpaF1 is a VirB11-like ATPase (60). We expressed both ATPase-mCherry fusions and an mCherry control from an IPTG-inducible plasmid (pBBR1MCS-2, Table 2.1) in wild-type strain Sm1021. We observed clear fluorescent signals from CpaE1-mCherry and mCherry in the presence of 50 and 200 μM IPTG. The expression of CpaF1-mCherry did not result in any detectable fluorescence, presumably due to incorrectly folded fusion protein. As anticipated, mCherry displayed a uniform distribution throughout the cell (Fig. 2.2A). In contrast, CpaE1-mCherry localized laterally by forming filament-like structures along one side in more than 60% and in the polar region in approximately 15% of the cells (Fig. 2.2B). The asymmetric localization of CpaE1 is in accordance with the TEM data where several pili bundles were observed on one side and at the pole of the cell. Taken together, the microscopic data suggest that bundle-forming Flp pili and the pili assembly machinery in *S. meliloti* are predominantly localized on one side of the cell.

S. meliloti requires Flp pili for efficient nodulation of the alfalfa host

Based on the function of related Flp pili in the virulence of the plant-pathogenic bacterium *R. solanacearum* (19), we hypothesized that *S. meliloti* Flp pili are important for host-microbe interaction and therefore symbiosis. *S. meliloti* wild type and Sm1021Δ*pilA1* strain were used in competitive nodulation assays with the alfalfa host. In this assay, alfalfa plants are co-inoculated with two bacterial strains in a 1:1 ratio and nodule occupancy is determined after 2 weeks of growth. Using the reporter gene plasmid pGUS3 (Table 2.1), nodules occupied by Sm1021 bearing pGUS3 would stain blue when exposed to the cleavable substrate X-Gluc, while those occupied by the test strain remain unstained (white) (39). A competition between Sm1021 and Sm1021/pGUS3 was carried out to confirm that the pGUS3 plasmid was being maintained in *S. meliloti* during the assay and that its presence does not impede nodulation. Ideally, this competition should yield a 1:1 ratio of nodules occupied by Sm1021 (white) and Sm1021/pGUS3 (blue), equaling 100% nodulation efficiency. In our analyses, Sm1021 displayed a nodulation efficiency of 85±14%. The competition experiment between Sm1021Δ*pilA1* and Sm1021/pGUS3 revealed that nodule occupancy of the deletion strain was 63±14%, which was a significant reduction compared to the wild type (27%; $p < 0.05$; Fig. 2.3). For comparison, we analyzed the competitive ability of a strain deficient in the *sinR*/*sinI* quorum sensing system, which plays an important role in establishing symbiosis (31, 61). The Sm1021Δ*sinI* mutant strain is unable to produce autoinducer signal molecules (*N*-acyl homoserine lactones, AHLs), which impairs the quorum sensing system. Thus, this strain is deficient in its ability to invade the host. Sm1021Δ*sinI* exhibited similar impairment in the competitive nodulation assay as Sm1021Δ*pilA1* (Fig. 2.3). To confirm that the reduction in nodulation efficiency of the *pilA1* deletion strain is solely caused by the targeted gene deletion, we analyzed the nodulation efficiency of a complementation strain

Sm1021Δ*pilA1*/pBS396 and compared it to wild type Sm1021. The complementation strain yielded a nodulation efficiency of 103±18%, and therefore not only regained nodulation ability but exceeded efficiency compared to wild type. In conclusion, Flp pili play an important role in efficient symbiosis of *S. meliloti* with its alfalfa host.

To assess the possible role of Flp pili in surface motility, we analyzed twitching and sliding motility behavior of *S. meliloti* wild-type and *pilA1* deletion strain. Twitching motility is typically mediated by Tfpa and is displayed at the edge of bacterial colonies through the presence of individual rafts of cells with jagged edges when cells migrate over the agar surface (11, 13). When bacterial colonies of strain Sm1021 and Sm1021Δ*pilA1* grown between SMM agar (1.0 or 1.5%) and the polystyrene surface of the petri dish were compared under a light microscope, colony edges of both strains appeared smooth and a characteristic twitch zone was absent, indicating a lack of twitching motility. *S. meliloti* can move over semisolid surfaces by two different types of motility, flagellum-mediated swarming, and EPS- mediated sliding (52, 62, 63). To evaluate the role of Flp pili in surface spreading, the expansion of *S. meliloti* Sm1021 and Sm1021Δ*pilA1* colonies on the surface of semisolid SMM agar (0.6%) was analyzed. Both strains were indistinguishable in their colony morphology, suggesting that Flp pili do not contribute to translocation on semisolid surfaces (data not shown).

Flp pili transcription is repressed by ExpR

To determine Flp pili expression during culture growth, we used plasmid-borne transcriptional *lacZ* fusions of the 254-bp upstream region of *pilA1* (pBS326, Table 2.1). Expression of *pilA1* in strain Sm1021 increased during exponential growth (at 16–24 h), peaked in early stationary growth (at 24–36 h), and then slowly tapered off to about half of the maximum level (Fig. 2.4A). *S. meliloti*

strain Sm1021 lacks an intact quorum-sensing system because of an insertion in the ExpR-encoding gene (37, 64). In contrast to Sm1021, *S. meliloti* strain Sm8530 is capable of quorum sensing because of a spontaneous excision of the native insertion sequence in the *expR* gene (37). Thus, we examined the expression of *pilA1* in strain Sm8530. While promoter activity was half of that in Sm1021, a similar expression profile with peak expression during early stationary growth was observed (Fig. 2.4A). The data indicate that *pilA1* expression is regulated by ExpR. To conclusively prove the regulatory role of ExpR in *pilA1* expression, we analyzed *pilA1* promoter activity in strain Sm1021 ExpR$^+$, which carries a restored copy of the *expR* gene (Table 2.1). We found that the activity of the *pilA1* promoter reduced to basal levels (Fig. 2.4B). However, this activity was 5 times higher than the background activity observed in a strain carrying a promoter plasmid (data not shown). Therefore, the presence of a functional copy of *expR* represses *pilA1* transcription. It should be mentioned that the expression profiles of *pilA1* in the two strains with the restored *expR* locus, Sm8530 (spontaneous excision) and Sm1021 ExpR$^+$ (genetic manipulation), vary slightly for reasons that are not well understood. Lastly, in the absence of activating AHL, due to a deleted *sinI* gene, *pilA1* activity in the resulting strain Sm1021ExpR$^+$Δ*sinI* (Table 2.1) was restored to the levels observed in strain Sm1021 (Fig. 2.4B). Thus, AHL-activated ExpR represses transcription of *pilA1*, and therefore, the expression of Flp pili.

AHL-activated ExpR binds to the *pilA1* promoter region

Transcriptional analyses indicate that ExpR controls the expression of Flp pili in *S. meliloti*. To determine whether ExpR-based repression is direct or indirect, we examined the binding of purified His$_6$-ExpR to the 254-bp promoter region of *pilA1* using an electrophoretic mobility shift

assay (55). As a positive control, we used the promoter region of the *visN-visR* operon, which has been previously identified as the direct target of AHL-activated ExpR (29, 33, 36). VisN and VisR are class IA regulators of the hierarchy cascade of the *S. meliloti* flagellar regulon and activate structural class II genes via the class IB regulator Rem (43, 65). The promoter region of one of the class II genes, *fliF*, served as a negative control for the DNA-binding assay because it is not directly regulated by ExpR (43). His_6-ExpR exhibited minimal levels of binding to the promoter regions of *visN* and *pilA1* in the absence of AHL (Fig. 2.5, lanes 2 and 5). Binding was observed for the *visN* and *pilA1* promoters, as indicated by the shift in mobility (Fig. 2.5, lanes 3 and 6), in the presence of 3-oxo-C_{14}-HSL, which was previously shown to stimulate binding of ExpR to the *sinI* promoter region (55). No binding was detected in the control experiment with p*fliF* (Fig. 2.5, lanes 8 and 9). Therefore, *pilA1* is a direct target of regulation by AHL-activated ExpR.

Binding of AHL-activated ExpR protects a 28-bp region on the *pilA1* promoter

To determine the specific ExpR binding site on the *pilA1* promoter, DNase I footprinting experiments with His_6-ExpR in the presence of 3-oxo-C_{14}-HSL were performed using a 6-FAM labeled DNA-fragment (56). The results in Fig. 2.6A indicate that the ExpR-protected region is a 28-bp sequence located 74 bp upstream of the start codon of *pilA1*. The sequence of the protected region in the electropherogram was identified by dideoxynucleotide sequencing as 5'-TAGCCCCCGCTAAATTCAGGGTATCCG-3' (Fig. 2.6B). This region was aligned with four previously identified ExpR binding sites (29, 66), which are located in the promoter region of genes upregulated (*sinI* and *expR*) or downregulated (*visN* and *sinR*) by ExpR (Fig. 2.7). The *pilA1* binding region aligns well with these sequences and with the 17-bp ExpR binding consensus established from 33 experimentally validated ExpR binding sites (Fig. 2.7, (66)). The ExpR

binding sequence is distinguished by its degenerate dyad symmetry with 3–4 Cs and 3–4 Gs separated by 10–12 nucleotides rich in A and T (29, 66). All these features are well conserved for the ExpR binding site in the *pilA1* promoter. Our findings further support the regulation of *pilA1* transcription by AHL-activated ExpR and identify a region upstream of the *pilA1* gene, which is specifically involved in ExpR binding.

DISCUSSION

Type IVb pili (Tfpb) have been most intensely studied in enteropathogenic bacteria, where they generally contribute to virulence by mediating cell-cell interaction and surface attachment (21). Details about the characteristics of Tfpb in other systems, specifically plant-associated bacteria, are only slowly emerging (19). The genome of the plant-symbiont *S. meliloti* contains two gene clusters coding for Tfpb which belong to the Flp (fimbrial low-molecular-weight protein) subfamily. We describe here the characterization, function and regulation of Flp pili encoded by the *flp-1* cluster on the chromosome of *S. meliloti*.

Our studies focused on the *pilA1* gene that encodes the putative pilin protein, an abundant structural subunit of the Flp pilus filament. Transmission electron microscopy revealed the presence of bundle-forming pili in strain Sm1021 and their absence in Sm1021Δ*pilA1* (Fig. 2.1). Although isolated pili filaments were observed in a very small percentage of *pilA1* deletion cells, the origin of these rare pili-like structures remains elusive at this point. The phenotype might be attributed to the expression of Flp pili from the *flp-2* locus and/or incorporation of an alternate pilin subunit encoded by Smc02446. This orphan chromosomal gene is assigned as putative fimbriae associated protein (Flp/Fab pilin component) and exhibits 60% identity to PilA1. Interestingly, wild-type cells occasionally had two or three Flp pili bundles emanating from one side of the cell. The lateral localization of Flp pili was corroborated by the filament-like, unilateral presence of CpaE1-mCherry in *S. meliloti* cells (Fig. 2.2B). CpaE1 is a TadZ-like protein, which is a member of the ParA/MinD superfamily (67, 68). In *A. actinomycetemcomitans*, TadZ localizes to the cell pole independent of any other *tad* locus proteins. It has been suggested that TadZ mediates polar localization of the Tad secretion apparatus (67). We hypothesize that CpaE1 has a similar function in positioning the Flp pilus machinery to one site of the *S. meliloti* cell. It remains to be seen,

whether CpaE1 itself forms an cytoskeletal filament such as ParA (69), or whether it binds to an intermediate filament like the one formed by crescentin which localizes to the inner cell curvature in *Caulobacter crescentus* (70).

In the *S. meliloti* Flp system, we observed that host plant nodulation was significantly impaired in the *pilA1* deletion strain (Fig. 2.3). We hypothesize that Flp pili confer a symbiotic advantage to *S. meliloti* by enhancing attachment to plant roots. Bacterial cell attachment is a prerequisite for successful nodulation and this interaction could be mediated by Flp pili in *S. meliloti*. It is an attractive assumption that the arrangement of several pili bundles on one side of the bacterial surface maximizes effective contact between bacteria and host cells, similar to the multiple *vir*-T4SS complexes and lateral attachment points during *A. tumefaciens* infection (71). It remains to be elucidated whether pili bind along the entire root surface or whether their binding is restricted to specialized sites, as postulated for rhicadhesin in *Rhizobium leguminosarum* (10). The reason for *S. meliloti* to possess two distinct Tfpb loci is not clear, but the maintenance of the *flp-2* locus on pSymA suggests a specific function during the free-living or symbiotic state. The role of *flp-2* in symbiosis is currently being investigated.

The regulation of Flp pili expression by ExpR and therefore by the *sinR/sinI* quorum sensing system is rather intriguing and demonstrates a remarkable coordination of cellular processes. Based on DNA microarray data in quorum sensing mutants, Hoang *et al.* (36) have suggested the regulation of *pilA1* expression by the Sin/ExpR quorum sensing system. Thus far, experimental data for direct regulation of *pilA1* expression by ExpR were lacking. Our studies not only confirm the direct binding of ExpR to the promoter region of *pilA1*, but also define the DNA sequence of the binding site. The ExpR binding site on the *pilA1* promoter exhibits a high degree of similarity to the ExpR binding consensus sequence (Figs. 2.6 and 2.7). It is known that ExpR can act as a

repressor or an activator of transcription. A recent publication by Charoenpanich *et al.* (66) suggests that the location of the ExpR binding site, with respect to the promoter and transcription start site, may determine the type of regulation exerted by ExpR. Binding within or upstream of the −35 region activates the promoter, whereas ExpR binding downstream of the −35 region represses promoter activity. A search of the *pilA1* promoter, based on the predicted and experimentally confirmed *S. meliloti* promoter characteristics (72), identified 5′-CTAAAT-3′ within the ExpR binding site as a putative −10 sequence (Fig. 2.5). In this case, ExpR binding would cover the −10 region of the *pilA1* promoter, thereby repressing its activity. Studies using modified promoter regions in the ExpR binding site would shed further light on the exact nucleotides involved in the repression of *pilA1* transcription.

Details of the transcriptional organization of the *flp-1* gene cluster are not known. We did not find evidence from *in silico* analysis for the regulation of any other gene besides *pilA1* by ExpR, which is also supported by previous microarray analyses (36). At this point, two scenarios are possible: (i) low level constitutive expression of genes encoding the remaining pilus assembly machinery as these proteins are required in much lower numbers than the pilin subunit itself (24) or (ii) the presence of a different regulatory mechanism, because Tfpb expression in other bacterial species is characteristically controlled by multiple complex systems including species-specific controls (24, 28, 73, 74).

The current study allows for the integration of Flp pili synthesis in the Sin/ExpR quorum sensing-based transcriptional regulation in *S. meliloti*. Fig. 2.8 depicts the expanded regulatory network of ExpR targets with demonstrated cellular functions. In this scheme, the ExpR-AHL complex activates the production of two extracellular polysaccharides, galactoglucan and succinoglycan, and represses flagella-driven motility, Flp pili synthesis, and the Sin quorum sensing system in *S.*

meliloti (29, 62, 66, 75). We propose an ExpR-regulated expression program, which provides a dynamic and precise transcriptional control of cellular processes important for host interaction (66). One of the first steps in host invasion is chemotaxis-driven flagellar-based motility in the rhizosphere. Once the symbiont reaches the roots of its host plant, swimming motility is no longer required, which is reflected in the repression of flagella production (65). Since gene activation via ExpR occurs at low AHL concentrations as opposed to repression, EPS synthesis is activated prior to the down-regulation of flagella (66). Both the EPS systems, galactoglucan and succinoglycan, are symbiotically important and mediate nodule invasion (3, 6, 76). Our study revealed that Flp pili are symbiotically relevant appendages and presumably function by mediating initial attachment to root hairs. We can only speculate about the integration of pili function in the early stages of host interaction. As a working model, we propose a contribution of pili in host attachment before EPS function becomes prevailing. Although repression of symbiotically important pili at high cell density might seem counterintuitive, it is important to note that basal level expression of *pilA1* still exists at that time which might be sufficient for pili production. However, additional research is needed to fully integrate the function of type IVb pili systems in symbiosis.

Our transcriptional studies demonstrated that peak expression of *pilA1* is during mid-log to early stationary phase in the absence of ExpR. Therefore, an activating mechanism in addition to the repression exerted by ExpR-AHL is responsible for this expression profile. The inverse regulation of EPS and pili guarantees the presence of one or more mechanisms that enable *S. meliloti* cells to adhere to host roots. This sophisticated control mechanism allows *S. meliloti* to achieve a cost-effective regulation of gene expression without compromising its ability to adjust to changing environments. Additional studies are required to unravel the detailed biological background of the inverse temporal regulation of EPS and pili.

In this work, the role and regulation of Tfpb in the symbiotic interaction between rhizobial bacteria and legume hosts have been analyzed. We revealed that Flp pili are important for efficient symbiosis between *S. meliloti* and its host legume alfalfa. It will be intriguing to determine their specific function during nodulation, along with the role of the second Tfpb locus present on the pSymA megaplasmid. This knowledge will shed some light on the purpose of two separate Tfpb loci in gram-negative bacteria. We also established the direct regulation of Flp pili expression through the Sin/ExpR quorum sensing system in *S. meliloti*. The temporal inverse regulation of pili and EPS synthesis is an interesting conclusion from this work and provides an attractive focal area for future studies.

ACKNOWLEDGEMENTS

This study was supported by start-up funds and seed funds from the Fralin Life Science Institute at Virginia Tech to Birgit E. Scharf. We thank Ann Hirsch for the donation of *Medicago sativa* serovar Iroquois seeds, Roger Y. Tsien for plasmid pRSET-B mCherry, and Anke Becker, María José Soto, and Ann Hirsch for *S. meliloti* strains Sm1021 ExpR$^+$, Sm1021, and Sm8530, respectively. We are indebted to the reviewers for their helpful comments, Veronika Meier for her initial analysis of the *pilA1* promoter activity, Anjali Sharma for experimental assistance with β-galactosidase assays, Revathy Ramachandran for technical advice with EMSA and footprint analyses, Kathy Lowe for technical assistance with TEM, Katherine Broadway, Kuntan Dhanoya, and Benjamin Webb for critical reading of the manuscript.

REFERENCES

1. **Gage DJ.** 2004. Infection and invasion of roots by symbiotic, nitrogen-fixing rhizobia during nodulation of temperate legumes. Microbiol Mol Biol Rev **68:**280-300.
2. **van Rhijn P, Vanderleyden J.** 1995. The *Rhizobium*-plant symbiosis. Microbiol Rev **59:**124-142.
3. **Jones KM, Kobayashi H, Davies BW, Taga ME, Walker GC.** 2007. How rhizobial symbionts invade plants: the *Sinorhizobium-Medicago* model. Nat Rev Microbiol **5:**619-633.
4. **González JE, Marketon MM.** 2003. Quorum sensing in nitrogen-fixing rhizobia. Microbiol Mol Biol Rev **67:**574-592.
5. **Jones KM.** 2012. Increased production of the exopolysaccharide succinoglycan enhances *Sinorhizobium meliloti* 1021 symbiosis with the host plant *Medicago truncatula*. J Bacteriol **194:**4322-4331.
6. **Pellock BJ, Cheng HP, Walker GC.** 2000. Alfalfa root nodule invasion efficiency is dependent on *Sinorhizobium meliloti* polysaccharides. J Bacteriol **182:**4310-4318.
7. **Yao SY, Luo L, Har KJ, Becker A, Ruberg S, Yu GQ, Zhu JB, Cheng HP.** 2004. *Sinorhizobium meliloti* ExoR and ExoS proteins regulate both succinoglycan and flagellum production. J Bacteriol **186:**6042-6049.
8. **Hirsch AM, Long SR, Bang M, Haskins N, Ausubel FM.** 1982. Structural studies of alfalfa roots infected with nodulation mutants of *Rhizobium meliloti*. J Bacteriol **151:**411-419.
9. **Wang D, Yang S, Tang F, Zhu H.** 2012. Symbiosis specificity in the legume: rhizobial mutualism. Cell Microbiol **14:**334-342.
10. **Rodríguez-Navarro DN, Dardanelli MS, Ruíz-Saínz JE.** 2007. Attachment of bacteria to the roots of higher plants. FEMS Microbiol Lett **272:**127-136.
11. **Mattick JS.** 2002. Type IV pili and twitching motility. Annu Rev Microbiol **56:**289-314.
12. **Pelicic V.** 2008. Type IV pili: *e pluribus unum*? Mol Microbiol **68:**827-837.
13. **Burrows LL.** 2012. *Pseudomonas aeruginosa* twitching motility: type IV pili in action. Annu Rev Microbiol **66:**493-520.
14. **Giltner CL, van Schaik EJ, Audette GF, Kao D, Hodges RS, Hassett DJ, Irvin RT.** 2006. The *Pseudomonas aeruginosa* type IV pilin receptor binding domain functions as an adhesin for both biotic and abiotic surfaces. Mol Microbiol **59:**1083-1096.
15. **Barken KB, Pamp SJ, Yang L, Gjermansen M, Bertrand JJ, Klausen M, Givskov M, Whitchurch CB, Engel JN, Tolker-Nielsen T.** 2008. Roles of type IV pili, flagellum-mediated motility and extracellular DNA in the formation of mature multicellular structures in *Pseudomonas aeruginosa* biofilms. Environ Microbiol **10:**2331-2343.
16. **Luke NR, Jurcisek JA, Bakaletz LO, Campagnari AA.** 2007. Contribution of *Moraxella catarrhalis* type IV pili to nasopharyngeal colonization and biofilm formation. Infect Immun **75:**5559-5564.
17. **Meng Y, Li Y, Galvani CD, Hao G, Turner JN, Burr TJ, Hoch HC.** 2005. Upstream migration of *Xylella fastidiosa* via pilus-driven twitching motility. J Bacteriol **187:**5560-5567.
18. **Nguyen LC, Taguchi F, Tran QM, Naito K, Yamamoto M, Ohnishi-Kameyama M, Ono H, Yoshida M, Chiku K, Ishii T, Inagaki Y, Toyoda K, Shiraishi T, Ichinose Y.** 2012. Type IV pilin is glycosylated in *Pseudomonas syringae* pv. tabaci 6605 and is required for surface motility and virulence. Mol Plant Pathol **13:**764-774.
19. **Wairuri CK, van der Waals JE, van Schalkwyk A, Theron J.** 2012. *Ralstonia solanacearum* needs Flp pili for virulence on potato. Mol Plant Microbe Interact **25:**546-556.
20. **Strom MS, Lory S.** 1993. Structure-function and biogenesis of the type IV pili. Annu Rev Microbiol **47:**565-596.
21. **Roux N, Spagnolo J, de Bentzmann S.** 2012. Neglected but amazingly diverse type IVb pili. Res Microbiol **163:**659-673.
22. **Donnenberg MS, Giron JA, Nataro JP, Kaper JB.** 1992. A plasmid-encoded type IV fimbrial gene of enteropathogenic *Escherichia coli* associated with localized adherence. Mol Microbiol **6:**3427-3437.
23. **Mazariego-Espinosa K, Cruz A, Ledesma MA, Ochoa SA, Xicohtencatl-Cortes J.** 2010. Longus, a type IV pilus of enterotoxigenic *Escherichia coli*, is involved in adherence to intestinal epithelial cells. J Bacteriol **192:**2791-2800.
24. **Tomich M, Planet PJ, Figurski DH.** 2007. The *tad* locus: postcards from the widespread colonization island. Nat Rev Microbiol **5:**363-375.
25. **Planet PJ, Kachlany SC, Fine DH, DeSalle R, Figurski DH.** 2003. The Widespread Colonization Island of *Actinobacillus actinomycetemcomitans*. Nat Genet **34:**193-198.

26. **Inoue T, Tanimoto I, Ohta H, Kato K, Murayama Y, Fukui K.** 1998. Molecular characterization of low-molecular-weight component protein, Flp, in *Actinobacillus actinomycetemcomitans* fimbriae. Microbiol Immunol **42:**253-258.
27. **Kachlany SC, Planet PJ, Desalle R, Fine DH, Figurski DH, Kaplan JB.** 2001. flp-1, the first representative of a new pilin gene subfamily, is required for non-specific adherence of *Actinobacillus actinomycetemcomitans*. Mol Microbiol **40:**542-554.
28. **Schilling J, Wagner K, Seekircher S, Greune L, Humberg V, Schmidt MA, Heusipp G.** 2010. Transcriptional activation of the tad type IVb pilus operon by PypB in *Yersinia enterocolitica*. J Bacteriol **192:**3809-3821.
29. **McIntosh M, Krol E, Becker A.** 2008. Competitive and cooperative effects in quorum-sensing-regulated galactoglucan biosynthesis in *Sinorhizobium meliloti*. J Bacteriol **190:**5308-5317.
30. **Rinaudi LV, González JE.** 2009. The low-molecular-weight fraction of exopolysaccharide II from *Sinorhizobium meliloti* is a crucial determinant of biofilm formation. J Bacteriol **191:**7216-7224.
31. **Gurich N, González JE.** 2009. Role of quorum sensing in *Sinorhizobium meliloti*-Alfalfa symbiosis. J Bacteriol **191:**4372-4382.
32. **Marketon MM, Glenn SA, Eberhard A, González JE.** 2003. Quorum sensing controls exopolysaccharide production in *Sinorhizobium meliloti*. J Bacteriol **185:**325-331.
33. **Hoang HH, Gurich N, González JE.** 2008. Regulation of motility by the ExpR/Sin quorum-sensing system in *Sinorhizobium meliloti*. J Bacteriol **190:**861-871.
34. **Glenn SA, Gurich N, Feeney MA, González JE.** 2007. The ExpR/Sin quorum-sensing system controls succinoglycan production in *Sinorhizobium meliloti*. J Bacteriol **189:**7077-7088.
35. **Gao M, Chen H, Eberhard A, Gronquist MR, Robinson JB, Rolfe BG, Bauer WD.** 2005. *sinI*- and *expR*-dependent quorum sensing in *Sinorhizobium meliloti*. J Bacteriol **187:**7931-7944.
36. **Hoang HH, Becker A, González JE.** 2004. The LuxR homolog ExpR, in combination with the Sin quorum sensing system, plays a central role in *Sinorhizobium meliloti* gene expression. J Bacteriol **186:**5460-5472.
37. **Pellock BJ, Teplitski M, Boinay RP, Bauer WD, Walker GC.** 2002. A LuxR homolog controls production of symbiotically active extracellular polysaccharide II by *Sinorhizobium meliloti*. J Bacteriol **184:**5067-5076.
38. **Viands DR, Hansen JL, Thomas EM, Neally JL.** 2005. Registration of 'Guardsman II' alfalfa. Crop Science **45:**2644-2644.
39. **Olivares J, Casadesus J, Bedmar EJ.** 1980. Method for Testing Degree of Infectivity of *Rhizobium meliloti* Strains. Appl Environ Microbiol **39:**967-970.
40. **Rigaud J, Puppo A.** 1975. Indole-3-Acetic-Acid Catabolism by Soybean Bacteroids. J Gen Microbiol **88:**223-228.
41. **Scharf B, Schuster-Wolff-Bühring H, Rachel R, Schmitt R.** 2001. Mutational analysis of *Rhizobium lupini* H13-3 and *Sinorhizobium meliloti* flagellin genes: importance of flagellin A for flagellar filament structure and transcriptional regulation. J Bacteriol **183:**5334-5342.
42. **Götz R, Limmer N, Ober K, Schmitt R.** 1982. Motility and chemotaxis in two strains of *Rhizobium* with complex flagella. J Gen Microbiol **128:**789-798.
43. **Rotter C, Mühlbacher S, Salamon D, Schmitt R, Scharf B.** 2006. Rem, a new transcriptional activator of motility and chemotaxis in *Sinorhizobium meliloti*. J Bacteriol **188:**6932-6942.
44. **Bertani G.** 1951. Studies on lysogenesis. I. The mode of phage liberation by lysogenic *Escherichia coli*. J Bacteriol **62:**293-300.
45. **Labes M, Pühler A, Simon R.** 1990. A new family of RSF1010-derived expression and lac-fusion broad-host- range vectors for gram-negative bacteria. Gene **89:**37-46.
46. **Kovach ME, Elzer PH, Hill DS, Robertson GT, Farris MA, Roop RM, 2nd, Peterson KM.** 1995. Four new derivatives of the broad-host-range cloning vector pBBR1MCS, carrying different antibiotic-resistance cassettes. Gene **166:**175-176.
47. **Simon R, Priefer U, Pühler A.** 1983. A broad host range mobilisation system for *in vivo* genetic engineering: Transposon mutagenesis in gram negative bacteria. Bio/Technology **1:**783-791.
48. **Higuchi R.** 1989. Using PCR to engineer DNA, p 61-70. *In* Erlich HA (ed), PCR technology Principles and applications for DNA amplification. Stockton Press, New York.
49. **Simon R, O'Connell M, Labes M, Pühler A.** 1986. Plasmid vectors for the genetic analysis and manipulation of rhizobia and other gram-negative bacteria. Methods Enzymol **118:**640-659.
50. **Sourjik V, Schmitt R.** 1996. Different roles of CheY1 and CheY2 in the chemotaxis of *Rhizobium meliloti*. Mol Microbiol **22:**427-436.
51. **Domínguez-Ferreras A, Muñoz S, Olivares J, Soto MJ, Sanjuán J.** 2009. Role of potassium uptake

systems in *Sinorhizobium meliloti* osmoadaptation and symbiotic performance. J Bacteriol **191:**2133-2143.
52. **Nogales J, Bernabéu-Roda L, Cuéllar V, Soto MJ.** 2012. ExpR is not required for swarming but promotes sliding in *Sinorhizobium meliloti*. J Bacteriol **194:**2027-2035.
53. **Miller JH.** 1972. Experiments in molecular genetics. Cold Spring Harbor Laboratory Press, Cold Spring Harbor.
54. **Meier VM, Müschler P, Scharf BE.** 2007. Functional analysis of nine putative chemoreceptor proteins in *Sinorhizobium meliloti*. J Bacteriol **189:**1816-1826.
55. **Bartels FW, McIntosh M, Fuhrmann A, Metzendorf C, Plattner P, Sewald N, Anselmetti D, Ros R, Becker A.** 2007. Effector-stimulated single molecule protein-DNA interactions of a quorum-sensing system in *Sinorhizobium meliloti*. Biophys J **92:**4391-4400.
56. **Zianni M, Tessanne K, Merighi M, Laguna R, Tabita FR.** 2006. Identification of the DNA bases of a DNase I footprint by the use of dye primer sequencing on an automated capillary DNA analysis instrument. J Biomol Tech **17:**103-113.
57. **Bateman A, Coin L, Durbin R, Finn RD, Hollich V, Griffiths-Jones S, Khanna A, Marshall M, Moxon S, Sonnhammer EL, Studholme DJ, Yeats C, Eddy SR.** 2004. The Pfam protein families database. Nucleic Acids Res **32:**D138-141.
58. **Iyer LM, Leipe DD, Koonin EV, Aravind L.** 2004. Evolutionary history and higher order classification of AAA+ ATPases. J Struct Biol **146:**11-31.
59. **Frickey T, Lupas AN.** 2004. Phylogenetic analysis of AAA proteins. J Struct Biol **146:**2-10.
60. **Sagulenko E, Sagulenko V, Chen J, Christie PJ.** 2001. Role of *Agrobacterium* VirB11 ATPase in T-pilus assembly and substrate selection. J Bacteriol **183:**5813-5825.
61. **Marketon MM, Gronquist MR, Eberhard A, González JE.** 2002. Characterization of the *Sinorhizobium meliloti sinR/sinI* locus and the production of novel N-acyl homoserine lactones. J Bacteriol **184:**5686-5695.
62. **Bahlawane C, McIntosh M, Krol E, Becker A.** 2008. *Sinorhizobium meliloti* regulator MucR couples exopolysaccharide synthesis and motility. Mol Plant Microbe Interact **21:**1498-1509.
63. **Nogales J, Domínguez-Ferreras A, Amaya-Gómez CV, van Dillewijn P, Cuéllar V, Sanjuán J, Olivares J, Soto MJ.** 2010. Transcriptome profiling of a Sinorhizobium meliloti fadD mutant reveals the role of rhizobactin 1021 biosynthesis and regulation genes in the control of swarming. BMC Genomics **11:**157.
64. **Galibert F, Finan TM, Long SR, Pühler A, Abola P, Ampe F, Barloy-Hubler F, Barnett MJ, Becker A, Boistard P, Bothe G, Boutry M, Bowser L, Buhrmester J, Cadieu E, Capela D, Chain P, Cowie A, Davis RW, Dreano S, Federspiel NA, Fisher RF, Gloux S, Godrie T, Goffeau A, Golding B, Gouzy J, Gurjal M, Hernandez-Lucas I, Hong A, Huizar L, Hyman RW, Jones T, Kahn D, Kahn ML, Kalman S, Keating DH, Kiss E, Komp C, Lelaure V, Masuy D, Palm C, Peck MC, Pohl TM, Portetelle D, Purnelle B, Ramsperger U, Surzycki R, Thebault P, Vandenbol M, et al.** 2001. The composite genome of the legume symbiont *Sinorhizobium meliloti*. Science **293:**668-672.
65. **Sourjik V, Müschler P, Scharf B, Schmitt R.** 2000. VisN and VisR are global regulators of chemotaxis, flagellar, and motility genes in *Sinorhizobium* (*Rhizobium*) *meliloti*. J Bacteriol **182:**782-788.
66. **Charoenpanich P, Meyer S, Becker A, McIntosh M.** 2013. Temporal expression program of quorum sensing-based transcription regulation in *Sinorhizobium meliloti*. J Bacteriol **195:**3224-3236.
67. **Perez-Cheeks BA, Planet PJ, Sarkar IN, Clock SA, Xu Q, Figurski DH.** 2012. The product of *tadZ*, a new member of the *parA*/*minD* superfamily, localizes to a pole in *Aggregatibacter actinomycetemcomitans*. Mol Microbiol **83:**694-711.
68. **Lutkenhaus J.** 2012. The ParA/MinD family puts things in their place. Trends Microbiol **20:**411-418.
69. **Gerdes K, Howard M, Szardenings F.** 2010. Pushing and pulling in prokaryotic DNA segregation. Cell **141:**927-942.
70. **Ingerson-Mahar M, Gitai Z.** 2012. A growing family: the expanding universe of the bacterial cytoskeleton. FEMS Microbiol Rev **36:**256-266.
71. **Aguilar J, Cameron TA, Zupan J, Zambryski P.** 2011. Membrane and core periplasmic *Agrobacterium tumefaciens* virulence Type IV secretion system components localize to multiple sites around the bacterial perimeter during lateral attachment to plant cells. mBio **2:**e00218-00211.
72. **MacLellan SR, MacLean AM, Finan TM.** 2006. Promoter prediction in the rhizobia. Microbiology **152:**1751-1763.
73. **Bernard CS, Bordi C, Termine E, Filloux A, de Bentzmann S.** 2009. Organization and PprB-dependent control of the *Pseudomonas aeruginosa tad* Locus, involved in Flp pilus biology. J Bacteriol **191:**1961-1973.
74. **Scannapieco FA, Millar SJ, Reynolds HS, Zambon JJ, Levine MJ.** 1987. Effect of anaerobiosis on the surface ultrastructure and surface proteins of *Actinobacillus actinomycetemcomitans (Haemophilus*

actinomycetemcomitans). Infect Immun **55:**2320-2323.
75. **McIntosh M, Meyer S, Becker A.** 2009. Novel *Sinorhizobium meliloti* quorum sensing positive and negative regulatory feedback mechanisms respond to phosphate availability. Mol Microbiol **74:**1238-1256.
76. **González JE, York GM, Walker GC.** 1996. *Rhizobium meliloti* exopolysaccharides: synthesis and symbiotic function. Gene **179:**141-146.
77. **Hanahan D, Meselson M.** 1983. Plasmid screening at high colony density. Methods Enzymol **100:**333-342.
78. **Meade HM, Long SR, Ruvkun GB, Brown SE, Ausubel FM.** 1982. Physical and genetic characterization of symbiotic and auxotrophic mutants of *Rhizobium meliloti* induced by transposon Tn5 mutagenesis. J Bacteriol **149:**114-122.
79. **Chang AC, Cohen SN.** 1978. Construction and characterization of amplifiable multicopy DNA cloning vehicles derived from the P15A cryptic miniplasmid. J Bacteriol **134:**1141-1156.
80. **Gould J, Devey M, Hasegawa O, Ulian EC, Peterson G, Smith RH.** 1991. Transformation of *Zea mays* L. Using *Agrobacterium tumefaciens* and the Shoot Apex. Plant Physiol **95:**426-434.
81. **Schafer A, Tauch A, Jager W, Kalinowski J, Thierbach G, Pühler A.** 1994. Small mobilizable multi-purpose cloning vectors derived from the *Escherichia coli* plasmids pK18 and pK19: selection of defined deletions in the chromosome of *Corynebacterium glutamicum*. Gene **145:**69-73.
82. **Hubner P, Willison JC, Vignais PM, Bickle TA.** 1991. Expression of regulatory nif genes in *Rhodobacter capsulatus*. J Bacteriol **173:**2993-2999.
83. **Shaner NC, Campbell RE, Steinbach PA, Giepmans BN, Palmer AE, Tsien RY.** 2004. Improved monomeric red, orange and yellow fluorescent proteins derived from *Discosoma* sp. red fluorescent protein. Nat Biotechnol **22:**1567-1572.
84. **Bachmann BJ.** 1990. Linkage map of *Escherichia coli* K-12, edition 8 [published erratum appears in Microbiol Rev 1991 Mar;55(1):191]. Microbiol Rev **54:**130-197.
85. **Novick RP, Clowes RC, Cohen SN, Curtiss R, 3rd, Datta N, Falkow S.** 1976. Uniform nomenclature for bacterial plasmids: a proposal. Bacteriol Rev **40:**168-189.

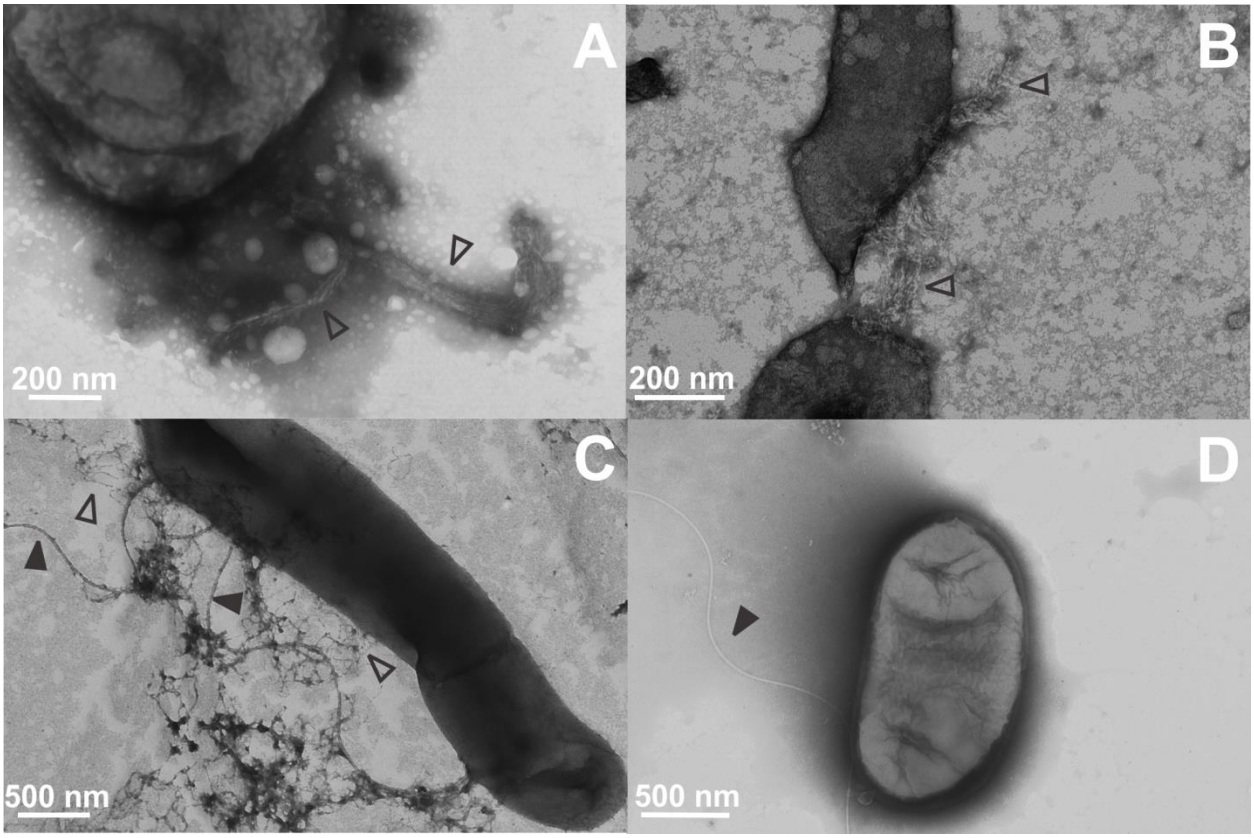

Fig. 2.1: Transmission electron micrographs of Flp pili in *S. meliloti*. Strains Sm1021 and Sm1021Δ*pilA1* cells were grown for 48 hours in SMM and negatively stained with aqueous phosphotungstic acid (0.5%) (A, C+D) or uranyl acetate (1%) (B). **A-C.** Sm1021, **D.** Sm1021Δ*pilA1*. Solid and open arrow heads indicate flagella and Flp pili, respectively.

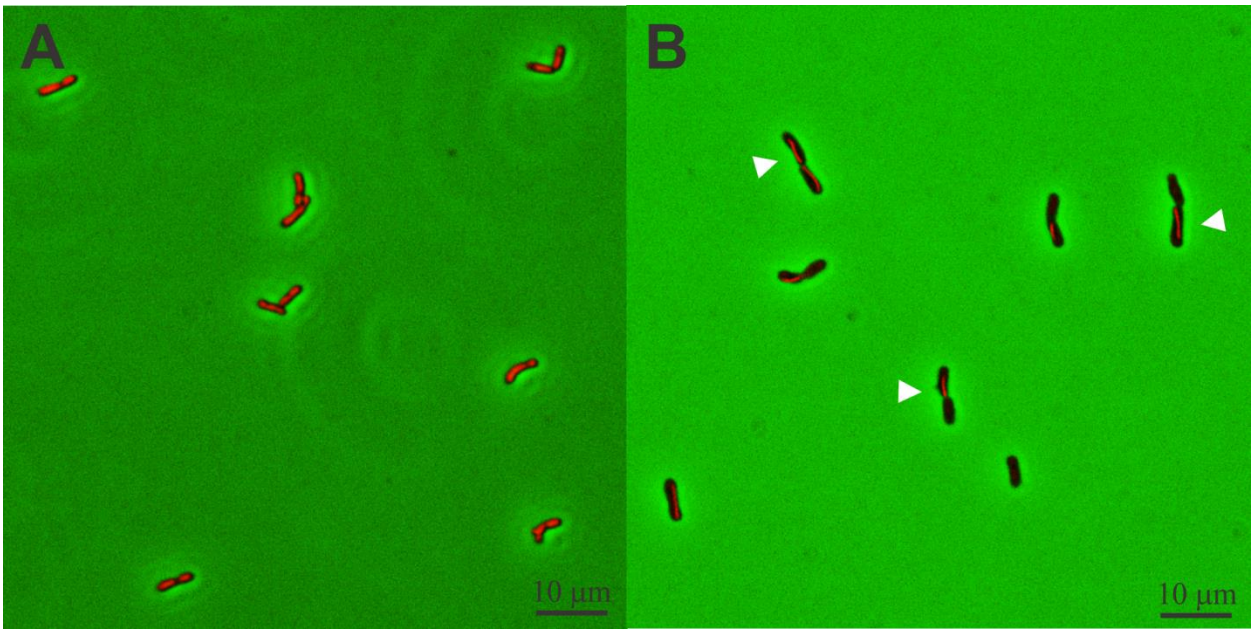

Fig. 2.2: Localization of CpaE1 in *S. meliloti* by fluorescence microscopy. **A.** mCherry expressed from pBS403 (control), and **B.** CpaE1 fused to mCherry expressed from pBS406 were monitored in *S. meliloti* Sm1021 grown for 14 hours in TYC in the presence of 200 mM IPTG.

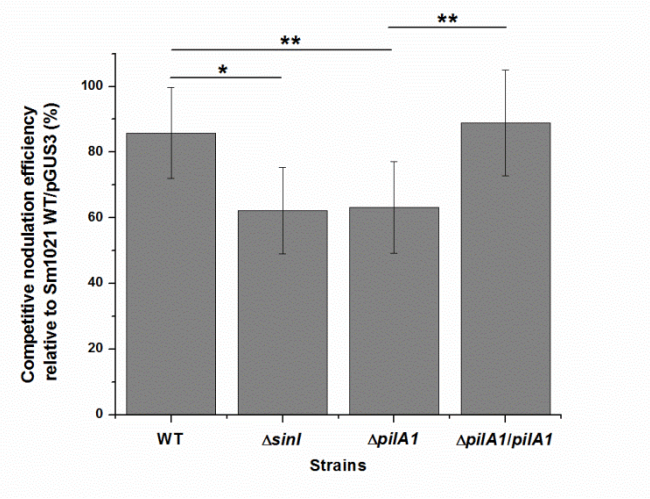

Fig. 2.3: Competitive nodulation assay of Sm1021, Sm1021Δ*sinI*, Sm1021Δ*pilA1*, and Sm1021Δ*pilA1*/*pilA1* with Sm1021 (pGUS3). Three weeks after germination, alfalfa plants were inoculated with equal numbers of *S. meliloti* cells from both competing strains. After two weeks of incubation, roots were harvested, incubated with the substrate X-Gluc, and blue and white nodule counts per plants were determined. Data are from four (Sm1021Δ*sinI* and Sm1021Δ*pilA1*/*pilA1*) or eight (Sm1021 and Sm1021Δ*pilA1)* independent experiments with 10–12 plants per competition per experiment. Error bars represent standard deviations. Data were analyzed for statistical significance using one-way analysis of variance (ANOVA) and a post hoc Tukey's test for pairwise comparisons. Sm1021 vs. Sm1021Δ*sinI* (*), $p < 0.06$; Sm1021 vs. Sm1021Δ*pilA1* and Sm1021Δ*pilA1* vs. Sm1021Δ*pilA1*/*pilA1* (**), $p < 0.05$.

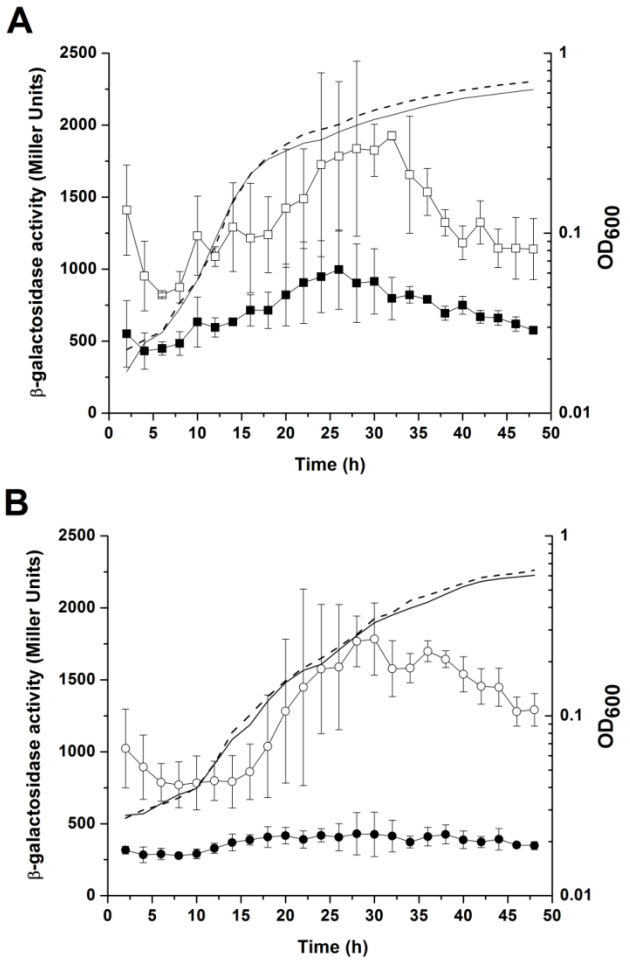

Fig. 2.4: Kinetics of *pilA1* expression in *S. meliloti* Sm1021 and Sm8530 strains during growth over a 48 hour period. **A.** Promoter activity in Miller units monitored by *lacZ* reporter gene construct in strains Sm1021 (□-□) and Sm8530 (■-■) and their respective growth curves (OD_{600}) (solid and dotted line). **B**. Promoter activity in strains Sm1021 $ExpR^+$ (●-●) and Sm1021 $ExpR^+\Delta sinI$ (○-○) and their respective growth curves (solid and dotted line). Points represent the mean of three independent experiments and bars represent standard deviations.

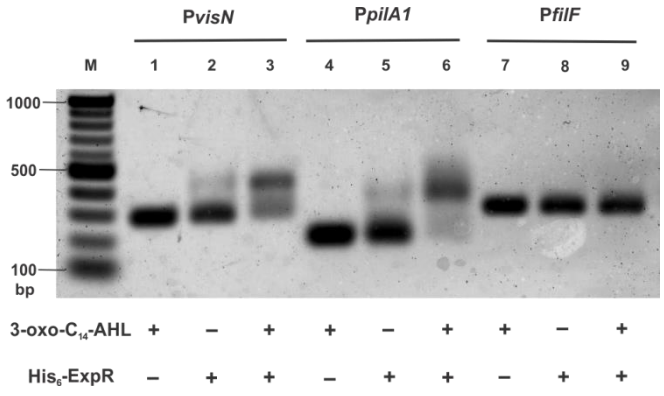

Fig. 2.5: AHL-dependent binding of His_6-ExpR to promoter regions of *visN* and *pilA1*. Reaction mixtures comprising 0.7 pmol of the upstream regions of *visN* (273 bp), *pilA1* (254 bp), and *fliF* (327 bp) were incubated with 15 pmol of His_6-ExpR in the presence and absence of 10 □M 3-oxo-C_{14}-HSL, and detected in an electrophoretic mobility shift assay after staining DNA with SYBR® Green.

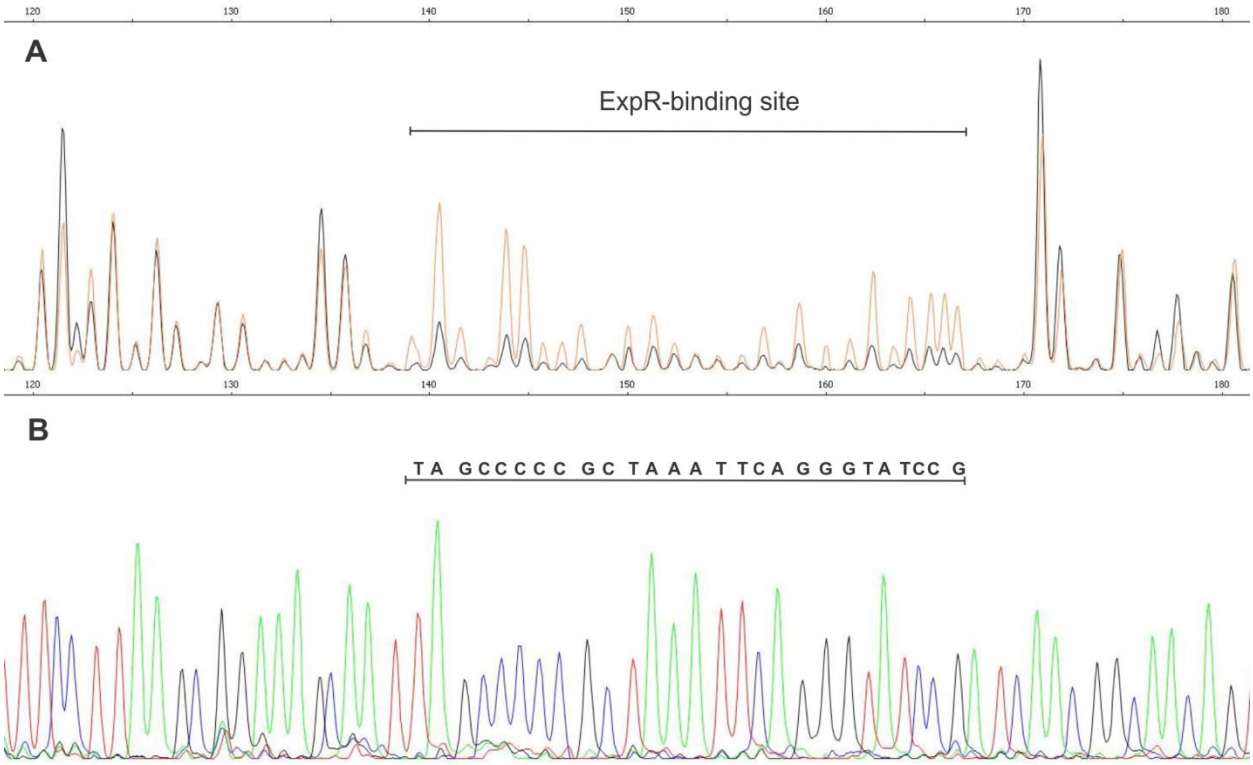

Fig. 2.6: DNase I footprinting of 6-FAM-labeled *pilA1* promoter with His_6-ExpR. **A.** Superimposed DNase I digestion pattern of the *pilA1* promoter region in the absence of ExpR (tan line) and in the presence of His_6-ExpR and 3-oxo-C_{14}-HSL (black line). The protected region is indicated by a horizontal line. **B.** Traces for the dideoxynucleotide sequencing reaction of the *pilA1* promoter fragment (A, green; C, blue; G, black; T, red). The DNA sequence protected by 3-oxo-C_{14}-HSL-activated His_6-ExpR is indicated above the corresponding region.

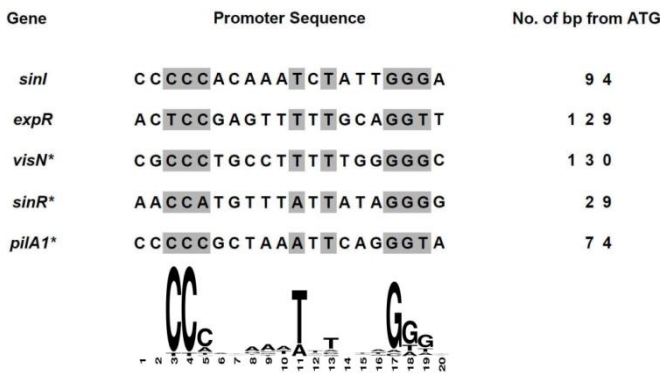

Fig. 2.7: ExpR-binding sites of selected genes from the ExpR regulon. The identified ExpR binding sites from the promoter regions of *sinI*, *expR*, *visN*, *sinR* (66), and *pilA1* are aligned in 5′-3′ orientation to show homology to the ExpR consensus sequence. Grey shading indicates highly conserved nucleotides. The frequency of each nucleotide within the ExpR consensus sequence is indicated below. The consensus sequence was generated using the WebLogo tool (http://weblogo.berkeley.edu/). The asterisk (*) indicates genes that are downregulated by ExpR.

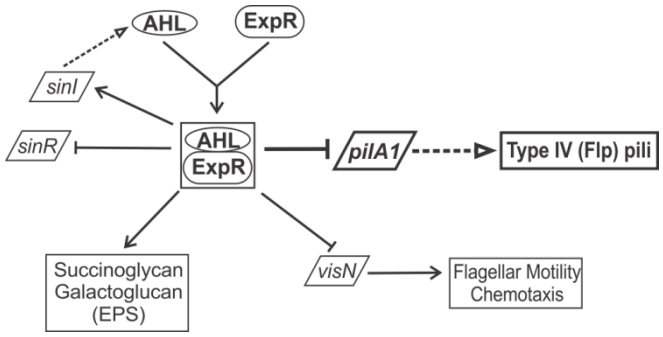

Fig. 2.8: Proposed scheme of the AHL-activated ExpR regulation network of EPS production, flagellar motility, and Flp pili synthesis in *S. meliloti* including Type IV (Flp) pili synthesis. Arrows indicate activation, blunt ended lines repression, and dotted arrows gene function. For more details, refer to the main text.

Table 2.1. Bacterial strains and plasmids

Strain/Plasmid	Relevant characteristics [a]	Source or Reference
Strain		
E. coli		
DH5α	*recA1 endA1*	(77)
M15/pREP4	Km^r; *lac ara gal mtl F recA uvr*	Qiagen
S17-1	*recA endA thi hsdR* RP4-2 Tc::Mu::Tn7 Tp^r Sm^r	(49)
S. meliloti		
Sm1021	Sm^r; *expR102*::IS*Rm*2011-1 *expR*	(78)
Sm1021Δ*pilA1*	Sm^r; Δ*pilA1*	This study
Sm1021Δ*sinI*	Sm^r; Δ*sinI*	This study
Sm1021 ExpR$^+$	Sm^R; Sm1021 with restored *expR* locus	Anke Becker
Sm1021 ExpR$^+$ Δ*sinI*	Sm^R; Sm1021 with restored *expR* locus, Δ*sinI*	This study
Sm8530	Sm^R; Sm1021 *expR*$^+$ (formerly *expR101*)	(37)
Plasmid		
pACYC184	Cp^r, Tc^r; source of *lacI*^{q}	(79)
pBBR1MCS-2	Km^r	(46)
pBS125	Km^r; 650-bp *Eco*RI/*Hin*dIII fragment containing a *sinI* in-frame deletion cloned into pK18*mobsacB*	This study
pBS126	Km^r; 650-bp *Eco*RI/*Hin*dIII fragment containing a *pilA1* in-frame deletion cloned into pK18*mobsacB*	This study
pBS189	Ap^r , *lacI*^{q} fragment from pBS189 cloned into the *Sac*I site of pBBR1MCS-2	This study
pBS326	Tc^r, *pilA1* promoter-*lacZ* in pPHU234	This study
pBS396	Km^r; 183-bp *Hin*dIII/*Bam*HI PCR fragment containing *pilA1* cloned into pBBR1MCS-2	This study
pBS401	Km^r; 696-bp *Eco*RI/*Sac*II PCR fragment containing mCherry (without stop codon) cloned into pBS189	This study
pBS403	Km^r; 699-bp *Eco*RI/*Sac*II PCR fragment containing mCherry (with stop codon) cloned into pBS189	This study
pBS406	Km^r; 1284-bp *Hin*dIII/*Eco*RI PCR fragment containing *cpaE1* cloned into pBS401	This study
pBS407	Km^r; 1401-bp *Hin*dIII/*Eco*RI PCR fragment containing *cpaF1* cloned into pBS401	This study
pBS1077	737-bp *Bam*HI-*Hin*dIII PCR fragment containing *expR* cloned into pQE30	This study
pGUS3	Km^r, GUS (β-glucuronidase)	(80)
pK18*mobsacB*	Km^r, *lacZ mob sacB*	(81)
pPHU234	Tc^r, promotorless *lacZ* fusion	(82)
pQE30	Ap^r; expression vector	Qiagen
pRSET-B mCherry	Ap^r; source of mCherry	(83)

[a] Nomenclature according to Bachmann (84) and Novick *et al*. (85).

Chapter 3 - The role of two Flp pili systems in *Sinorhizobium meliloti* symbiosis with its legume host

HARDIK M. ZATAKIA[1]*, NANCY A. FUJISHIGE[2]*, MICHELLE R. LUM[2], ANN M. HIRSCH[3], BIRGIT E. SCHARF[1]

[1] Department of Biological Sciences, Virginia Polytechnic Institute and State University, Life Sciences I, Blacksburg, VA 24061

[2] Frank R. Seaver College of Science and Engineering, Loyola Marymount University, Los Angeles, CA 90045

[3] Department of Molecular, Cell, and Developmental Biology, University of California, Los Angeles, CA 90095

* H.M.Z. and N.A.F. contributed equally to the work.

Running title: The role of Flp pili in symbiosis

Key words: biofilm, exopolysaccharides, nodulation, quorum sensing, rhizosphere, type IVb pili

Correspondence:

Birgit Scharf

Department of Biological Sciences, Virginia Tech, Life Sciences I, Blacksburg, VA 24061, USA

Tel: (+1) 540 231 0757

Fax: (+1) 540 231 4043

E-mail bscharf@vt.edu

Attribution: Hardik Zatakia has generated the data shown here in Fig. 3.1 - Fig. 3.3. Data generated by NAF, MRL, AMH have not been included here but will be part of the final manuscript.

ABSTRACT

The genome of the nitrogen-fixing plant symbiont, *Sinorhizobium meliloti*, contains two gene clusters encoding Type IVb pili of the Flp (fimbrial low-molecular-weight protein) subfamily. Our previous work revealed the importance of Flp1 for efficient symbiosis with alfalfa. The current study is aimed to identify the role of Flp2 in symbiosis and to give a detailed characterization of the functions of Flp1 and Flp2 in plant-host interaction. Nodulation assays with *S. meliloti* mutants lacking *pilA2* and *pilA1pilA2*, which encode the respective putative pilin subunits of Flp1 and Flp2, with alfalfa revealed that both *pilA* deletion strains are outcompeted by wild type with a 27% and 31% reduction for Δ*pilA1* and Δ*pilA2*, respectively. A *pilA1pi1A2* double deletion strain presented no significant additive effect. Our results show that both Flp systems are important for efficient symbioses of *S. meliloti* with its plant hosts. We hypothesize that Flp1 initiates contact with host roots, while Flp2 is more important for the later stages during symbiosis, when Flp1 may play an accessory role.

INTRODUCTION

Legumes, such as soybeans, peas, and alfalfa engage in a symbiotic relationship with rhizobial soil bacteria, which leads to the conversion of atmospheric di-nitrogen to a biologically available form of nitrogen in the root nodules. Two types of nodules are developed by legumes, determinate and indeterminate. The so-called 'slow growing' rhizobia such as *Bradyrhizobium* species are known to induce spherical determinate nodules in which the meristematic activity ceases early. Alternatively, indeterminate nodules, which are cylindrical in shape due to a persistent meristem, are induced by 'fast-growing' rhizobia like *Rhizobium leguminosarum* and *Sinorhizobium meliloti* (1).

The association between *S. meliloti* and its hosts, namely species of *Medicago*, *Melilotus*, and *Trigonella*, has been long studied as a model for symbiotic plant-microbe interactions (2-6). Investigations of the various processes involved in the establishment of nitrogen-fixing symbiotic associations led to a detailed understanding of this mutual relationship. Bacterial processes involved in the initiation of symbiosis include chemotaxis towards the rhizosphere, quorum sensing, exopolysaccharide synthesis, lipochitooligosaccharide (Nod factor) production, and biofilm formation (4, 6-8). Bacterial Nod factors, whose synthesis is induced by the release of host-produced flavonoids, cause root hairs to curl, thereby entrapping attached bacterial cells. After lowering of plant defenses and development of a plant-derived infection thread, bacteria enter plant cells, nodule tissue is formed, and bacteria differentiate into nitrogen-fixing bacteroids (9).

Adhesion of *S. meliloti* cells to plant roots, abiotic surfaces and each other leads to the development of biofilms (8, 10, 11). Biofilm structures are beneficial for a bacterial community in conferring resistance to antimicrobials and protection against host defenses (12). Rhizobial biofilm formation

is critical for the establishment of a successful symbiosis (9). Several bacterial cell surface components are involved in this early stage of nodulation, namely Nod factors, exopolysaccharides, flagella, and Type IV (Tfp) pili (8, 10, 11, 13, 14).

Tfp are classified into two types, a (Tfpa) and b (Tfpb). Tfpa are intensely studied and their function in twitching motility is well known (15). Tfbp mediate tight adherence (tad) to host cells (16-18). They are often found on the surface of intestinal pathogens where they function as host-colonizing factors (19-23). The *tad* locus is present in a similar arrangement in the genomes of many bacteria, including human pathogens (*Pseudomonas, Vibrio*) and plant-associated bacteria (*Agrobacterium, Sinorhizobium*), some having two or three *tad* loci (17). The Flp (fimbrial low-molecular-weight protein) subfamily represent a discrete monophyletic group within the Tad protein class, primarily facilitating host colonization and pathogenesis through nonspecific adhesion (24, 25). In plant-pathogenic bacteria such as *Agrobacterium tumefaciens* and *Ralstonia solanacearum* Flp pili mediate attachment to surfaces and are required for virulence (26, 27).

S. meliloti possesses two *flp* gene clusters, one on the chromosome (*flp-1*) and one on the pSymA megaplasmid (*flp-2*), respectively (13). We have shown previously that Flp pili encoded by *flp-1* are required for a competitive symbiosis of *S. meliloti* with its host. Expression of pilin-encoding *pilA1* is maximal in early stationary phase and is under direct negative control of ExpR, the global transcriptional regulator of quorum sensing, exopolysaccharide production and motility. The temporal inverse regulation of exopolysaccharides and pili by ExpR provides a coordinated expression of cellular processes during early stages of symbiosis (13).

In this study, we establish that *flp-2*, in addition to *flp-1*, is required for competitive symbiosis of *S. meliloti* with its hosts. Our results demonstrate that both Flp systems mediate root attachment and therefore are important for efficient symbiosis of *S. meliloti* with its plant hosts. We

hypothesize that Flp1 initiates contact with host roots, while Flp1 and Flp2 are engaged in later symbiotic stages.

MATERIALS AND METHODS

Bacterial strains and plasmids

Derivatives of *E. coli* K-12 and *S. meliloti* Sm1021 and the plasmids used are listed in Table 3.1. The following antibiotics were used in their final concentrations: for *E. coli*, kanamycin at 50 µg/ml and tetracycline at 10 µg/ml; for *S. meliloti* grown in TYC (28), neomycin at 40 µg/ml, streptomycin at 600 µg/ml, and tetracycline at 10 µg/ml, for *S. meliloti* grown in SMM (29, 30), streptomycin was omitted and tetracycline was used at 2.5 µg/ml.

Genetic manipulations and DNA methods

The promoter region of *pilA2* was amplified according to standard PCR protocols and cloned into the promoter-less plasmid pPHU234 (31) to make the *pilA2* promoter region-*lacZ* transcriptional fusion. An in-frame deletion construct of *pilA2* was generated *in vitro* by overlap extension PCR and cloned into the mobilizable suicide vector pK18*mobsacB* (32). Broad-host range plasmids were used to transform *E. coli* S17-1 and then conjugally transferred to *S. meliloti* by streptomycin-tetracycline or streptomycin-neomycin double selection (33). Allelic replacement was achieved by sequential selections on neomycin and 10% sucrose as described previously (34). Confirmation of allelic replacement and elimination of the vector was obtained by gene-specific primer PCR, DNA-sequencing, and Southern blotting.

Competitive nodulation assays

Alfalfa seeds (*Medicago sativa*, cultivar Iroquois and cultivar 'Guardsman II', developed from cultivar Iroquois (35)) were surface sterilized, germinated, and grown in hydroponic (HP) medium in a plant growth chamber (Conviron Adaptis A1000, Canada) with 16 hours day (light) cycle at

24°C with 50% humidity and 8 hours night (dark) cycle at 16-18°C with 50% humidity as described previously (13). After about two weeks of growth, when plant roots reached into the medium, they were co-inoculated with equal amounts of competing *S. meliloti* strains (Wt/pGUS3 versus test strain) grown in TYC at 30°C (28). After two weeks of inoculation, plants roots were harvested and assayed for β-glucuronidase activity (36). The number of blue and white nodules per plant were counted and the nodulation efficiency for each test strain was calculated as follows: [(*n*/*N*)*100]*2 where *n*, number of white nodules of test strain in a plant and *N*, total (blue and white) number of nodules on the same plant (37). Data were analyzed for statistically significant differences using a one-way analysis of variance (ANOVA). A post hoc Tukey's test was applied for pairwise comparisons.

β-galactosidase assays

Assays were performed as previously described (13). Briefly, stationary phase cultures of *S. meliloti* containing *lacZ* fusion plasmids were diluted to an OD_{600} of 0.02 in SMM medium and incubated at 30 ºC for 48 hours. Samples were taken every 2 hours, diluted 1:4 in Z buffer, permeabilized with 30 µL of 0.1% SDS and chloroform, and assayed for β-galactosidase activity by the method of Miller.

RESULTS

S. meliloti possesses two type IVb pili systems of the Flp subfamily

The *Sinorhizobium meliloti* genome contains two Type IVb pili-encoding gene clusters of the *flp* subfamily. These clusters have previously not been analyzed and thus are described here in detail. The *flp-1* cluster is on the chromosome and comprises 13 putative pilus assembly genes, while the *flp-2* cluster comprises 11 putative pilus assembly genes and is located on the pSymA megaplasmid (Fig. 3.1). A summary of the gene products and their predicted function for both clusters is given in Table 3.2. The *flp-1* cluster has been previously shown to play a role in Type IVb pili synthesis in *S. meliloti* (13). The pilin-encoding gene, *pilA1*, is in the *flp-1* cluster, while *pilA2* is the putative pilin encoding gene in the *flp-2* gene cluster. Other putative functional homologs of the *tad* and *cpa* loci involved in pilus biogenesis in *Aggregatibacter actinomycetemcomitans* and *Caulobacter crescentus* are also present on both *flp* clusters of *S. meliloti* (17). CpaA1 and CpaA2 are homologous to TadV, a prepilin peptidase, which processes prepilin to the mature pilin used for polymerization into a functional pilus filament. The genes *cpaB1*/*cpaB2*, *cpaC1*, and *cpaD1* are putative homologs of *rcpCAB* in *A. actinomycetemcomitans*. Their gene products are part of the pilus assembly apparatus embedded within the cytosolic and outer membrane. CpaE1 and CpaE2 are TadZ homologs, which are suggested to mediate polar localization of the Tad secretion apparatus (38). In fact, CpaE1 fused to mCherry predominantly exhibits lateral localization correlating with the formation of polar and lateral pili bundles in *S. meliloti* (13). Genes *cpaF1* and *cpaF2* encode the putative pilus assembly ATPase and are TadA homologs. Furthermore, six genes which encode for TadBCDG, CpaC, and PapD homologs are present on both *flp* clusters and are believed to take part in pilus assembly. Additionally, the TadE-

homologs SMc04117 and SMa1572 are putative pseudopilins which may play a role in Type IVb pilus biogenesis (17) (Table 3.2).

S. meliloti requires both Flp pili systems for efficient nodulation of the _Medicago sativa_ host

In our previous study, it was demonstrated that *pilA1* and therefore Type IVb pili are important for effective nodulation of *Medicago sativa* (13). To establish a role of the *flp-2* gene cluster in symbiosis, competitive nodulation assays were carried out between Sm1021 WT and Sm1021 Δ*pilA2*. Briefly, alfalfa plants were simultaneously inoculated with two bacterial strains in a 1:1 ratio and nodule occupancy was determined after two weeks. A pGUS3 reporter gene plasmid was used to differentiate between the nodules. Nodules occupied by Sm1021 bearing pGUS3 stain blue when exposed to the substrate X-Gluc, while those occupied by the test (deletion) strain remain white. To confirm that the pGUS3 plasmid was being maintained in *S. meliloti* during the assay and that it did not impact nodulation efficiency, a competition between Sm1021 and Sm1021/pGUS3 was carried out. A 1:1 ratio of nodules occupied by Sm1021 (white) and Sm1021/pGUS3 (blue), equaling to a 100 % nodulation efficiency, should be the ideal outcome of this competition. Our analyses showed that nodulation efficiency of Sm1021 WT was 87 ± 12 %. For comparison, we analyzed the competitive ability of a *sinI* deletion strain, which is deficient in its ability to invade the host (39, 40). This strain, Sm1021 Δ*sinI*, exhibited a 57 ± 12 % reduction in nodule occupancy and served as negative control for our assays (Fig. 3.2). We had previously presented that the Sm1021 Δ*pilA1* strain had a competitive nodulation efficiency of 61 ± 11 % (Fig. 3.2; (13)). In the competition experiment between Sm1021 Δ*pilA2* strain and Sm1021 WT, we observed a similar, significant reduction in nodulation efficiency of 60 ± 15 % ($p < 0.05$; Fig. 3.2). We next analyzed whether *pilA1* and *pilA2* had an additive effect on nodulation, by testing

the competitive nodulation efficiency of Sm1021 Δ*pilA1*Δ*pilA2*. The nodulation efficiency of the double deletion strain was determined to be 49 ± 5 % ($p < 0.05$; Fig. 3.2). Thus, the *pilA1pi1A2* double deletion strain exhibited no significant impact on nodulation. In conclusion, not only *pilA1* (*flp-1*) but also *pilA2* (*flp-2*) is important for efficient nodulation of *M. sativa* by *S. meliloti*.

Expression of *pilA2* in liquid cultures was negligible

In our previous study, we showed that *pilA1* expression peaked at early stationary phase in liquid cultures (13). It was also seen that throughout the growth phase the expression was maintained at moderate levels (~ 1000 Miller units). Using a transcriptional fusion of the *pilA2* promoter region with *lacZ*, we observed almost negligible levels of *pilA2* expression (< 50 Miller units) (Fig 3.3).

DISCUSSION

In this study, we characterized, using *in silico* analyses, the *flp*-1 and *flp-2* gene clusters on the *S. meliloti* chromosome and the pSymA megaplasmid, respectively. It was observed that the genes encoding the pilus synthesis machinery in both *flp*-1 and *flp-2* gene clusters are homologous to the *tad* and *rcp* genes, which fulfill a similar role of assembling type IVb pili, in *Aggregatibacter actinomycetemcomitans* (Fig. 3.1, Table 3.2). Using deletions and functional analyses, it would be interesting to confirm that the homologs in *S. meliloti* play a similar role as those in *A. actinomycetemcomitans*. Furthermore, we explored the role of the *flp-2* cluster in establishing symbiosis. PilA2, a PilA1-homolog with 60 % identity, encoded from the *flp-2* system also encodes for a putative pilin subunit. There was no expression of *pilA2* in liquid cultures unlike that seen in *pilA1* (Fig. 3.3). However, like the Δ*pilA1* strain, the Δ*pilA2* strain was shown to be defective in nodulation by 31 % as compared to the Sm1021 WT. A *pilA1pi1A2* double deletion strain presented a non-significant effect. Thus, it can be concluded that both *flp-1* and *flp-2* have a significant role in establishing a successful symbiotic relationship. Based on the lack of expression of *pilA2* in liquid cultures and a significant nodulation impairment by a Δ*pilA2* strain, we can hypothesize that *flp-1* has a primary functional role in establishing initial contact with the host roots while *flp-2* is important in the later stages of the symbiotic relationship, when *flp-1* may play an accessory role.

The above mentioned data from Chapter 3 will be published along with data from our collaborators, Dr. Ann Hirsch (UCLA) and Dr. Nancy Fujishige (LMU). They observed that a higher percentage of nodules induced by the Sm1021 Δ*pilA1*, Δ*pilA2*, and Δ*pilA1*Δ*pilA2* strains remained uninfected or partially infected. However, Sm1021 WT-induced nodules were mostly completely infected. Furthermore, the role of pili in *S. meliloti* biofilm formation was also

explored. It was demonstrated that biofilm formation was significantly reduced in Sm1021 Δ*pilA1* and Δ*pilA2* strains after 48 and 72 h on poly-vinyl chloride microtiter plates. The Δ*pilA1*Δ*pilA2* strain exhibited no additive defect on biofilm formation. The decrease in biofilm formation in pili mutants points to a role of pili in attachment and adhesion to host roots.

REFERENCES

1. **Hirsch AM.** 1992. Developmental Biology of Legume Nodulation. New Phytologist **122:**211-237.
2. **van Rhijn P, Vanderleyden J.** 1995. The *Rhizobium*-plant symbiosis. Microbiol Rev **59:**124-142.
3. **Lum MR, Hirsch AM.** 2002. Roots and their symbiotic microbes: Strategies to obtain nitrogen and phosphorus in a nutrient-limiting environment. Journal of Plant Growth Regulation **21:**368-382.
4. **Jones KM, Kobayashi H, Davies BW, Taga ME, Walker GC.** 2007. How rhizobial symbionts invade plants: the *Sinorhizobium-Medicago* model. Nat Rev Microbiol **5:**619-633.
5. **Gage DJ.** 2004. Infection and invasion of roots by symbiotic, nitrogen-fixing rhizobia during nodulation of temperate legumes. Microbiol Mol Biol Rev **68:**280-300.
6. **Cooper JE.** 2007. Early interactions between legumes and rhizobia: disclosing complexity in a molecular dialogue. J Appl Microbiol **103:**1355-1365.
7. **González JE, Marketon MM.** 2003. Quorum sensing in nitrogen-fixing rhizobia. Microbiol Mol Biol Rev **67:**574-592.
8. **Fujishige NA, Kapadia NN, Hirsch AM.** 2006. A feeling for the micro-organism: structure on a small scale. Biofilms on plant roots. Botanical Journal of the Linnean Society **150:**79-88.
9. **Rodriguez-Navarro DN, Dardanelli MS, Ruiz-Sainz JE.** 2007. Attachment of bacteria to the roots of higher plants. FEMS Microbiol Lett **272:**127-136.
10. **Fujishige NA, Kapadia NN, De Hoff PL, Hirsch AM.** 2006. Investigations of *Rhizobium* biofilm formation. FEMS Microbiol Ecol **56:**195-206.
11. **Fujishige NA, Lum MR, De Hoff PL, Whitelegge JP, Faull KF, Hirsch AM.** 2008. Rhizobium common *nod* genes are required for biofilm formation. Mol Microbiol **67:**504-515.
12. **Lopez D, Vlamakis H, Kolter R.** 2010. Biofilms. Cold Spring Harb Perspect Biol **2:**a000398.
13. **Zatakia HM, Nelson CE, Syed UJ, Scharf BE.** 2014. ExpR coordinates the expression of symbiotically important, bundle-forming Flp pili with quorum sensing in *Sinorhizobium meliloti*. Appl Environ Microbiol **80:**2429-2439.
14. **Rinaudi LV, González JE.** 2009. The low-molecular-weight fraction of exopolysaccharide II from *Sinorhizobium meliloti* is a crucial determinant of biofilm formation. J Bacteriol **191:**7216-7224.
15. **Burrows LL.** 2012. *Pseudomonas aeruginosa* twitching motility: type IV pili in action. Annu Rev Microbiol **66:**493-520.
16. **Craig L, Pique ME, Tainer JA.** 2004. Type IV pilus structure and bacterial pathogenicity. Nat Rev Microbiol **2:**363-378.
17. **Tomich M, Planet PJ, Figurski DH.** 2007. The *tad* locus: postcards from the widespread colonization island. Nat Rev Microbiol **5:**363-375.
18. **Pelicic V.** 2008. Type IV pili: *e pluribus unum*? Mol Microbiol **68:**827-837.
19. **Zhang Y, Tennent JM, Ingham A, Beddome G, Prideaux C, Michalski WP.** 2000. Identification of type 4 fimbriae in *Actinobacillus pleuropneumoniae*. FEMS Microbiol Lett **189:**15-18.
20. **Boyd JM, Dacanay A, Knickle LC, Touhami A, Brown LL, Jericho MH, Johnson SC, Reith M.** 2008. Contribution of type IV pili to the virulence of *Aeromonas salmonicida* subsp. *salmonicida* in Atlantic salmon (*Salmo salar L.*). Infection and immunity **76:**1445-1455.
21. **Bernard CS, Bordi C, Termine E, Filloux A, de Bentzmann S.** 2009. Organization and PprB-dependent control of the *Pseudomonas aeruginosa tad* locus, involved in Flp pilus biology. J Bacteriol **191:**1961-1973.
22. **Schilling J, Wagner K, Seekircher S, Greune L, Humberg V, Schmidt MA, Heusipp G.** 2010. Transcriptional activation of the *tad* type IVb pilus operon by PypB in *Yersinia enterocolitica*. J Bacteriol **192:**3809-3821.
23. **Salomonsson EN, Forslund A-L, Forsberg Å.** 2011. Type IV pili in *Francisella*–a virulence trait in an intracellular pathogen. *Francisella tularensis* and tularemi**:**64.
24. **Roux N, Spagnolo J, de Bentzmann S.** 2012. Neglected but amazingly diverse type IVb pili. Res Microbiol **163:**659-673.
25. **Kachlany SC, Planet PJ, Desalle R, Fine DH, Figurski DH, Kaplan JB.** 2001. *flp-1*, the first representative of a new pilin gene subfamily, is required for non-specific adherence of *Actinobacillus actinomycetemcomitans*. Mol Microbiol **40:**542-554.
26. **Wang Y, Haitjema CH, Fuqua C.** 2014. The Ctp type IVb pilus locus of *Agrobacterium tumefaciens* directs formation of the common pili and contributes to reversible surface attachment. J Bacteriol **196:**2979-2988.

27. **Wairuri CK, van der Waals JE, van Schalkwyk A, Theron J.** 2012. *Ralstonia solanacearum* needs Flp pili for virulence on potato. Mol Plant Microbe Interact **25:**546-556.
28. **Scharf B, Schuster-Wolff-Bühring H, Rachel R, Schmitt R.** 2001. Mutational analysis of *Rhizobium lupini* H13-3 and *Sinorhizobium meliloti* flagellin genes: importance of flagellin A for flagellar filament structure and transcriptional regulation. J Bacteriol **183:**5334-5342.
29. **Götz R, Limmer N, Ober K, Schmitt R.** 1982. Motility and chemotaxis in two strains of *Rhizobium* with complex flagella. J Gen Microbiol **128:**789-798.
30. **Rotter C, Mühlbacher S, Salamon D, Schmitt R, Scharf B.** 2006. Rem, a new transcriptional activator of motility and chemotaxis in *Sinorhizobium meliloti*. J Bacteriol **188:**6932-6942.
31. **Labes M, Pühler A, Simon R.** 1990. A new family of RSF1010-derived expression and lac-fusion broad-host- range vectors for gram-negative bacteria. Gene **89:**37-46.
32. **Schafer A, Tauch A, Jager W, Kalinowski J, Thierbach G, Pühler A.** 1994. Small mobilizable multi-purpose cloning vectors derived from the *Escherichia coli* plasmids pK18 and pK19: selection of defined deletions in the chromosome of *Corynebacterium glutamicum*. Gene **145:**69-73.
33. **Simon R, Priefer U, Pühler A.** 1983. A broad host range mobilisation system for *in vivo* genetic engineering: Transposon mutagenesis in gram negative bacteria. Bio/Technology **1:**783-791.
34. **Sourjik V, Schmitt R.** 1996. Different roles of CheY1 and CheY2 in the chemotaxis of *Rhizobium meliloti*. Mol Microbiol **22:**427-436.
35. **Viands DR, Hansen JL, Thomas EM, Neally JL.** 2005. Registration of 'Guardsman II' alfalfa. Crop Science **45:**2644-2644.
36. **Domínguez-Ferreras A, Muñoz S, Olivares J, Soto MJ, Sanjuán J.** 2009. Role of potassium uptake systems in *Sinorhizobium meliloti* osmoadaptation and symbiotic performance. J Bacteriol **191:**2133-2143.
37. **Olivares J, Casadesus J, Bedmar EJ.** 1980. Method for Testing Degree of Infectivity of *Rhizobium meliloti* Strains. Appl Environ Microbiol **39:**967-970.
38. **Perez-Cheeks BA, Planet PJ, Sarkar IN, Clock SA, Xu Q, Figurski DH.** 2012. The product of *tadZ*, a new member of the *parA*/*minD* superfamily, localizes to a pole in *Aggregatibacter actinomycetemcomitans*. Mol Microbiol **83:**694-711.
39. **Gurich N, González JE.** 2009. Role of quorum sensing in *Sinorhizobium meliloti*-Alfalfa symbiosis. J Bacteriol **191:**4372-4382.
40. **Marketon MM, Gronquist MR, Eberhard A, González JE.** 2002. Characterization of the *Sinorhizobium meliloti sinR*/*sinI* locus and the production of novel N-acyl homoserine lactones. J Bacteriol **184:**5686-5695.
41. **Simon R, O'Connell M, Labes M, Pühler A.** 1986. Plasmid vectors for the genetic analysis and manipulation of rhizobia and other gram-negative bacteria. Methods Enzymol **118:**640-659.
42. **Meade HM, Long SR, Ruvkun GB, Brown SE, Ausubel FM.** 1982. Physical and genetic characterization of symbiotic and auxotrophic mutants of *Rhizobium meliloti* induced by transposon Tn5 mutagenesis. J Bacteriol **149:**114-122.
43. **Gould J, Devey M, Hasegawa O, Ulian EC, Peterson G, Smith RH.** 1991. Transformation of *Zea mays* L. Using *Agrobacterium tumefaciens* and the Shoot Apex. Plant Physiol **95:**426-434.
44. **Bachmann BJ.** 1990. Linkage map of *Escherichia coli* K-12, edition 8 [published erratum appears in Microbiol Rev 1991 Mar;55(1):191]. Microbiol Rev **54:**130-197.
45. **Novick RP, Clowes RC, Cohen SN, Curtiss R, 3rd, Datta N, Falkow S.** 1976. Uniform nomenclature for bacterial plasmids: a proposal. Bacteriol Rev **40:**168-189.
46. **Bateman A, Coin L, Durbin R, Finn RD, Hollich V, Griffiths-Jones S, Khanna A, Marshall M, Moxon S, Sonnhammer EL, Studholme DJ, Yeats C, Eddy SR.** 2004. The Pfam protein families database. Nucleic Acids Res **32:**D138-141.

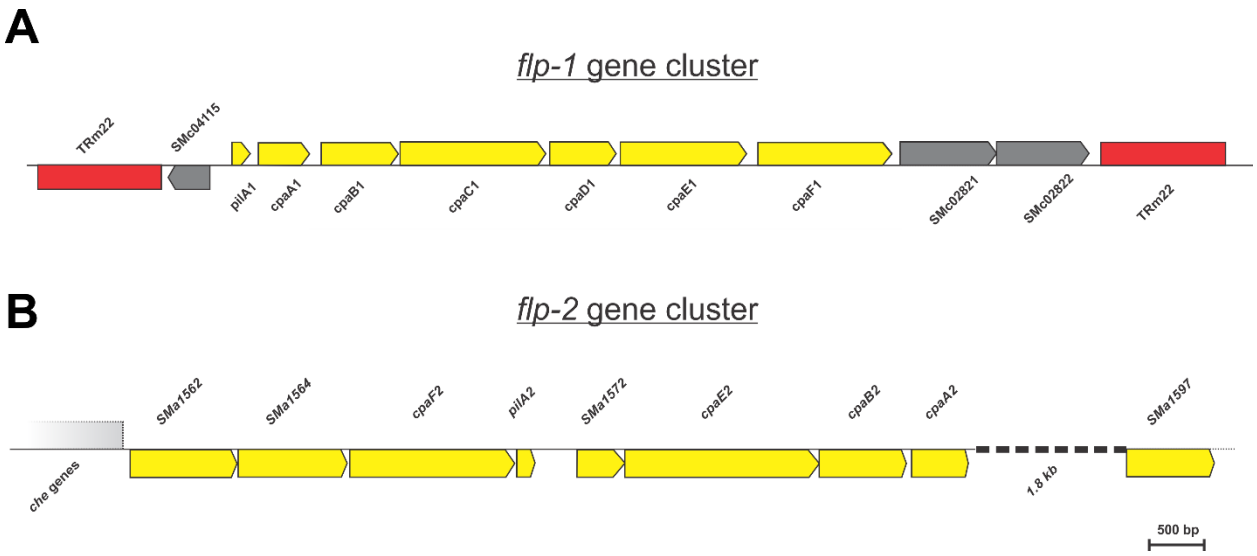

Fig. 3.1: Gene maps of the two *flp* pili clusters in *S. meliloti*. **A.** *flp-1* gene cluster located on the chromosome and **B.** *flp-2* gene cluster located on the pSymA megaplasmid. Open reading frames marked in yellow are putative pilus assembly genes, open reading frames marked in grey are genes unrelated to pili function, and insertion sequences are marked in red. See Table 3.2 for gene descriptions and putative functions.

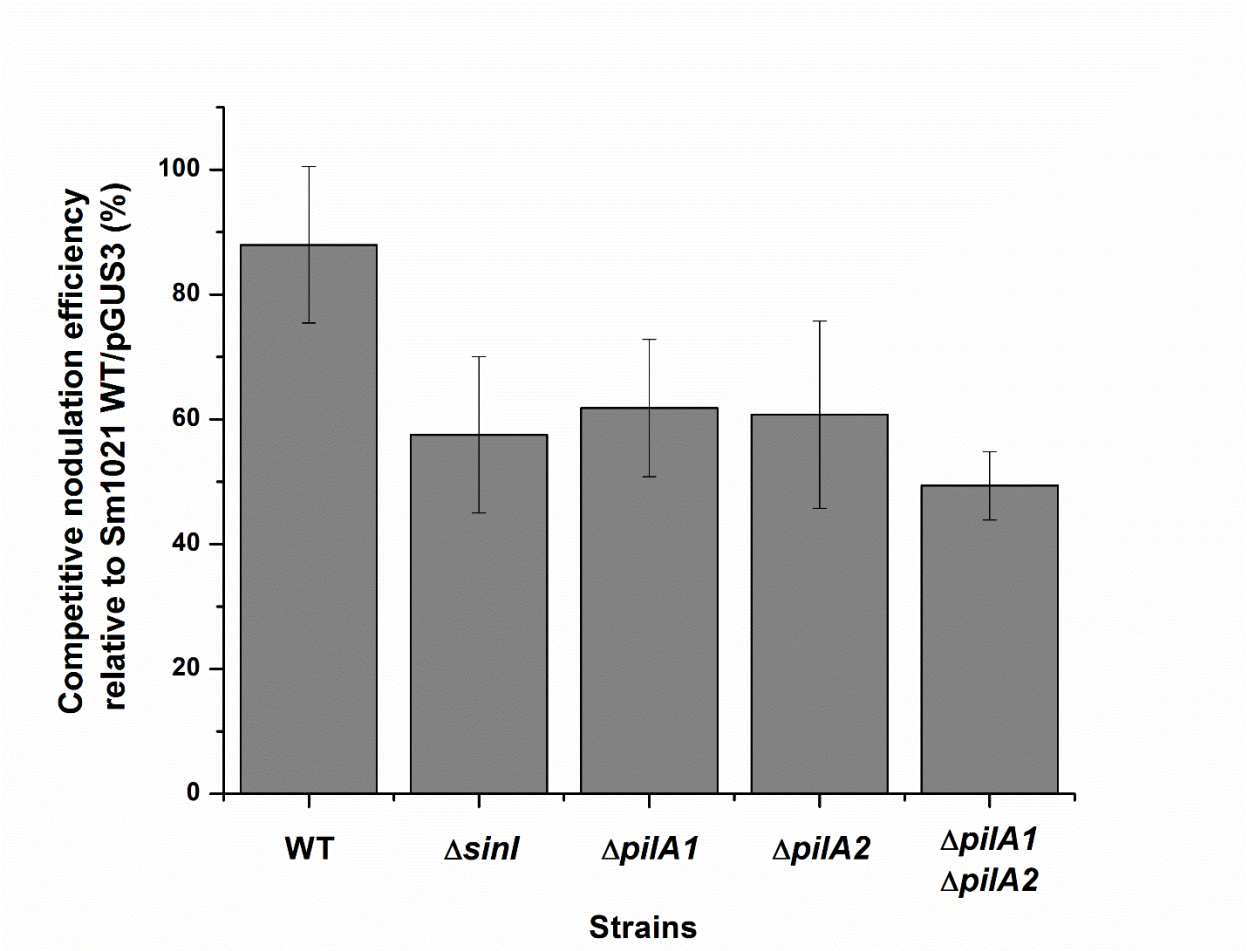

Fig. 3.2: Competitive nodulation assay of Sm1021, Sm1021 Δ*sinI*, Sm1021 Δ*pilA1*, Sm1021 Δ*pilA2* and Sm1021 Δ*pilA1*Δ*pilA2* with Sm1021/pGUS3. Three weeks after germination, alfalfa plants were inoculated with equal numbers of *S. meliloti* cells from both competing strains. After two weeks of incubation, roots were harvested and incubated with the substrate X-Gluc, and blue and white nodule counts per plants were determined. Data are from at least four independent experiments with ten to twelve plants per competition per experiment. Error bars represent standard deviations. Data were analyzed for statistical significance using one-way ANOVA and a post hoc Tukey's test for pairwise comparisons. Data from strains Sm1021 Δ*sinI*, Δ*pilA1*, Δ*pilA2* and Δ*pilA1*Δ*pilA2* were significantly different from the value of Sm1021 WT ($p < 0.05$).

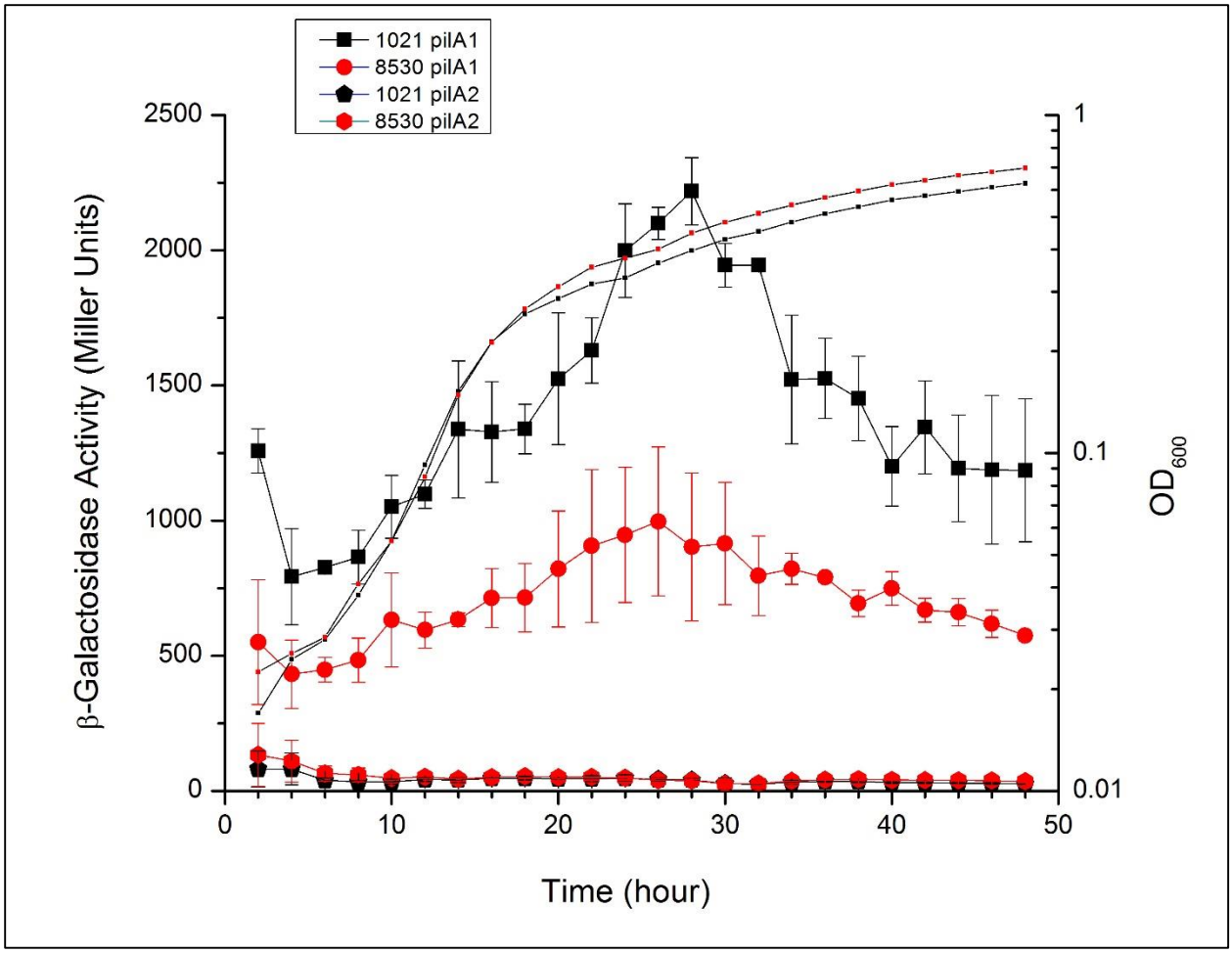

Fig 3.3: Kinetics of *pilA1* and *pilA2* expression in *S. meliloti* Sm1021 and Sm8530 strains during growth over a 48 hour period. Promoter activity in Miller units monitored by *lacZ* reporter gene constructs in strains Sm1021 (black) and Sm8530 (red) and their respective growth curves (OD_{600}) (solid and dotted line). Points represent the mean of three independent experiments and bars represent standard deviations. (Modified from (13))

Table 3.1. Bacterial strains and plasmids

Strains/Plasmids Primers	Relevant Characteristics/Sequence [a]	Reference
Strain		
E. coli		
S17-1	*recA endA thi hsdR* RP4-2 Tc::Mu::Tn7 Tp^r Sm^r	(41)
S. meliloti		
Sm1021	Sm^r; *expR102*::IS*Rm*2011-1 *expR*	(42)
Sm1021Δ*sinI*	Sm^r; Δ*sinI*	(13)
Sm1021Δ*pilA1*	Sm^r; Δ*pilA1*	(13)
Sm1021Δ*pilA2*	Sm^r; Δ*pilA2*	This study
Sm1021Δ*pilA1*Δ*pilA2*	Sm^r; Δ*pilA1*Δ*pilA2*	This study
Plasmid		
pGUS3	Km^r, GUS (β-glucuronidase)	(43)
pK18*mobsacB*	Km^r, *lacZ mob sacB*	(32)

[a] Nomenclature according to Bachmann (44) and Novick *et al*. (45).

Table 3.2. Products of the two *flp* gene clusters of *S. meliloti*, their predicted lengths, sequence identities, and putative functions.

Flp protein [a]	Size (aa) Flp1	Size (aa) Flp2	Identity (%) [b]	Putative Function	Tad homolog
PilA	60	56	60	Major pilin subunit	PilA
CpaA	174	170	39	Prepilin peptidase	TadV
CpaB	269	263	36	Pilus assembly (secretion)	RcpC
CpaC	511	-	N.A.	Secretin	RcpA
CpaD	226	-	N.A.	Pilus assembly	RcpB
CpaE	428	586	42	Pilus localization	TadZ
CpaF	466	497	73	Pilus assembly ATPase	TadA
SMc02821/SMa1564	336	333	46	Pilus assembly (secretion)	TadB
SMc02822/SMa1562	327	321	49	Pilus assembly (secretion)	TadC
SMc02824/-	269	-	N.A.	Pilus assembly (OM)	TadD
SMc04115/SMa1580	138	170	36	Pilus assembly	CpaC-like
SMc04117/SMa1572	204	141	41	Pseudopilin	TadE
SMc04118/SMa1579	194	431	44	Pilus Assembly (IM)	TadG
-/SMa1597	-	260	N.A.	Pilus assembly chaperone	PapD-like

[a] Prediction according to Pfam (protein families database of alignments) (46).

[b] Protein sequence alignment was performed with NCBI Blastp.

Chapter 4 - Cellular stoichiometry of methyl-accepting chemotaxis proteins in *Sinorhizobium meliloti*

HARDIK M. ZATAKIA[1], TIMOFEY D. ARAPOV[1], VERONIKA M. MEIER[2+], BIRGIT E. SCHARF[1, 2*]

(Manuscript in preparation)

[1]Department of Biological Sciences, Life Sciences I, Virginia Polytechnic Institute and State University, Blacksburg, VA 24061, USA

[2] Lehrstuhl für Genetik, Universität Regensburg, D-93040 Regensburg, Germany

Running title: Stoichiometry of *Sinorhizobium meliloti* chemoreceptors

Key words: alfalfa, chemoreceptors, flagellar motor, plant symbiosis, transcriptional control

* For correspondence:
E-mail bscharf@vt.edu
Tel (+1) 540 231 0757
Biological Sciences, Life Sciences I
Virginia Tech
Blacksburg, VA 24061, USA

[+] Present Address: BKD (bloembollenkeuringsdienst), Zwartelaan 2, NL-2161 AL Lisse, Veronika.Wallner@bkd.eu

Attributions: Hardik Zatakia generated the data shown in Figures 4.1 – 4.7, 4.9, and Table 4.3.

ABSTRACT

The chemosensory system in *Sinorhizobium meliloti* has several important deviations from the widely studied enterobacterial paradigm. To better understand the differences between the two systems and how they are optimally tuned, we determined the cellular stoichiometries of the methyl-accepting chemotaxis proteins (MCPs, six transmembrane and two cytosolic) and the histidine kinase CheA in *S. meliloti*. Quantitative immunoblotting was used to determine the total amount of MCPs and CheA per cell in *S. meliloti*. The MCPs are present in the cell in either high abundance (McpV and IcpA), low abundance (McpU, McpX, and McpW), or extremely low abundance (McpT, McpY, and McpZ). The approximate cellular ratio of these three receptor groups is 300:30:1. The chemoreceptor to CheA ratio is 37:1, similar to that seen in *Bacillus subtilis* (23:1) and about 10 times higher than that in *Escherichia coli* (3.4:1). Different from *E. coli*, the high abundance receptors in *S. meliloti* are lacking the carboxy-terminal NWETF pentapeptide that binds the CheR methyltransferase and CheB methylesterase. Using transcriptional *lacZ* fusions, we showed that chemoreceptors are positively controlled by the master regulators of motility, VisNR and Rem. In addition, FlbT, a class IIA transcriptional regulator of flagellin, also positively regulates the expression of most of the chemoreceptors except for McpT and McpY, placing chemoreceptors as class III genes. Taken together, these results demonstrate that the chemosensory complex and the adaptation system in *S. meliloti* deviates significantly from the established enterobacterial paradigm, but shares some similarities with that of *B. subtilis*.

INTRODUCTION

Chemotaxis is a mechanism by which bacteria rapidly respond to their immediate environment, ultimately moving toward favorable niches and moving away from repellents (1-3). Chemotaxis has been implicated in various bacterial processes like pathogenicity, nodulation, and biofilm production (4, 5). It has been most widely studied in the enterobacterium *Escherichia coli*, which swims in a series of runs and tumbles through the rotation of peritrichous flagella (6). Runs are driven by counter-clockwise (CCW) flagellar rotation, leading to the formation of a flagellar bundle with synchronous rotation speeds. In *E. coli*, tumbles are achieved by the reversal of one or more flagella in the clockwise (CW) direction which causes the flagellar bundle to splay apart, randomly reorienting the cell in three dimensional space (7). However, some bacterial flagellar motors exhibit only unidirectional rotation. In the case of *Rhodobacter sphaeroides*, the single polar flagellum stops, causing the cell to tumble, while resuming flagellar rotation results in a straight run (8). In *Sinorhizobium meliloti*, the asynchrony caused by the slowing down of one or more of the strictly CW rotating flagella causes the cell to tumble (9-11).

Bacterial chemotaxis is accomplished due to the sensing of environmental signals by receptors called methyl-accepting chemotaxis proteins (MCPs). *E. coli* has four transmembrane MCPs: Tap, Tar, Trg, and Tsr. While Tap senses dipeptides, Tar mediates taxis towards aspartate and maltose. Trg recognizes ribose and galactose, and Tsr responds to serine. A fifth receptor, Aer, which is anchored to the inside of the cytoplasmic membrane, acts as an oxygen sensor (12, 13). The number of different chemoreceptors varies within species. Although *Mesorhizobium loti* has only one putative chemoreceptor gene, *Vibrio cholerae* has 45 (14). Chemoreceptors form stable homodimers which are in turn arranged in trimers. These ‘trimers of dimers’ along with other cytoplasmic chemotaxis proteins are packaged in large hexagonal arrays called ‘chemoreceptor

clusters' (15). MCPs typically consist of a periplasmic ligand-binding domain, two membrane-spanning helices, and a cytoplasmic signaling domain (12). Binding of ligand to the periplasmic domain causes a piston-like movement through the transmembrane domains to the cytoplasmic domain where it acts as a signal to the cytosolic chemotaxis proteins. While the periplasmic domains of MCPs are highly diverse to accommodate various ligands, the cytoplasmic signaling domains are highly conserved, even amongst different species (2). A two-component system using a histidine-aspartate phosphorelay mediates the chemotactic signal transduction from the chemoreceptor cluster to the flagellar motors. The first component, CheA, is the histidine kinase that binds to the cytoplasmic domain of the MCPs via a coupling protein, CheW (2, 3). The second component, CheY, is the response regulator that interacts with the flagellar motor complex when phosphorylated, thereby controlling its rotation. Binding of an attractant to the periplasmic domain of an MCP induces a conformational change in the cytoplasmic domain that inhibits the autophosphorylation of CheA. In *E. coli*, when CheA is inactive and no signal is being passed to the flagellar motors, continued CCW rotation results in a run. In the absence of a bound attractant or presence of a repellent, ATP-dependent CheA autophosphorylation is stimulated. Phosphorylated CheA (CheA-P) transfers the phosphate group to a conserved aspartate residue in CheY (16). CheY-P interacts with FliM of the flagellar motor complex and signals the motor to switch to the CW direction, subsequently resulting in a tumble (17, 18). In *E. coli*, CheZ is a phosphatase which increases the dephosphorylation rate of CheY-P and thereby allows for signal termination (19-21). An adaptation system involving CheR and CheB is employed for increased sensitivity and real-time modulation of chemotactic activity based on the local environment. CheR is a methyltransferase which constitutively adds methyl groups on conserved sites on the cytoplasmic signaling domain of MCPs. CheB acts as a methylesterase and is activated through its

phosphorylation by CheA-P (2, 14). In *E. coli*, only the high abundant MCPs, Tar and Tsr, have a conserved pentapeptide NWETF at their carboxy terminus, which serves as the site for CheR and CheB docking (22). The concerted addition and removal of methyl groups by CheR and CheB, respectively, brings about the conformational changes in MCPs required for the resetting and adaptation of the chemotaxis system (23, 24).

The importance of bacterial chemotaxis in establishing symbiosis with plant hosts has been well documented for members of the *Rhizobiaceae* family including *S. meliloti* (25-27). Recent studies of *S. meliloti* motility and chemotaxis have uncovered marked deviations from the enterobacterial paradigm (14, 28). Unlike *E. coli*, *S. meliloti* not only has six transmembrane chemoreceptors (McpT-McpX, and McpZ) but also has two soluble cytosolic receptors (McpY and IcpA). Our group has shown that the chemoreceptor McpU plays a role in host interaction by sensing the plant-derived amino acid, proline (29). However, the function of the remaining seven chemoreceptor proteins is not known. Furthermore, *S. meliloti* does not utilize a CheZ phosphatase but employs an indirect phosphate sink mechanism for signal termination. Here, phosphate groups from the response regulator CheY2 are shuttled back via CheA to an additional response regulator protein, CheY1 (30). *S. meliloti* possesses three additional proteins involved in chemotaxis as compared to *E. coli* , namely CheD, CheS, and CheT (31). A CheD analog in *Bacillus subtilis* serves as an MCP deamidase and thus plays a role in adaptation (32). However, it is unclear whether *S. meliloti* CheD exerts a similar function. CheS and CheT have no homologs in enteric bacteria but display homology to some unassigned proteins in other α-proteobacteria like *Caulobacter crescentus* and *Rhizobium leguminosarum* (33). The function of CheT in chemotaxis is currently unknown. We have established that CheS enhances phosphate flow from CheA-P to CheY1 by increasing the affinity between CheA-P and CheY1 by 100-fold (33). The one kinase-two response regulator

system and presence of an auxiliary protein allows the implementation of tunable switch-like signal processing (34).

Up to now, two studies have investigated the cellular quantities of bacterial chemotaxis proteins, one in *E. coli* and one in *B. subtilis* (35, 36). While protein amounts may change depending on growth conditions and nutrient availability, cellular ratios of chemotaxis proteins were fairly robust. Both studies also revealed that ratios between certain proteins, such as CheA and CheW, remained constant, while the ratio of others, such as CheA and the MCPs, differed greatly between species. To gain a better understanding of deviations evolved in the *S. meliloti* chemotaxis system and to understand how the system is tuned for optimum performance and sensitivity, we determined the cellular amounts and ratios of all eight chemoreceptors and CheA in *S. meliloti* using quantitative immunoblots. Furthermore, we explored the regulation of chemoreceptor gene expression within the flagellar hierarchy. Ultimately, computational models can be used to simulate the interactions of all chemotaxis proteins and to evaluate the chemotaxis system holistically under various physiologically relevant conditions (37).

MATERIALS AND METHODS

Bacterial strains and plasmids

Derivatives of *E. coli* K12 and *S. meliloti* MV II-1 and the plasmids used are listed in Table 4.1.

Media and growth conditions

E. coli strains were grown in lysogeny broth (LB) (38) at indicated temperatures. *S. meliloti* strains were grown in TYC (0.5 % tryptone, 0.3 % yeast extract, 0.13 % $CaCl_2.6H_2O$ [pH 7.0]) (39) or SMM (Sinorhizobium motility medium; RB [6.1 mM K_2HPO_4, 3.9 mM KH_2PO_4, 1 mM $MgSO_4$, 1 mM $(NH_4)_2SO_4$, 0.1 mM $CaCl_2$, 0.1 mM NaCl, 0.01 mM Na_2MoO_4, 0.001 mM $FeSO_4$, 2 µg/l biotin] (40), 0.2 % Mannitol. 2 % TY) (41). Motile cells for immunoblots were grown in SMM for two days, diluted to an OD_{600} of 0.02 and incubated at 30 °C to an OD_{600} of 0.25. The following antibiotics were used in their final concentrations: for *E. coli*, ampicillin at 100 µg/ml, kanamycin at 50 µg/ml and tetracycline at 10 µg/ml; for *S. meliloti*, neomycin at 120 µg/ml, streptomycin at 600 µg/ml, and tetracycline at 10 µg/ml.

Genetic and DNA manipulations

S. meliloti DNA was isolated and purified as described previously (42). Plasmid DNA, DNA fragments or PCR products were purified according to manufacturers' instructions, and PCR amplification of chromosomal DNA was carried out according to published protocols (42). The Δ*flbT* strain was generated *in vitro* by overlap extension PCR as described (43). Constructs containing the mutations were cloned into the mobilizable suicide vector pK18*mobsac*B, used to transform *E. coli* S17-1, and conjugally transferred to *S. meliloti* by filter mating (44). Allelic replacement was achieved by sequential selections on neomycin and 10 – 15 % sucrose as

described previously (42). Confirmation of allelic replacement and elimination of the vector was obtained by gene-specific primer PCR and DNA-sequencing. Derivatives of the broad-host-range plasmids pPHU235 and pPHU236 were used to transform *E. coli* S17-1 and conjugally transferred to *S. meliloti* by streptomycin-tetracycline double selection as described above (45).

β-galactosidase assays

Cultures of *S. meliloti* containing *lacZ* fusions grown on over-layered Bromfield agar (0.04 % Bacto tryptone, 0.01 % yeast extract, 0.01 % $CaCl_2.2H_2O$) plates were sampled, diluted 1:1 in Z buffer (46), permeabilized with 1 drop of toluene, and assayed for β-galactosidase activity by the method of Miller (46) as previously described (47).

Purification of recombinant proteins

McpT-LBD (ligand-binding domain) (aa 30 – 178) was expressed from pBS1030, McpU-LBD (aa 40 – 287) was expressed from pBS0353, McpV-LBD (aa 31 – 189) from pBS0409, McpW-LBD (aa 39 – 180) from pBS1031, McpX-LBD (aa 34 – 320) from pBS0352, McpZ-LBD (aa 39 – 445) from pBS0426, IcpA from pRU2550, and CheA from (pBS0057) in *E. coli* ER2566 (Table 4.1) as described by Riepl *et al.* (48). Briefly, cells were grown to an OD_{600} of 0.6 - 0.8 at 37 °C in LB, and expression was induced by 0.3 mM isopropyl-β-$_D$-thiogalactopyranoside (IPTG) at 16 °C for 16 h. Cells were harvested, resuspended in IMPACT buffer (20 mM Tris/HCl, pH 8.0, 500 mM NaCl, and 1 mM EDTA), and lysed by three passages through a French pressure cell at 20,000 lb/in^2 (SLM Aminco, Silver Spring, MD). A modified IMPACT buffer (20 mM Tris/HCl, pH 8.0, 2 M NaCl, and 1 mM EDTA) along with Halt™ Protease Inhibitor cocktail (Life Technologies) was used for CheA purification. The soluble fraction was loaded on a Chitin agarose (NEBiolabs,

Beverly, MA) column (6 cm x 5 cm) and Intein-mediated cleavage was induced by equilibration of the column with IMPACT buffer containing 50 mM dithiothreitol (DTT) and further incubation at 4 °C for two to three days. Proteins were eluted with IMPACT buffer and pooled fractions of each protein were further purified by fast-performance liquid chromatography (FPLC, Äktaprime Plus, GE Healthcare) gel filtration on HiPrep 26/60 Sephacryl S-200 HR (GE Healthcare). The column was equilibrated and developed using 80 mM Na_2HPO_4, 20 mM NaH_2PO_4, 100 mM NaCl, 5 % (v/v) glycerol, pH 7.5 at 0.5 ml/min, and protein-containing fractions were combined.

McpY protein was overproduced in inclusion bodies from plasmid pRU2790 in *E. coli* BL21(DE3) (Table 4.1). Cells were grown at 37 °C in LB at 300 rpm to an OD_{600} of 0.6 - 0.8, and expression was induced by 1 mM IPTG. Cells were harvested after 4 h of incubation at 37 °C, resuspended in 20 ml 0.5 mM EDTA, 20 mM Tris/HCl, pH 7.5, and cell lysates were prepared as described before. The lysate was centrifuged at 55,000 g and 4 °C for 20 min, the soluble fraction was discarded, and the pellet was washed twice with 20 mM Tris/HCl, pH 7.5, 1 % (v/v) Triton X-100, 1 mM EDTA. Inclusion bodies were suspended in 10 ml denaturation buffer (8 M urea, 5 mM DTT, 50 mM Tris/HCl, pH 8.0), centrifuged and the supernatant was filtered through a 0.2 µm cellulose acetate syringe filter. Ten-ml samples were subjected to FPLC (Äktaprime Plus, GE Healthcare) gel filtration on HiPrep 26/60 Sephacryl S-200 HR (GE Healthcare). The column was equilibrated and the protein eluted in denaturation buffer at 0.5 ml/min, and protein-containing fractions were combined. The protein was then refolded by dialysis against a 30-fold volume of 50 mM Tris/HCl, pH 8.0, 1 mM EDTA, 1 mM DTT, 20 % (v/v) glycerol, 100 mM NaCl for 24 h at 4 °C. Subsequently, dialysis was performed with 50 mM Tris/HCl, pH 8.0, 1 mM EDTA, 1 mM DTT, 10 % (v/v) glycerol, 100 mM NaCl for 24 h at 4 °C. Lastly, the protein was dialyzed in phosphate-

buffered saline (PBS; 80 mM Na_2HPO_4, 20 mM NaH_2PO_4, 100 mM NaCl, pH 7.5) for 24 h at 4 °C and stored in 5 % glycerol at -80 °C.

Immunoblotting

Polyclonal antibodies raised against purified ligand-binding domains of McpT-McpX, and McpZ were purified as described here (39). Briefly, one mg of purified protein was separated on a 12.5 % acrylamide gel and transferred to a nitrocellulose membrane (Amersham Protran 0.45 NC, GE Healthcare). Proteins were stained on the membrane using 1 % Ponceau S and the protein containing membrane was cut into pieces (1 cm x 0.5 cm). Membrane pieces were then incubated 16 h at 4 °C with two ml of crude serum. The blots were washed three times with PBS/0.1 % bovine serum albumin (BSA), twice with PBS/0.1 % BSA/0.1 % Nonidet P40, and three times with PBS/0.1 % BSA for 5 min per wash step. The specific antibodies were eluted from the membrane by incubating with 750 µl of 0.2 M glycine/HCl, pH 2.5 for 1 min followed by neutralization with 375 µl of prechilled 1M potassium phosphate, pH 9.0. The elution was repeated once and the combined eluates were dialyzed three times against PBS (30x) and stored at -80 °C. Samples for immunoblots were prepared as follows. For whole cell extracts, one ml cell culture of RU11/001 at OD_{600} 0.250 ± 0.002 was pelleted and resuspended in 15 µl of supernatant and 15 µl of Laemmli Buffer (4.5 % SDS, 18.75 mM Tris/HCl pH 6.5, 43.5 % Glycerin, 0.0125 % Bromophenol Blue, and 5 % β-mercaptoethanol). Samples were then boiled at 100 °C for 10 min and stored at -30 °C. Control samples comprised cell extracts from appropriate deletion strains treated identically. Standard curves were made by adding defined quantities of purified protein to appropriate deletion strain lysates. Immunoblots were carried out as described (49). Briefly, proteins from cell extracts were separated on 12.5 % acrylamide gels and then transferred to a 0.45 µm nitrocellulose membrane. The membrane was blocked overnight with 5 % non-fat dry milk

solution made in PBS/0.1 % Tween 20. The blots were probed with a 1:200 dilution of purified antibodies or 1:5000 dilution of crude serum. Mouse monoclonal anti-GFP was used at a 1:5,000 dilution to detect McpW-eGFP fusion protein. Blots were washed three times with PBS/0.1 % Tween 20 and then probed with 1:5,000 dilution of donkey anti-rabbit horseradish peroxidase-linked whole antibody. The blots were washed three times with PBS/0.1 % Tween 20. Detection was performed by chemiluminescence (Amersham ECL Western Blotting Detection Kit or SuperSignal™ West Femto Maximum Sensitivity Substrate for McpY) using Hyperfilm ECL (GE Healthcare). Images were captured by using an Epson Perfection 1640SU scanner and intensities were quantified using ImageJ. Variations caused by improper blotting of proteins and manual error were minimized by only using those blots for quantification that had a standard curve with an R^2 value of > 0.95. Values shown in Table 4.3 are obtained from six independent immunoblots.

Protein concentrations were initially determined by the standard Bradford Assay using Quick Start™ Bradford 1x Dye Reagent (BIO-RAD) and a bovine serum albumin standard curve as per the manufacturer's protocol. Amounts of proteins stated in the figure legends were calculated using this method. Accurate protein concentrations were obtained by quantitative amino acid analyses after total acid hydrolysis performed at the Protein Chemistry Lab, Texas A&M University.

Determination of dry weight

Dry weight was determined as previously described (18). Five 25-ml samples were harvested by centrifugation, resuspended in 77 mM ammonium acetate, pH 7.0, transferred to tared Sarstedt tubes, centrifuged, washed in the same buffer, and lyophilized for 3 days. Medium and buffer were prefiltered (0.2 μm). A value of 0.053 ± 0.008 mg/ml of culture (mean ± SD for five determinations) was obtained.

RESULTS

The *mcp* genes are part of the flagellar regulon and transcribed as class III genes: Previously, we have shown that all genes in the flagellar gene cluster are organized in a four-class hierarchy (41, 49). The LuxR-type VisNR and the OmpR-like Rem act as class IA and IB transcriptional regulators, respectively. They control the expression of class II (comprising flagellar assembly and motility genes) and class III (comprising flagellin and chemotaxis genes), which require the expression of class IIA for expression (41). While *icpA* is the first gene of the *che* operon and therefore classified as a class III gene, the regulation of the remaining seven chemoreceptor genes is unknown. With the exception of *mcpW*, which is co-transcribed with a putative *cheW*, the remaining *mcp* genes are monocistronic and all are scattered throughout the genome (47, 50). To answer whether expression of those *mcp* genes, not located in the flagellar gene cluster, follows the same control mechanisms, we used the broad-host-range plasmids pPHU235 and pPHU236 as vectors for transcriptional fusions of six of the *mcp* promotors, and of the promoter of the *che* operon as a control (47). The resulting *lacZ* fusion plasmids were transferred to RU11/001 (WT), RU11/814 (Δ*visNR*), and RU11/555 (Δ*rem*), and assayed for ß-galactosidase activity as listed in Table 4.2. Both, *visNR* and *rem*, were required for the transcription of chemoreceptor genes. In most cases, promoter activities dropped to zero. Only two of the genes with weaker promoters, namely *mcpT* and *mcpY*, exhibited some residual transcriptional activity. In conclusion, *mcp* genes are part of the flagellar regulon and positively regulated by its master transcriptional regulators. We also analyzed the transcription of receptor genes in a strain carrying a deletion in the class IIA flagellar regulatory gene, *flbT*. In *C. crescentus*, deletion of *flbT* results in increased levels of flagellin synthesis (51, 52). FlbT in *C. crescentus* is therefore a negative regulatory protein for flagellin protein synthesis (53). In contrast, *S. meliloti* FlbT is a positive regulator for flagellin and

chemotaxis gene expression, as examined by reporter gene and western blot analysis (data not shown). In *Brucella melitensis*, FlbT plays a similar role and is an activator of the flagellin, FliC (54). When we analyzed the transcription of *mcp* genes in RU13/110, a strain carrying a deletion in *flbT* (Table 4.2), the activities of most promoters clearly decreased to residual activities between 1% and 20%. However, two exceptions were noticed. The *mcpT* and *mcpY* promoters still exhibited 80% activity levels in Δ*flbT* compared to those measured in wild type. Therefore, in contrast to the majority of the chemoreceptor genes, these two genes are not regulated by FlbT.

Quantification of transmembrane chemoreceptors

To quantify the six transmembrane chemoreceptors (McpT-X, and McpZ), we raised and purified polyclonal antibodies against the periplasmic ligand-binding region of each MCP. Thus, we avoided generating antibodies targeting the highly conserved cytosolic domains and obviated cross reactivity with other chemoreceptors in the cell extracts. Stable expression of proteins is important for consistent results. In *S. meliloti*, expression of flagellar and chemotaxis genes (including the *che* operon) are under a tight transcriptional control through the activity a class IB regulator, Rem (55). Furthermore, it has been previously shown that chemoreceptors in *S. meliloti* follow the expression pattern of Rem, and are maximally expressed at mid-exponential phase (56). Thus, an OD_{600} of 0.25 was selected for harvesting cells for immunoblots (47). Standard curves were established by adding varying amounts of the purified periplasmic regions of each MCP to cell extracts of the corresponding deletion strains. Signals from immunoblots were detected using X-ray films with different exposures, and band intensities were determined with ImageJ. Six independent immunoblots containing three wild-type cell lysates each were used to quantify each protein.

A representative blot for McpV (65.34 kDa) showed a distinct band below the 75 kDa marker in lanes 2-4 containing wild-type cell extracts, which is markedly absent in lane 1 containing the *mcpV* deletion cell extract (Fig. 4.1). McpV-LBD (20.23 kDa) which was used to create a standard curve can be seen below the 25 kDa marker in the lanes containing *mcpV* deletion cell extracts and purified McpV-LBD in decreasing amounts. A similar blot is seen for McpZ (90.15 kDa), with varying amounts of McpZ-LBD (45.97 kDa) added to extracts from the *mcp*Z deletion strain (Fig. 4.2).

Purified McpU-LBD (27.66 kDa) and McpX-LBD (32.55 kDa) were used to quantify the corresponding proteins in *S. meliloti* wild-type cell extracts. Although the proteins were separated under denaturing conditions and a reducing agent was added to the loading buffer, both proteins existed in monomeric and dimeric forms (Figs. 4.3 & 4.4). The McpU-LBD standard curve showed that the ratio of monomer to dimer was approximately 80:20. In contrast, McpX-LBD mainly existed as a dimer with the ratio of monomer to dimer being approximately 20:80. Thus, the intensities of both bands in each case, monomer and dimer, were added for the quantification of McpU and McpX.

For immunoblots probed with anti-McpW antibodies, McpW-LBD (15.96 kDa) was used as a standard. We observed that the McpW (72.50 kDa) band in wild-type extracts overlapped with a cross-reacting band of similar size, as indicated in Fig. 4.5 by the more intense band marked by an asterisk compared to lane 4 containing the *mcpW* deletion strain extract. To confirm that the additional band intensity was caused by McpW, we loaded extracts of strain RU13/143 expressing McpW-eGFP from its native chromosomal locus in lane 1 and 3. McpW-eGFP (104.84 kDa) appeared above the 100 kDa marker band and the band intensity of the 75-kDa band was decreased to that of the *mcpW* deletion strain (Fig. 4.5, lane 4). Next, we subtracted the 75-kDa band

appearing in the *mcpW* deletion strain extract from the 75-kDa band of the wild-type extract to quantify McpW. Additionally, we quantified the band intensity of McpW-eGFP. Both quantification methods yielded the same amount of McpW.

To quantify the number of MCP molecules per cell, we determined the number of *S. meliloti* cells in one ml of cell culture grown in minimal medium at OD_{600} 0.25. Using serial dilutions and spread plating, we determined that one ml cell culture of *S. meliloti* at OD_{600} 0.25 contained 2.56 ± 0.31 x 10^8 cells. For the six transmembrane chemoreceptors, the numbers ranged from a few molecules to several hundred per cell (Table 4.3). McpT-LBD could not be detected between 0.1 µg to 1.0 pg using either crude serum or affinity-purified antibodies raised against McpT-LBD. Moreover, no band corresponding to McpT was detected in the WT cell lysates. Of the five transmembrane receptors quantified, McpV was the most abundant chemoreceptor, being present in more than six fold higher numbers compared to McpU (Table 4.3). The others followed the order: McpU > McpX > McpW > McpZ.

Quantification of cytosolic chemoreceptors

For the two cytosolic chemoreceptors, IcpA (57.54 kDa) and McpY (64.30 kDa), full length proteins were used to serve as controls for a standard curve and polyclonal antibodies already existed (56). IcpA was one of the most abundant receptor at levels comparable to McpV (Fig. 4.6). The amounts of McpY were the lowest of any chemoreceptor (Fig. 4.7) (Table 4.3).

Quantification of CheA

To determine the stoichiometry of chemoreceptors to the kinase CheA and to compare our data with the *E. coli* and *B. subtilis* studies (35, 36), we quantified the cellular amounts of CheA.

Purified full length CheA (81.12 kDa) and existing polyclonal antibodies were used for quantification (30). A typical blot (Figure 4.8) exhibited a band above the 75 kDa marker in WT cell lysates, which was absent in the lane containing Δ*cheA* cell lysates. A standard curve was established by adding increasing amounts of the purified full-length CheA protein. As shown in Table 4.3, CheA was found to present in low abundance at levels similar to the low abundance chemoreceptor, McpW.

DISCUSSION

Chemotaxis is a complex process that aids in the survival of a bacterial cell. Since it consumes considerable amounts of a cell's energy, tight regulation on the expression of all components of the chemotaxis machinery is required (57). Our group has shown previously that motility and chemotaxis genes in the *S. meliloti* flagellar regulon are expressed in a transcriptional hierarchy (41). Our current studies expand the previously established scheme by including the *mcp* genes as class III genes and FlbT (class IIA) as a positive regulator for class III genes (with *mcpT* and *mcpY* as exceptions). Similar to the coordinated regulation in enterobacteria (58), class III gene expression is dependent on the completion of basal body structure and flagellar export. This suggests that a control mechanism related to the one operating in enterobacteria exists in *S. meliloti*.

A number of different chemotaxis proteins have to interact to bring about the desired changes in motility. It can be hypothesized that the cellular amounts of these proteins may be at the exact levels tuned for optimal performance. We set out to quantify the amounts of chemoreceptors and the histidine kinase CheA in an *S. meliloti* cell. The total number of all eight chemoreceptors in an *S. meliloti* cell is 690 ± 142 (Table 4.3). This is extremely low as compared to 59,960 ± 5,960 in *B. subtilis* and 26,000 ± 1800 in *E. coli* (35, 36). From our viable cell counts and dry weight analyses, it is evident that an *S. meliloti* cell is about half the size of an *E. coli* cell (18). The smaller size may enable the *S. meliloti* cell to function efficiently with a lower number of chemoreceptors. Fluorescence studies with GFP-tagged chemoreceptors showed that not all cells from the population have expressed GFP-fusions. Therefore, it is possible that the actual numbers of chemotaxis proteins per cell is higher. However, this observation does not have any effect on protein ratios.

In *E. coli*, the chemoreceptors are present in either high (Tsr and Tar) or low (Trg, Tap, and Aer) abundance (22, 35). Similarly in *S. meliloti*, the chemoreceptors are present in high (McpV and IcpA), low (McpU, McpW, and McpX), or extremely low (McpZ and McpY) abundance. The approximate ratios of receptors are 1 (McpT, Y, Z) : 30 (McpU, W, X) : 300 (McpV and IcpA). The high abundance of McpV and IcpA correlates with the CheA- and CheW-independent localization of these receptors in *S. meliloti* (56). It can be hypothesized that their abundance enables them to localize at the pole independently of other chemotaxis proteins and, in fact, act as the scaffold receptors to recruit other receptors to localize at the poles. The function of McpV and IcpA in sensing environmental cues is not known and the subject of current investigations. However, the low-abundance receptor McpU has been identified as proline sensor (29). Additionally, we found indications suggesting McpU functions as a general amino acid receptor (Webb and Scharf, personal communication). In *B. subtilis*, the major receptors for taxis towards all amino acids and sugars, McpB and McpC, are also present in relatively lower abundance in the cell (36). This feature might be commonplace in soil bacteria as it is not seen in *E. coli*, where the high abundance receptor Tsr mediates taxis toward serine and Tar mediates taxis towards aspartate and maltose (22).

Finally, two of the three receptors that are present in very low numbers (McpT and McpY) appear to be regulated differently from the other receptors: (i) the transcription of both genes is not controlled by the class IIA regulator FlbT, and (ii) promoters of both genes exhibit 30-40 % residual expression in alfalfa root nodules while all other chemoreceptors are not expressed (data not shown). This different mechanism of regulation suggests a role of McpT and McpY *in planta* and could be the cause of their extremely low expression levels under our assay conditions.

In *E. coli*, the presence of the carboxy-terminal pentapeptide, representing the CheR and CheB binding site, correlates with receptor abundance (59, 60). Despite the absence of this binding motif in low-abundance receptors of *E. coli*, receptor methylation and demethylation occur efficiently due to assistance by high-abundance receptors within chemoreceptor clusters (61). In *S. meliloti*, high abundance receptors McpV and IcpA are lacking the motif. Instead, only McpT, McpW, McpX, and McpY, which are low or extremely-low abundance chemoreceptors possess the conserved carboxy-terminal pentapeptide (47). The adaptation process in *S. meliloti* has not been analyzed and the composition of chemoreceptor arrays is unknown. Therefore, the reason for the opposite correlation of receptor abundance and presence of the CheR/CheB binding motif remains to be elucidated.

The ratio of chemoreceptors to CheA in *S. meliloti* is approximately 37:1. This ratio is lower in *E. coli* (3.4:1) but is closer to the levels in *B. subtilis* (23:1) (35, 36). It remains to be investigated, whether the structure of the CheA-CheW-receptor complex is different in *S. meliloti* from the one described for *E. coli* (62). It can be hypothesized that the ratios of chemotaxis proteins across genera are adapted and optimized according to their lifestyle. Our ongoing efforts to confirm the amounts of cytosolic chemotaxis proteins would provide us with a snapshot of the chemotaxis protein stoichioimetry in an *S. meliloti* cell. This, in turn, would shed more light on the various unique features of the *S. meliloti* chemosensory system.

ACKNOWLEDGEMENTS

This study was supported by grant Scha914/2-1/2 from the Deutsche Forschungsgemeinschaft and NSF grant MCB-1253234. We are indebted to Michael Süss for construction of plasmid pRU2550, Verena Wagner for the purification of IcpA, Jinny Johnson for her help with the amino acid analyses, and the members of the Scharf lab for critical reading of the manuscript.

REFERENCES

1. **Bren A, Eisenbach M.** 2000. How signals are heard during bacterial chemotaxis: protein-protein interactions in sensory signal propagation. J Bacteriol **182:**6865-6873.
2. **Wadhams GH, Armitage JP.** 2004. Making sense of it all: Bacterial chemotaxis. Nat Rev Mol Cell Bio **5:**1024-1037.
3. **Porter SL, Wadhams GH, Armitage JP.** 2011. Signal processing in complex chemotaxis pathways. Nat Rev Microbiol **9:**153-165.
4. **Broek AV, Vanderleyden J.** The role of bacterial motility, chemotaxis, and attachment in bacteria-plant interactions.
5. **Pratt LA, Kolter R.** 1998. Genetic analysis of *Escherichia coli* biofilm formation: roles of flagella, motility, chemotaxis and type I pili. Mol Microbiol **30:**285-293.
6. **Stock JB, Surette MG.** 1996. Chemotaxis. Escherichia coli**:**1103-1129.
7. **Macnab RM.** 2003. How bacteria assemble flagella. Annu Rev Microbiol **57:**77-100.
8. **Armitage JP, Macnab RM.** 1987. Unidirectional, intermittent rotation of the flagellum of *Rhodobacter sphaeroides*. J Bacteriol **169:**514-518.
9. **Platzer J, Sterr W, Hausmann M, Schmitt R.** 1997. Three genes of a motility operon and their role in flagellar rotary speed variation in *Rhizobium meliloti*. J Bacteriol **179:**6391-6399.
10. **Scharf B, Schmitt R.** 2002. Sensory transduction to the flagellar motor of *Sinorhizobium meliloti*. Journal of molecular microbiology and biotechnology **4:**183-186.
11. **Attmannspacher U, Scharf B, Schmitt R.** 2005. Control of speed modulation (chemokinesis) in the unidirectional rotary motor of *Sinorhizobium meliloti*. Molecular microbiology **56:**708-718.
12. **Falke JJ, Hazelbauer GL.** 2001. Transmembrane signaling in bacterial chemoreceptors. Trends Biochem Sci **26:**257-265.
13. **Parkinson JS, Hazelbauer GL, Falke JJ.** 2015. Signaling and sensory adaptation in *Escherichia coli* chemoreceptors: 2015 update. Trends Microbiol **23:**257-266.
14. **Szurmant H, Ordal GW.** 2004. Diversity in chemotaxis mechanisms among the bacteria and archaea. Microbiol Mol Biol Rev **68:**301-319.
15. **Hazelbauer GL, Falke JJ, Parkinson JS.** 2008. Bacterial chemoreceptors: high-performance signaling in networked arrays. Trends Biochem Sci **33:**9-19.
16. **Hess JF, Oosawa K, Kaplan N, Simon MI.** 1988. Phosphorylation of three proteins in the signaling pathway of bacterial chemotaxis. Cell **53:**79-87.
17. **Bren A, Eisenbach M.** 1998. The N terminus of the flagellar switch protein, FliM, is the binding domain for the chemotactic response regulator, CheY. J Mol Biol **278:**507-514.
18. **Scharf BE, Fahrner KA, Turner L, Berg HC.** 1998. Control of direction of flagellar rotation in bacterial chemotaxis. Proc Natl Acad Sci U S A **95:**201-206.
19. **McEvoy MM, Bren A, Eisenbach M, Dahlquist FW.** 1999. Identification of the binding interfaces on CheY for two of its targets, the phosphatase CheZ and the flagellar switch protein fliM. J Mol Biol **289:**1423-1433.
20. **Blat Y, Eisenbach M.** 1994. Phosphorylation-dependent binding of the chemotaxis signal molecule CheY to its phosphatase, CheZ. Biochemistry **33:**902-906.
21. **Lukat GS, Stock JB.** 1993. Response regulation in bacterial chemotaxis. Journal of cellular biochemistry **51:**41-46.
22. **Feng X, Baumgartner JW, Hazelbauer GL.** 1997. High- and low-abundance chemoreceptors in *Escherichia coli*: differential activities associated with closely related cytoplasmic domains. J Bacteriol **179:**6714-6720.
23. **Djordjevic S, Stock AM.** 1998. Chemotaxis receptor recognition by protein methyltransferase CheR. Nat Struct Biol **5:**446-450.
24. **Anand GS, Goudreau PN, Stock AM.** 1998. Activation of methylesterase CheB: evidence of a dual role for the regulatory domain. Biochemistry **37:**14038-14047.
25. **Caetano-Anollés G, Wall LG, De Micheli AT, Macchi EM, Bauer WD, Favelukes G.** 1988. Role of Motility and Chemotaxis in Efficiency of Nodulation by *Rhizobium meliloti*. Plant Physiol **86:**1228-1235.
26. **Miller LD, Yost CK, Hynes MF, Alexandre G.** 2007. The major chemotaxis gene cluster of *Rhizobium leguminosarum* bv. *viciae* is essential for competitive nodulation. Mol Microbiol **63:**348-362.

27. **Gulash M, Ames P, Larosiliere RC, Bergman K.** 1984. Rhizobia are attracted to localized sites on legume roots. Appl Environ Microbiol **48:**149-152.
28. **Schmitt R.** 2002. *Sinorhizobial* chemotaxis: a departure from the enterobacterial paradigm. Microbiology **148:**627-631.
29. **Webb BA, Hildreth S, Helm RF, Scharf BE.** 2014. *Sinorhizobium meliloti* chemoreceptor McpU mediates chemotaxis toward host plant exudates through direct proline sensing. Appl Environ Microbiol **80:**3404-3415.
30. **Sourjik V, Schmitt R.** 1998. Phosphotransfer between CheA, CheY1, and CheY2 in the chemotaxis signal transduction chain of *Rhizobium meliloti*. Biochemistry **37:**2327-2335.
31. **Sourjik V, Sterr W, Platzer J, Bos I, Haslbeck M, Schmitt R.** 1998. Mapping of 41 chemotaxis, flagellar and motility genes to a single region of the *Sinorhizobium meliloti* chromosome. Gene **223:**283-290.
32. **Glekas GD, Plutz MJ, Walukiewicz HE, Allen GM, Rao CV, Ordal GW.** 2012. Elucidation of the multiple roles of CheD in *Bacillus subtilis* chemotaxis. Mol Microbiol **86:**743-756.
33. **Dogra G, Purschke FG, Wagner V, Haslbeck M, Kriehuber T, Hughes JG, Van Tassell ML, Gilbert C, Niemeyer M, Ray WK, Helm RF, Scharf BE.** 2012. *Sinorhizobium meliloti* CheA complexed with CheS exhibits enhanced binding to CheY1, resulting in accelerated CheY1 dephosphorylation. J Bacteriol **194:**1075-1087.
34. **Amin M, Kothamachu VB, Feliu E, Scharf BE, Porter SL, Soyer OS.** 2014. Phosphate sink containing two-component signaling systems as tunable threshold devices. PLoS Comput Biol **10:**e1003890.
35. **Li M, Hazelbauer GL.** 2004. Cellular Stoichiometry of the Components of the Chemotaxis Signaling Complex. J Bacteriol **186:**3687-3694.
36. **Cannistraro VJ, Glekas GD, Rao CV, Ordal GW.** 2011. Cellular stoichiometry of the chemotaxis proteins in *Bacillus subtilis*. J Bacteriol **193:**3220-3227.
37. **Levin MD, Morton-Firth CJ, Abouhamad WN, Bourret RB, Bray D.** 1998. Origins of individual swimming behavior in bacteria. Biophys J **74:**175-181.
38. **Bertani G.** 1951. Studies on lysogenesis. I. The mode of phage liberation by lysogenic *Escherichia coli*. J Bacteriol **62:**293-300.
39. **Scharf B, Schuster-Wolff-Buhring H, Rachel R, Schmitt R.** 2001. Mutational analysis of the *Rhizobium lupini* H13-3 and *Sinorhizobium meliloti* flagellin genes: importance of flagellin A for flagellar filament structure and transcriptional regulation. J Bacteriol **183:**5334-5342.
40. **Götz R, Limmer N, Ober K, Schmitt R.** 1982. Motility and Chemotaxis in Two Strains of *Rhizobium* with Complex Flagella. Journal of General Microbiology **128:**789-798.
41. **Rotter C, Mühlbacher S, Salamon D, Schmitt R, Scharf B.** 2006. Rem, a new transcriptional activator of motility and chemotaxis in *Sinorhizobium meliloti*. J Bacteriol **188:**6932-6942.
42. **Sourjik V, Schmitt R.** 1996. Different roles of CheY1 and CheY2 in the chemotaxis of *Rhizobium meliloti*. Mol Microbiol **22:**427-436.
43. **Higuchi R.** 1989. Using PCR to engineer DNA. PCR technology**:**61-70.
44. **Simon R, O'Connell M, Labes M, Pühler A.** 1986. Plasmid vectors for the genetic analysis and manipulation of rhizobia and other gram-negative bacteria. Methods Enzymol **118:**640-659.
45. **Labes M, Pühler A, Simon R.** 1990. A new family of RSF1010-derived expression and lac-fusion broad-host-range vectors for gram-negative bacteria. Gene **89:**37-46.
46. **Miller JH.** 1972. Experiments in molecular genetics. Cold Spring Harbor Laboratory Press, Cold Spring Harbor.
47. **Meier VM, Müschler P, Scharf BE.** 2007. Functional analysis of nine putative chemoreceptor proteins in *Sinorhizobium meliloti*. J Bacteriol **189:**1816-1826.
48. **Riepl H, Maurer T, Kalbitzer HR, Meier VM, Haslbeck M, Schmitt R, Scharf B.** 2008. Interaction of CheY2 and CheY2-P with the cognate CheA kinase in the chemosensory-signalling chain of *Sinorhizobium meliloti*. Mol Microbiol **69:**1373-1384.
49. **Sourjik V, Müschler P, Scharf B, Schmitt R.** 2000. VisN and VisR are global regulators of chemotaxis, flagellar, and motility genes in *Sinorhizobium* (*Rhizobium*) *meliloti*. J Bacteriol **182:**782-788.
50. **Galibert F, Finan TM, Long SR, Pühler A, Abola P, Ampe F, Barloy-Hubler F, Barnett MJ, Becker A, Boistard P, Bothe G, Boutry M, Bowser L, Buhrmester J, Cadieu E, Capela D, Chain P, Cowie A, Davis RW, Dreano S, Federspiel NA, Fisher RF, Gloux S, Godrie T, Goffeau A, Golding B, Gouzy J, Gurjal M, Hernandez-Lucas I, Hong A, Huizar L, Hyman RW, Jones T, Kahn D, Kahn ML, Kalman S, Keating DH, Kiss E, Komp C, Lelaure V, Masuy D, Palm C, Peck MC, Pohl TM, Portetelle D,**

Purnelle B, Ramsperger U, Surzycki R, Thebault P, Vandenbol M, et al. 2001. The composite genome of the legume symbiont *Sinorhizobium meliloti*. Science **293:**668-672.
51. **Schoenlein PV, Ely B.** 1989. Characterization of strains containing mutations in the contiguous *flaF*, *flbT*, or *flbA-flaG* transcription unit and identification of a novel *fla* phenotype in *Caulobacter crescentus*. J Bacteriol **171:**1554-1561.
52. **Schoenlein PV, Gallman LS, Ely B.** 1989. Organization of the *flaFG* gene cluster and identification of two additional genes involved in flagellum biogenesis in *Caulobacter crescentus*. J Bacteriol **171:**1544-1553.
53. **Llewellyn M, Dutton RJ, Easter J, O'Donnol D, Gober JW.** 2005. The conserved *flaF* gene has a critical role in coupling flagellin translation and assembly in *Caulobacter crescentus*. Mol Microbiol **57:**1127-1142.
54. **Ferooz J, Lemaire J, Letesson J-J.** 2011. Role of FlbT in flagellin production in *Brucella melitensis*. Microbiology **157:**1253-1262.
55. **Rotter C, Mühlbacher S, Schmitt R, Scharf B.** 2006. Rem, a new transcriptional regulator of motility and chemotaxis in *Sinorhizobium meliloti*. J Bacteriol **submitted for publication**.
56. **Meier VM, Scharf BE.** 2009. Cellular Localization of Predicted Transmembrane and Soluble Chemoreceptors in *Sinorhizobium meliloti*. J Bacteriol **191:**5724-5733.
57. **Soutourina OA, Bertin PN.** 2003. Regulation cascade of flagellar expression in Gram-negative bacteria, vol 27.
58. **Aldridge P, Hughes KT.** 2002. Regulation of flagellar assembly. Curr Opin Microbiol **5:**160-165.
59. **Barnakov AN, Barnakova LA, Hazelbauer GL.** 1999. Efficient adaptational demethylation of chemoreceptors requires the same enzyme-docking site as efficient methylation. Proc Natl Acad Sci U S A **96:**10667-10672.
60. **Wu J, Li J, Li G, Long DG, Weis RM.** 1996. The receptor binding site for the methyltransferase of bacterial chemotaxis is distinct from the sites of methylation. Biochemistry **35:**4984-4993.
61. **Li M, Hazelbauer GL.** 2005. Adaptational assistance in clusters of bacterial chemoreceptors. Mol Microbiol **56:**1617-1626.
62. **Gegner JA, Graham DR, Roth AF, Dahlquist FW.** 1992. Assembly of an MCP receptor, CheW, and kinase CheA complex in the bacterial chemotaxis signal transduction pathway. Cell **70:**975-982.
63. **Pleier E, Schmitt R.** 1991. Expression of two *Rhizobium meliloti* flagellin genes and their contribution to the complex filament structure. J Bacteriol **173:**2077-2085.
64. **Kovach ME, Elzer PH, Hill DS, Robertson GT, Farris MA, Roop RM, 2nd, Peterson KM.** 1995. Four new derivatives of the broad-host-range cloning vector pBBR1MCS, carrying different antibiotic-resistance cassettes. Gene **166:**175-176.
65. **Schafer A, Tauch A, Jager W, Kalinowski J, Thierbach G, Pühler A.** 1994. Small mobilizable multi-purpose cloning vectors derived from the *Escherichia coli* plasmids pK18 and pK19: selection of defined deletions in the chromosome of *Corynebacterium glutamicum*. Gene **145:**69-73.
66. **Hübner P, Willison JC, Vignais PM, Bickle TA.** 1991. Expression of regulatory *nif* genes in *Rhodobacter capsulatus*. J Bacteriol **173:**2993-2999.

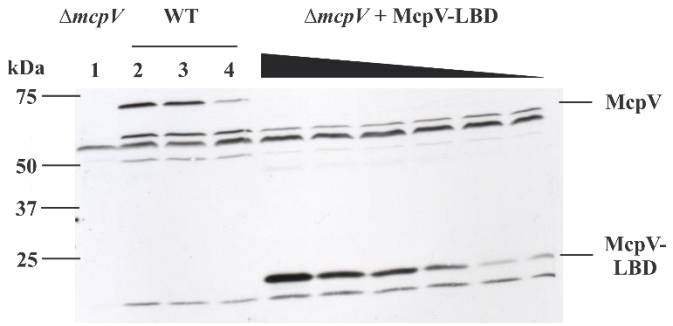

Fig. 4.1: Representative immunoblot used to quantify McpV. Lane 1 (Δ*mcpV*) contains RU11/830 (*mcpV* deletion strain) cell lysate from 1 ml culture at OD_{600} 0.25. Lanes 2 - 4 contain RU11/001 (WT) cell lysates from 1 ml of culture at OD_{600} 0.25 and show bands corresponding to McpV (65.34 kDa). Δ*mcpV* + McpV-LBD lanes contain purified McpV-LBD (7.5, 5.0, 4.0, 3.0, 2.0, and 1.0 ng) mixed with RU11/830 cell lysates.

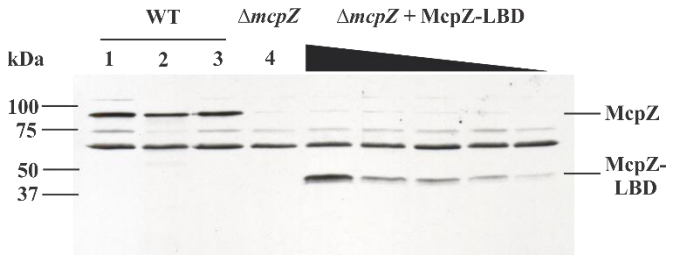

Fig. 4.2: Representative immunoblot used to quantify McpZ. Lanes 1 - 3 contain RU11/001 (WT) cell lysates from 1 ml of culture at OD_{600} 0.25 and show bands corresponding to McpZ (90.15 kDa). Lane 4 (Δ*mcpZ*) contains RU11/818 (*mcpZ* deletion strain) cell lysate from 1 ml culture at OD_{600} 0.25. Δ*mcpZ* + McpZ-LBD lanes contain purified McpZ-LBD (2.6, 1.3, 0.78, 0.52, and 0.26 ng) mixed with RU11/830 cell lysates.

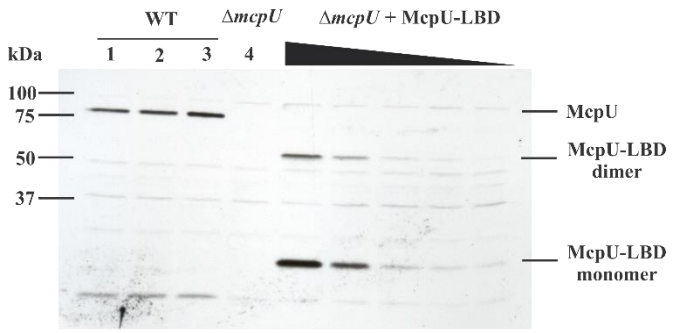

Fig. 4.3: Representative immunoblot used to quantify McpU. Lanes 1 - 3 contain RU11/001 (WT) cell lysates from 1 ml of culture at OD_{600} 0.25 and show bands corresponding to McpU (74.36 kDa). Lane 4 (Δ*mcpU*) contains RU11/828 (*mcpU* deletion strain) cell lysate from 1 ml culture at OD_{600} 0.25. Δ*mcpU* + McpU-LBD lanes contain purified McpU-LBD (2.0, 1.0, 0.5, 0.1, and 0.05 ng) mixed with RU11/828 cell lysates. McpU-LBD exists in a monomeric and dimeric form, as indicated.

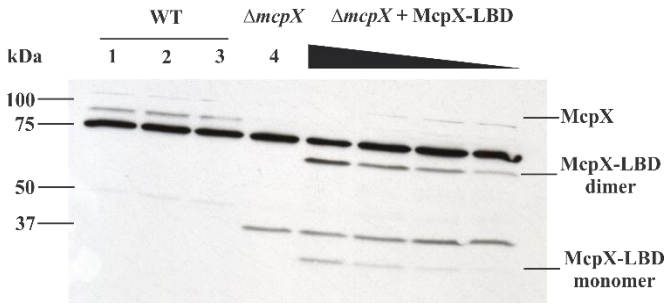

Fig. 4.4: Representative immunoblot used to quantify McpX. Lanes 1 - 3 contain RU11/001 (WT) cell lysates from 1 ml of culture at OD_{600} 0.25 and show bands corresponding to McpX (83.71 kDa). Lane 4 (Δ*mcpX*) contains RU11/805 (*mcpX* deletion strain) cell lysate from 1 ml culture at OD_{600} 0.25. Δ*mcpX* + McpX-LBD lanes contain purified McpX-LBD (1.0, 0.75, 0.5, and 0.25 ng) mixed with RU11/805 cell lysates. McpX-LBD exists in a monomeric and dimeric form, as indicated.

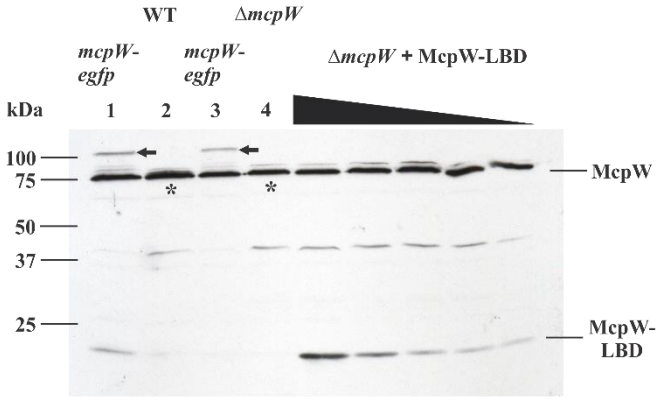

Fig. 4.5: Representative immunoblot used to quantify McpW. Lanes 1 and 3 contain RU13/143 (*mcpW-egfp*) cell lysates from 1 ml of culture at OD_{600} 0.25. Lane 2 contains RU11/001(WT) cell lysates from 1 ml of culture at OD_{600} 0.25. Lane 4 (Δ*mcpW*) contains RU11/803 (*mcpW* deletion strain) cell lysate from 1 ml culture at OD_{600} 0.25. Δ*mcpW* + McpW-LBD lanes contain purified McpW-LBD (0.5, 0.25, 0.1, 0.075, and 0.05 ng) mixed with RU11/803 cell lysates. The intensity of the McpW-GFP band in lanes 1 and 3 (arrows) is equal to the difference in intensities between the band in lane 2 (asterisk) and it corresponding non-specific band in lane 4.

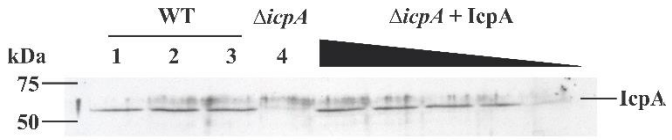

Fig. 4.6: Representative immunoblot used to quantify IcpA. Lanes 1 - 3 contain RU11/001 (WT) cell lysates from 1 ml of culture at OD_{600} 0.25 and show bands corresponding to IcpA (57.54 kDa). Lane 4 (Δ*icpA*) contains RU11/815 (*icpA* deletion) cell lysate from 1 ml culture at OD_{600} 0.25. Δ*icpA* + IcpA lanes contain purified IcpA (12.0, 10.0, 8.0, 6.0, and 4.0 ng) mixed with RU11/815 cell lysates.

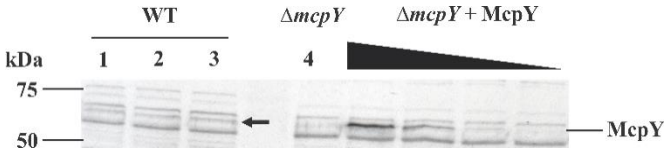

Fig. 4.7: Representative immunoblot used to quantify McpY. Lanes 1 - 3 contain RU11/001 (WT) cell lysates from 1 ml of culture at OD_{600} 0.25 and show bands corresponding to McpY (64.30 kDa). Lane 4 (Δ*mcpY*) contains RU11/804 (*mcpY* deletion strain) cell lysate from 1 ml culture at OD_{600} 0.25. Δ*mcpY* + McpY lanes contain purified McpY (0.1, 0.05, 0.01, and 0.005 ng) mixed with RU11/804 cell lysates. Arrow indicates the McpY protein the WT cell lysate.

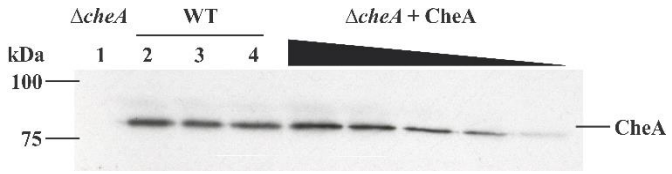

Fig. 4.8: Representative immunoblot used to quantify CheA. Lane 1 (Δ*cheA*) contains RU11/310 (*cheA* deletion strain) cell lysate from 1 ml culture at OD_{600} 0.25. Lanes 2 - 4 contain RU11/001 (WT) cell lysates from 1 ml of culture at OD_{600} 0.25 and show bands corresponding to CheA (81.12 kDa). Δ*cheA* + CheA lanes contain purified CheA (1.0, 0.8, 0.6, 0.4, and 0.2 ng) mixed with RU11/310 cell lysates.

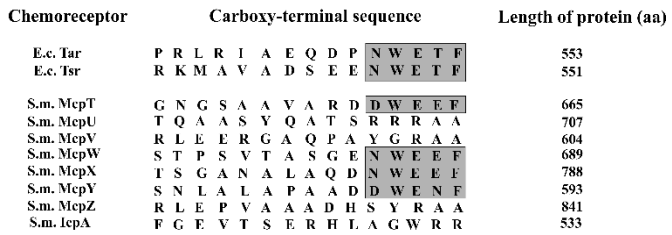

Fig. 4.9: Sequence comparison of the last 15 amino acid residues for NWETF-motif containing *E.coli* (E.c.) receptors Tar and Tsr and all eight *S. meliloti* (S.m.) chemoreceptors. The conserved pentapeptide sequence is marked in grey.

Table 4.1. Bacterial strains and plasmids

Strains/Plasmids	Relevant Characteristics/Sequence	Reference or Source
Strain		
E. coli		
BL21(DE3)	F$^-$ *ompT hsdS*$_B$(r_b^- m_b^-) *gal dcm* λ (DE3)	Novagen
ER2566	*lon ompT lacZ*::*T7*	NEBiolabs
S17-1	*recA endA thi hsdR* RP4-2 Tc::Mu::Tn7 Tp^r Sm^r	(44)
S. meliloti		
RU11/001	Sm^r, spontaneously streptomycin-resistant wild-type strain	(63)
RU11/310	Sm^r, Δ*cheA*	(42)
RU11/555	Sm^r, Δ*rem*	(41)
RU11/803	Sm^r, Δ*mcpW*	(47)
RU11/804	Sm^r, Δ*mcpY*	(47)
RU11/805	Sm^r, Δ*mcpX*	(47)
RU11/814	Sm^r, Δ*visNR*	(49)
RU11/815	Sm^r, Δ*icpA*	(47)
RU11/818	Sm^r, Δ*mcpZ*	(47)
RU11/828	Sm^r, Δ*mcpU*	(47)
RU11/830	Sm^r, Δ*mcpV*	(47)
RU11/838	Sm^r, Δ*mcpT*	(47)
RU13/143	Sm^r, *mcpW-egfp*	(56)
RU13/310	Sm^r, Δ*flbT*	This study
Plasmids		
pHT28	Ap^r, expression vector for *E. coli* fliM	(64)
pK18*mobsacB*	Km^r, *lacZ mob sacB*	(65)
pTYB1	Ap^r, protein expression vector	NEBiolabs
pTYB11	Ap^r, protein expression vector	NEBiolabs
pBS352	Ap^r, 858 bp *Nde*I/*Sap*I PCR fragment containing periplasmic domain of *mcpX* cloned into pTYB1	This study
pBS353	Ap^r, 741 bp *Nde*I/*Sap*I PCR fragment containing periplasmic domain of *mcpU* cloned into pTYB1	This study
pBS409	Ap^r, 474 bp *Sap*I/*Pst*I PCR fragment containing periplamic domain of *mcpV* cloned into pTYB11	This study
pBS426	Ap^r, 1218 bp *Sap*I/*Spe*I PCR fragment containing periplamic domain of *mcpZ* cloned into pTYB11	This study
pBS1030	Ap^r, 444 bp *Nde*I/*Pst*I PCR fragment containing periplamic domain of *mcpT* cloned into pTYB1	This study
pBS1031	Ap^r, 423 bp *Nde*I/*Pst*I PCR fragment containing periplamic domain of *mcpW* cloned into pTYB1	This study
pRU2250	Tc^r, *icpA* (1974 bp)-*lacZ* (*che*) fusion cloned into pPHU236	(66)

pRU2550	Ap^r, 1602 bp *Sap*I/*Sma*I PCR fragment containig *icpA* cloned into pTYB11	This study
pRU2782	Tc^r, *mcpT* (320 bp)-*lacZ* fusion cloned into pPHU235	(66)
pRU2783	Tc^r, *mcpU* (456 bp)-*lacZ* fusion cloned into pPHU236	(66)
pRU2784	Tc^r, *mcpW* (303 bp)-*lacZ* fusion cloned into pPHU236	(66)
pRU2787	Tc^r, *mcpZ* (409 bp)-*lacZ* fusion cloned into pPHU236	(66)
pRU2790	Ap^r, 1779 bp KpnI/PstI PCR fragment containig *mcpY* replacing *E. coli fliM* in pHT28	
pRU2898	Tc^r, *mcpY* (786 bp)-*lacZ* fusion cloned into pPHU236	(66)
pRU2994	Tc^r, *mcpX* (590 bp)-*lacZ* fusion cloned into pPHU236	(66)

Table 4.2. *In vivo mcp* promoter activities in wild type (WT), Δ*visN/R*, Δ*rem*, and Δ*flbT* mutant strains

Plasmid [a] (*lacZ*-fusion)	β-galactosidase activity [b] (Miller units)			
	RU11/001[c] WT	RU11/814 Δ*visNR*	RU11/555 Δ*rem*	RU13/110 Δ*flbT*
pRU2728 (*mcpT*)	42	7	7	35
pRU2283 (*mcpU*)	235	0	0	4
pRU2784 (*mcpW*)	127	2	0	6
pRU2994 (*mcpX*)	417	0	0	6
pRU2898 (*mcpY*)	29	13	12	23
pRU2787 (*mcpZ*)	154	0	0	17
pRU2250 (*icpA* = *che*)	156	0	0	25

[a] Transcription from nine chemoreceptor promoters was assessed with plasmid-borne *lacZ* fusions (47) in wild-type (RU11/001; (63), Δ*visN/R* (RU11/814; (55), Δ*rem* (RU11/555; (55), and Δ*flbT* (RU13/110) during exponential growth. Cells diluted in RB were layered on Bromfield agar plates and grown to an OD_{600} of 0.15-0.25. The *che*-operon (*che*) is composed of the genes *icpA orf2 cheY1 cheA cheW cheR cheB cheY2 cheD orf10*.

[b] β-galactosidase activities (46) of three to five independent experiments were averaged.

[c] Values for wild type were taken from Meier *et al.* (2007;(47)).

Table 4.3. Cellular chemotaxis protein contents in *S. meliloti*

Protein	No. of molecules/cell[*+]
McpT	ND
McpU	47 ± 6
McpV	299 ± 55
McpW	17 ± 4
McpX	39 ± 7
McpY	1 ± 1
McpZ	3 ± 1
IcpA	285 ± 69
Total Receptors	691 ± 143
CheA	18 ± 5

[*] Mean ± Standard deviation

Quantitative immunoblots were performed with 1 ml cell lysates of *S. meliloti* RU11/001 strain and purified Mcp (ligand-binding domain or full-length) proteins were used to generate a standard curve. ImageJ analyses was performed on each immunoblot to quantify the amount of protein in 1 ml cell culture.

[+]Values obtained from six independent immunoblots

Chapter 5 - Final Discussion

Nitrogen is an essential element in building amino acids and nucleic acids in living cells and thus is indispensable in sustaining life on Earth. Di-nitrogen (N_2) present in the atmosphere cannot be utilized directly by most living cells as a source of nitrogen. Some bacteria and archaea have the unique ability to fix atmospheric nitrogen to forms like ammonia (NH_3) or nitrogen dioxide (NO_2) which can be easily assimilated in living cells. This process can occur in free-living bacteria as well as those living in symbiosis with plants and animals. Most of symbiotic nitrogen fixation occurs between bacteria and plants (leguminous and non-leguminous) leading to increased soil fertility and crop yields and ultimately playing an extremely important role in the nitrogen cycle. Symbiotic nitrogen fixation saves almost $10 billion annually in United States alone by reducing the dependence on synthetic and expensive nitrogenous fertilizers (1).

Alfalfa (*Medicago sativa*) is a major component of animal feed and is the fourth largest crop grown in the United States. *Sinorhizobium meliloti*, a Gram-negative bacterium fixes atmospheric nitrogen in symbiosis with alfalfa. While the *Sinorhizobium – Medicago* model has been studied, deeper understanding of this symbiosis could not only potentially help us increase crop yields but also do so in an environmentally sustainable manner (2-4). Our focus in this study are two *S. meliloti* traits, Type IVb pili and chemotaxis, and their importance in establishing a successful symbiotic relationship.

In Chapter 2, we characterize the role of Type IVb pili in establishing symbiosis by *S. meliloti*. Type IVb pili are encoded from two putative *pil* clusters in the *S. meliloti* genome, *flp-1* on the chromosome and *flp-2* on the pSymA megaplasmid. Studies in this chapter are focused on *pilA1* gene which codes for the putative pilin protein, the structural subunit of the pilus filament. We demonstrated the presence of Type IVb pili in discrete bundles (bundle-forming pili) in strain Sm1021 and their absence in strain Sm1021 Δ*pilA1* using transmission electron microscopy. The

pilus bundles exhibited lateral localization where two or three pilus bundles emanated from one side of the cell. Lateral localization of pilus bundles was corroborated by the filament-like unilateral localization of CpaE1-mCherry, a putative cytoplasmic pilus assembly protein encoded from the *flp-1* gene cluster fused with mCherry. CpaE1 shows 24 % identity to TadZ from *Aggregatibacter actinomycetemcomitans*, which is thought to mediate the polar localization of Flp pilus machinery by independently localizing to the poles (5). It remains to be elucidated whether CpaE1 performs a similar function in *S. meliloti*.

Furthermore, using competitive nodulation assays with alfalfa, we observed that nodulation was significantly impaired by about 27 % in the Sm1021 Δ*pilA1* strain as compared to the Sm1021 WT. We hypothesize that *S. meliloti* uses Flp pili to attach to plant roots and thereby impact nodulation. Although nodulation efficiency is significantly reduced, it is not abolished. This points to an accessory role for Type IVb pili in nodulation, rather than an essential one. It can be postulated that the bundles of pili on one side of the cell help maximize contact between bacteria and plant-host cells. It is similar to the multiple lateral *vir*-type IV secretion system complexes used in attachment of *Agrobacterium tumefaciens* to plant cells (6). This demonstrates the importance of the *flp-1* cluster in symbiosis.

Additionally, we investigated the expression pattern of *pilA1* during culture growth. Using transcriptional fusions with *lacZ*, we observed that *pilA1* expression peaked in late exponential to early stationary phase. It was also confirmed that *pilA1* is regulated via the *sinRI* quorum sensing regulator, ExpR. Electrophoretic mobility shift assays (EMSAs) further proved a direct binding of acylated homoserine lactone-activated ExpR to the *pilA1* promoter. A 17-bp ExpR-binding site on the *pilA1* promoter, as confirmed by DNase I footprinting analyses, exhibited a high degree of similarity to other ExpR-binding sites of the ExpR regulon. It has also been shown that when ExpR

binds upstream of the -35 site it activates the gene, while when ExpR binds downstream of the -35 site it represses the gene (7). This also holds true for *pilA1* where the ExpR-binding site is downstream of the -35 site and thus ExpR represses *pilA1* expression. In fact, comparing the *pilA1* promoter with predicted and experimentally confirmed *S. meliloti* promoter characteristics shows that a sequence identified as 5´ - CTAAAT - 3´ within the ExpR-binding site would be the -10 site. In conclusion, ExpR on binding to the *pilA1* promoter covers the -10 site preventing the binding of RNA polymerase to the *pilA1* promoter and thereby, repressing the transcription of *pilA1*.

This study assimilates the Flp pilus synthesis into the *sinRI* quorum sensing system-based transcriptional regulation via ExpR in *S. meliloti*. While ExpR activates EPS production, it represses motility and chemotaxis and type IVb pili. These activities of ExpR have been shown to be dependent on the levels of AHLs in the culture and thus are growth phase dependent (7). A model can be imagined where the cell uses chemotaxis and motility to sense and reach the plant roots. The cell would then use type IVb pili to attach to the plant roots, while simultaneously repressing the transcription of the motility and chemotaxis activator, *visNR*, via ExpR. On attaching to the plant roots using pili, the cell activates the expression of exopolysaccharides important for infection thread formation and nodule invasion while repressing the expression of *pilA1*, both via ExpR. Thus, through ExpR, *S. meliloti* has implemented a dynamic and precise transcriptional control over symbiotically important processes like motility and chemotaxis, EPS production, and type IVb pili.

In Chapter 3, we explore the role of the *flp-2* cluster in establishing symbiosis. PilA2, a PilA1-homolog with 60 % identity, encoded from the *flp-2* system is a putative pilin subunit. There was no expression of *pilA2* in liquid cultures unlike that seen in *pilA1*. However, like the Δ*pilA1* strain, the Δ*pilA2* strain was shown to be defective in nodulation by 31 % as compared to the

Sm1021 WT. A Δ*pilA1*Δ*pi1A2* strain presented a non-significant effect. Thus, it can be concluded that both *flp-1* and *flp-2* have a significant role in establishing a successful symbiotic relationship. Based on the lack of expression of *pilA2* in liquid cultures and a significant nodulation impairment in a Δ*pilA2* strain, we can hypothesize that *flp-1* has a primary functional role in establishing initial contact with the host roots while *flp-2* is important in the later stages of the symbiotic relationship, when *flp-1* may play an accessory role.

The above mentioned data from Chapter 3 will be published along with data from our collaborators, Dr. Ann Hirsch (UCLA) and Dr. Nancy Fujishige (LMU). Using plant infectivity assays, they were able to establish that a higher percentage of nodules induced by the Sm1021 Δ*pilA1*, Δ*pilA2*, and Δ*pilA1*Δ*pilA2* strains remained uninfected or partially infected. On the other hand, the nodules induced by Sm1021 WT were mostly completely infected. Their study also explored the role of pili in *S. meliloti* biofilm formation. It was demonstrated that biofilm formation after 48 and 72 h on poly-vinyl chloride microtiter plates was significantly reduced in Sm1021 Δ*pilA1* and Δ*pilA2* strains. No additive defect on biofilm formation was seen in a Δ*pilA1*Δ*pilA2* strain. Since attachment to plant roots may be a precursor to localized biofilm production, which in turn is required for efficient nodulation, the decrease in biofilm formation in pili mutants point to a role of pili in attachment and adhesion to host roots. Taken together, Chapter 2 and Chapter 3 are the first reports establishing the function of Type IVb pili in a plant-bacterial symbiotic relationship.

Future studies related to Type IV pili in *S. meliloti* should focus on confirming the role of pili in attachment by performing plant root attachment assays. Furthermore, it would be interesting to explore the purpose of *flp-2*, *in planta*, by analyzing the expression of *pilA2* within infection threads and nodules. Since a chemotaxis- like operon, *che2*, is present immediately upstream of

the *flp-2* operon, it can be postulated that the *flp-2* operon is regulated by the proteins encoded from the *che2* operon, as seen in *Pseudomonas aeruginosa* (8). It has been shown before that the *che2* operon played no role in chemotaxis (9). It is exciting to explore the possibility that specific plant-derived compounds may be sensed by the chemoreceptor encoded by *che2* when the *S. meliloti* cell is in contact with the plant roots or within the infection thread. The two-component chemotaxis-like signaling system, in turn, may regulate the *flp-2* gene cluster. Finally, using deletion mutants and fluorescent protein-fusions, the exact role and localization of pilus synthesis machinery proteins should be elucidated.

Another *S. meliloti* trait important for establishing a symbiotic relationship is chemotaxis towards the plant roots (10). While chemotaxis is widely studied in the enteric *Escherichia coli*, there are several significant deviations in the *S. meliloti* chemotaxis system from the established paradigm. For greater in-depth understanding of the role chemotaxis on the two *S. meliloti* life styles, free-living and symbiotic, it is important to study the aberrations and their corresponding effects in *S. meliloti* chemotaxis. An important deviation is the number of methyl-accepting chemotaxis proteins (MCPs) which are the chemoreceptors in the chemotaxis system. *E. coli* has four transmembrane MCPs and one soluble MCP (11). In contrast, *S. meliloti* has six transmembrane (McpT-McpX, and McpZ) and two soluble (McpY and IcpA) chemoreceptors (9).

In Chapter 4, we showed that the chemoreceptor genes belong to the class III genes in the transcriptional hierarchy of the motility and chemotaxis genes in *S. meliloti* (RU11/001) (12). Additionally, it was observed that the expression of *mcp* genes except (*mcpT* and *mcpY*) is regulated by a class IIA regulator, FlbT, which also regulates the synthesis of flagellin in *S. meliloti*.

Furthermore, we determined the cellular stoichiometry of chemoreceptors and the histidine kinase, CheA. The total number of all eight chemoreceptors in an *S. meliloti* cell is 690 ± 142 as compared to 59,960 ± 5,960 in *B. subtilis* and 26,000 ± 1800 in *E. coli* (13, 14). Due to the smaller size of an *S. meliloti* cell, as per our dry weight analyses and viable cell counts, it is possible that its chemotaxis system may be uniquely optimized to function at low numbers of chemoreceptors. Moreover, fluorescence microscopy studies with mRFP-tagged proteins showed that not all cells in the population expressed a chemoreceptor cluster (Arapov and Scharf, personal communication). Thus, the actual number of chemoreceptors per cell value is higher than reported.

E. coli chemoreceptors are present in varied abundance: high (Tsr and Tar) or low (Trg, Tap, and Aer) (13, 15). A similarly distribution is seen in *S. meliloti*. The chemoreceptors are present in high (McpV and IcpA), low (McpU, McpW, and McpX), or extremely low (McpY and McpZ) abundance. The approximate ratios for these are 300 (high) : 30 (low) : 1 (extremely low). It has been shown that McpV and IcpA exhibit CheA- and CheW-independent localization, which might be a result of their high abundance (16). In *B. subtilis*, McpB and McpC are the sensors of amino acids and are present in relatively low abundance (14). Similarly, in *S. meliloti*, McpU senses proline and other amino acids and is also present in low abundance (17). McpT-LBD could not be detected using antibodies raised against it. Moreover, no band corresponding to McpT was detected in the WT cell lysates. The amounts of McpT in the cell are expected to be low based on the low transcriptional activity shown in a previous study (9, 16). Since McpT and McpY are not regulated by FlbT, there might exist another regulatory mechanism to control their expression. The reason for their extremely low amounts could be the continuous repression via this alternative regulator. It can be hypothesized that these MCPs may have a role *in planta* and may respond to plant-derived compounds as a stimulus for expression.

In *E. coli*, a characteristic pentapeptide, NWETF, which serves as a docking site for the adaptation proteins CheB and CheR is present at the carboxy terminus of the high-abundance chemoreceptors (Tar and Tsr) (18). The chemoreceptors in *S. meliloti* that have a NWETF-like motif belong to the low-abundance group (McpW and McpX) and the extremely low-abundance group (McpT and McpY). However, the chemoreceptors in *Thermotoga maritima* and *Rhodobacter sphaeroides* have no such pentapeptide at their carboxy termini. A pentapeptide-independent docking mechanism of the adaptation proteins has been suggested (19). While CheR docks exclusively to the pentapeptide-containing chemoreceptors in *E. coli* (pentapeptide-dependent CheR), it remains to be elucidated if the receptor methylation by CheR in *S. meliloti* is pentapeptide-dependent or pentapeptide–independent as, both, chemoreceptors with and without the pentapeptide are seen in *S. meliloti*.

Lastly, we show that CheA is present in the cell at levels comparable to the low-abundance chemoreceptor McpW. The ratio of chemoreceptor to CheA in *S. meliloti* is 37:1. This is comparable to that in *B. subtilis* of 24:1, while very different from that in *E. coli* of 3.4:1 (13, 14). It can be postulated that the chemoreceptor to CheA ratio is a hallmark of the milieu of the organism, and thus the soil bacteria (*S. meliloti* and *B. subtilis*) show such a level of similarity.

Future studies in this area would be to calculate the amounts of McpT in the cell using a 3xFLAG tag. McpT-LBD-3xFLAG can be used to establish a standard curve and a RU11/001 strain expressing McpT-3xFLAG from the native promoter would be used to determine the amounts of McpT per cell. Furthermore, the elucidation of the cellular stoichiometry of all the chemotaxis proteins in *S. meliloti* should be undertaken. These studies will also answer whether the stoichiometry of the CheA-CheW-receptor complex is different in *S. meliloti* from the one described for *E. coli* (20). This data along with the reaction constants of each of the

phosphotransfer reactions as well as receptor modifications (methylation and demethylation) in *S. meliloti* can be implemented into a computational model to generate a robust simulation of the *S. meliloti* chemotaxis system. Such a simulation would shed light on the questions of how the deviations in *S. meliloti* chemotaxis system help its lifestyle choices and how it effectively senses roots of its host plant and moves through the soil.

Overall, the results presented in this study have enhanced our understanding of the exact molecular processes that enable the plant and bacteria to enter into a successful symbiotic relationship. This knowledge paves the way for experimentation to further optimize these processes to help increase crop yields and benefit the environment.

REFERENCES

1. **van Rhijn P, Vanderleyden J.** 1995. The *Rhizobium*-plant symbiosis. Microbiological Reviews **59:**124-142.
2. **Jones KM, Kobayashi H, Davies BW, Taga ME, Walker GC.** 2007. How rhizobial symbionts invade plants: the *Sinorhizobium-Medicago* model. Nat Rev Microbiol **5:**619-633.
3. **Oldroyd GE, Murray JD, Poole PS, Downie JA.** 2011. The rules of engagement in the legume-rhizobial symbiosis. Annual review of genetics **45:**119-144.
4. **Gubry-Rangin C, Garcia M, Béna G.** 2010. Partner choice in *Medicago truncatula–Sinorhizobium* symbiosis. Proceedings of the Royal Society of London B: Biological Sciences **277:**1947-1951.
5. **Perez-Cheeks BA, Planet PJ, Sarkar IN, Clock SA, Xu Q, Figurski DH.** 2012. The product of *tadZ*, a new member of the *parA*/*minD* superfamily, localizes to a pole in *Aggregatibacter actinomycetemcomitans*. Mol Microbiol **83:**694-711.
6. **Aguilar J, Cameron TA, Zupan J, Zambryski P.** 2011. Membrane and core periplasmic *Agrobacterium tumefaciens* virulence Type IV secretion system components localize to multiple sites around the bacterial perimeter during lateral attachment to plant cells. mBio **2:**e00218-00211.
7. **Charoenpanich P, Meyer S, Becker A, McIntosh M.** 2013. Temporal Expression Program of Quorum Sensing-Based Transcription Regulation in *Sinorhizobium meliloti*. J Bacteriol **195:**3224-3236.
8. **Kato J, Kim HE, Takiguchi N, Kuroda A, Ohtake H.** 2008. *Pseudomonas aeruginosa* as a model microorganism for investigation of chemotactic behaviors in ecosystem. J Biosci Bioeng **106:**1-7.
9. **Meier VM, Müschler P, Scharf BE.** 2007. Functional analysis of nine putative chemoreceptor proteins in *Sinorhizobium meliloti*. J Bacteriol **189:**1816-1826.
10. **Caetano-Anollés G, Wall LG, De Micheli AT, Macchi EM, Bauer WD, Favelukes G.** 1988. Role of Motility and Chemotaxis in Efficiency of Nodulation by *Rhizobium meliloti*. Plant Physiol **86:**1228-1235.
11. **Parkinson JS, Hazelbauer GL, Falke JJ.** 2015. Signaling and sensory adaptation in *Escherichia coli* chemoreceptors: 2015 update. Trends Microbiol **23:**257-266.
12. **Rotter C, Mühlbacher S, Salamon D, Schmitt R, Scharf B.** 2006. Rem, a new transcriptional activator of motility and chemotaxis in *Sinorhizobium meliloti*. J Bacteriol **188:**6932-6942.
13. **Li M, Hazelbauer GL.** 2004. Cellular Stoichiometry of the Components of the Chemotaxis Signaling Complex. J Bacteriol **186:**3687-3694.
14. **Cannistraro VJ, Glekas GD, Rao CV, Ordal GW.** 2011. Cellular stoichiometry of the chemotaxis proteins in *Bacillus subtilis*. J Bacteriol **193:**3220-3227.
15. **Feng X, Baumgartner JW, Hazelbauer GL.** 1997. High- and low-abundance chemoreceptors in *Escherichia coli*: differential activities associated with closely related cytoplasmic domains. J Bacteriol **179:**6714-6720.
16. **Meier VM, Scharf BE.** 2009. Cellular Localization of Predicted Transmembrane and Soluble Chemoreceptors in *Sinorhizobium meliloti*. J Bacteriol **191:**5724-5733.
17. **Webb BA, Hildreth S, Helm RF, Scharf BE.** 2014. *Sinorhizobium meliloti* chemoreceptor McpU mediates chemotaxis toward host plant exudates through direct proline sensing. Appl Environ Microbiol **80:**3404-3415.
18. **Barnakov AN, Barnakova LA, Hazelbauer GL.** 1999. Efficient adaptational demethylation of chemoreceptors requires the same enzyme-docking site as efficient methylation. Proc Natl Acad Sci U S A **96:**10667-10672.
19. **Perez E, Stock AM.** 2007. Characterization of the *Thermotoga maritima* chemotaxis methylation system that lacks pentapeptide-dependent methyltransferase CheR:MCP tethering. Mol Microbiol **63:**363-378.
20. **Gegner JA, Graham DR, Roth AF, Dahlquist FW.** 1992. Assembly of an MCP receptor, CheW, and kinase CheA complex in the bacterial chemotaxis signal transduction pathway. Cell **70:**975-982.